Towards optimized spark ignition for hydrogen and biogas heavy-duty engines

Saha, Anupam

2026

Document Version:
Publisher's PDF, also known as Version of record

Towards optimized spark ignition for hydrogen and biogas heavy-duty engines

ANUPAM SAHA
DEPARTMENT OF ENERGY SCIENCES | FACULTY OF ENGINEERING | LUND UNIVERSITY

Towards optimized spark ignition for hydrogen and biogas heavy-duty engines

Towards optimized spark ignition for hydrogen and biogas heavy-duty engines

Anupam Saha

LUND
UNIVERSITY

DOCTORAL DISSERTATION

Doctoral dissertation for the degree of Doctor of Philosophy (PhD)
at the Faculty of Engineering at Lund University to be publicly defended on
Friday, the 12th of June 2026 at 10:15 in M:A, M-huset, Ole Römers väg 1, Lund.

Thesis advisors: Prof. Öivind Andersson and Prof. Per Tunestål

Faculty opponent: Dr. Isaac Ekoto

Organization: Lund University

Document name: Doctoral Disstertation

Date of issue 2026-06-12

Author: Anupam Saha

Sponsoring organization: Swedish Energy Agency, Volvo Trucks AB and SEM AB

Title and subtitle: Towards optimized spark ignition for hydrogen and biogas heavy-duty engines

Abstract:

Heavy-duty transport is one of the major contributors to global greenhouse gas (GHG) emissions, with internal combustion engines (ICEs) expected to remain an important propulsion technology in long-haul applications during the transition to sustainable transport. The use of renewable gaseous fuels such as biogas and hydrogen offers a promising pathway to significantly reduce the climate impact of ICE-based powertrains. Due to their high octane rating and excellent knock resisting properties, these fuels are well suited for spark ignition (SI) engines. However, achieving robust combustion in SI engines is strongly dependent on the spark ignition process, which becomes increasingly challenging under lean and highly diluted operating conditions. At the same time, excessive spark energy can accelerate spark plug wear and increase the risk of abnormal combustion, particularly in hydrogen engines. To address this, this thesis investigates spark ignition processes in ICEs operating on hydrogen and biogas.

A central focus of the thesis is to improve the understanding of how electrical energy from the spark is transferred to the surrounding gas and how this governs ignitability, combustion stability, and spark plug wear. To achieve this, a combination of experimental approaches is employed, including fundamental investigations in constant-volume chambers and application-oriented studies in single-cylinder heavy-duty research engines. The results reveal that ignition performance is not determined by the total spark energy, but by how effectively the spark energy is delivered during different phases of the spark discharge. The initial breakdown and arc phases are shown to be highly efficient in transferring energy to the gas, whereas the glow phase contributes less efficiently and is associated with increased thermal losses to the spark plug electrodes.

Further investigations demonstrate that ignitability in hydrogen engines is strongly governed by early flame kernel development, which is sensitive to in-cylinder flow, fuel-air mixture conditions, and heat losses to the electrodes. By systematically analyzing the interaction between spark ignition parameters, electrode geometries, and operating condition, this work identifies optimal spark ignition control strategies for both biogas and hydrogen engines. These strategies enable robust combustion while minimizing excessive spark energy discharge, thereby reducing spark plug wear and the risk of abnormal combustion phenomena such as pre-ignition.

Overall, this thesis provides new insights into the fundamental physics of spark ignition and establishes a framework for optimized ignition control in heavy-duty engines operating on renewable gaseous fuels. The findings support the development of more efficient, durable, and scalable combustion technologies, contributing to a practical pathway toward sustainable heavy-duty transport.

Key words: Heavy-duty vehicles, Internal combustion engines, Gaseous fuels, Spark ignition, Breakdown-arc, Glow, Spark plasma, Biogas, Hydrogen, Direct injection, Ignitability, Combustion stability, Spark plug wear

Classification system and/or index terms (if any)

Supplementary bibliographical information

Language: English

Number of pages: 100

ISSN and key title: 0282-1990

ISBN: 978-91-90202-31-9 (print) 978-91-90202-32-6) (electronic)

Recipient's notes

Price

Security classification

Signature

Date 2026-04-17

Towards optimized spark ignition for hydrogen and biogas heavy-duty engines

Anupam Saha

LUND
UNIVERSITY

A doctoral thesis at a university in Sweden takes either the form of a single, cohesive research study (monograph) or a summary of research papers (compilation thesis), which the doctoral student has written alone or together with one or several other author(s).

In the latter case the thesis consists of two parts. An introductory text puts the re search work into context and summarizes the main points of the papers. Then, the research publications themselves are reproduced, together with a description of the individual contributions of the authors. The research papers may either have been already published or are manuscripts at various stages (in press, under review, or in draft).

Published by:
Department of Energy Sciences
Faculty of Engineering
Lund University
Lund 2026

ISBN 978-91-90202-31-9 (print)
ISBN 978-91-90202-32-6) (electronic)
ISSN 0282-1990

Printed in Sweden by Media-Tryck, Lund University,
Lund, 2026

Dedicated to spark ignition engines.

Table of Contents

List of publications

This thesis is based on the following publications, referred to by their Roman numerals:

I. **The Influence of Ignition Control Parameters on Combustion Stability and Spark Plug Wear in a Large Bore Gas Engine**
A. Saha, A. Ojanperä, J. Hyvonen, J. Ängeby, J. Tidholm, Ö. Andersson, P. Tunestål
SAE Technical Paper 2023-01-0257, 2023, https://doi.org/10.4271/2023-01-0257

II. **Characterization of Spark Ignition Energy Transfer at Different Phases Using Pressure-Rise Calorimetry**
A. Saha, P. Tunestål, J. Ängeby, Ö. Andersson
SAE Technical Paper 2025-01-8402, 2025, https://doi.org/10.4271/2025-01-8402

III. **High-Speed Optical Diagnostics of Misfire Limits in a Spark-Ignited Heavy-Duty Hydrogen Engine**
P. Hallstadius, **A. Saha**, A. Sridhara, Ö. Andersson
SAE Int. J. Adv. & Curr. Prac. in Mobility 7(5):2383-2397, 2025, https://doi.org/10.4271/2025-01-8401

IV. **Calorimetric Study of the Influence of Spark Ignition System Parameters on the Energy Transfer to the Gas**
A. Saha, P. Tunestål, J. Ängeby, Ö. Andersson
SAE Technical Paper 2025-24-0033, 2025, https://doi.org/10.4271/2025-24-0033

V. **Ignitability Study in a Spark-Ignited Hydrogen Direct Injection Heavy-Duty Engine**
A. Saha, E. Zanjani, J. Engström, P. Tunestål, Ö. Andersson
Will be submitted to *the International Journal of Hydrogen Energy*.

Publications not included in this thesis

i. **Spark Ignition - Searching for the Optimal Spark Profile**
J. Ängeby, **A. Saha**, M. Lundgren, O. Björnsson
Heintzel, A. (eds) Internationaler Motorenkongress 2022. AUDR 2022. Proceedings. Springer Vieweg, Wiesbaden. https://doi.org/10.1007/978-3-658-44740-3_26

Acknowledgements

The completion of this PhD marks the end of a challenging and rewarding journey, which would not have been possible without the support and encouragement of many individuals. I would like to express my sincere gratitude to all those who contributed to the initiation and development of this project, for their trust in my ability to carry it forward and for creating the conditions that enabled its successful completion.

First and foremost, I would like to express my sincere gratitude to my main supervisor, Öivind Andersson. Your critical feedback and clear direction have been extremely valuable throughout this project. You taught me how to approach research questions from a broader scientific perspective—how to define, formulate, and motivate them in a structured and meaningful way. During the early stages of my PhD, when I was developing the spark calorimeter, you gave me the freedom to explore different ideas through trial and error. This trust and flexibility played an important role in shaping both the experimental work and my development as a researcher. I am also especially thankful for your guidance in scientific writing. I still remember working on my first technical paper—your advice helped me understand how to structure and communicate research effectively within a limited time.

I would also like to thank my co-supervisor, Per Tunestål, for all the insightful discussions we had on spark ignition throughout my PhD. I truly appreciated how approachable you were—whether it was about new results, figures, or ideas from the literature. Your support meant a lot, particularly during the early stages of my work when things were not progressing as expected. Your encouragement and perspective helped me stay motivated and move forward. I also appreciate the support from other seniors in the division, including Martin Tunér, Sebastian Verhelst, Marcus Lundgren and Kerstin Sernhed.

I would also like to express my sincere appreciation to my mentors from industry. In particular, I would like to thank Jakob Ängeby and Anders Johnsson from Phinia (formerly SEM AB) for your support throughout my PhD journey. Your guidance was extremely valuable in helping me understand different ignition systems and in deepening my perspective on the spark ignition process through many insightful discussions. I am also grateful to Johan Engström and Djordje Purkovic from Volvo Trucks for all the discussions we had during our weekly progress meetings. Your support during the final experimental campaign at Chalmers University was especially important. Without your support, it would not have been possible, and my thesis would not have been complete.

I would like to thank my colleagues who collaborated with me during some of the experimental campaigns, including Peter Hallstadius and Aravind Sridhara at Lund

University, and Elvin Zanjani at Chalmers University. Your commitment and teamwork were essential for carrying out this work.

My sincere thanks go to all the technicians whose expertise and efforts made the experiments possible, including Anders Olsson and Patrik Johanson at Lund, and Timothy Benham at Chalmers University. A special thanks to Getachew Darge from the IEA department of Lund University for supporting and guiding me with the electrical measurement equipment for spark ignition I needed during my PhD.

I am also grateful to the administrative staff at the department, including Linda Engh, Catarina Lindén, Anders Schyllert, Andrea Frydenlund, and Sissela Silvmarker, as well as our IT specialist, Robert-Zoltán Szász, for their continuous support with practical matters.

To my fellow PhD students and postdoctoral colleagues at the division—Alexandra, André, Axel, Beyza, Brian, Carlos, Christoffer, Frank, Luis, Magnus, Maja, Miaoxin, Mirjam, Menno, Nika, Ola, Peter, Xiufei, Yuxinang, Yachao, and Yannick—thank you for contributing to a friendly, collaborative, and stimulating research environment. I truly appreciate the collegial atmosphere and the friendships that have developed over the years.

To all my colleagues at the department—please forgive me for not naming everyone—thank you for the laughter, the lunch and fika conversations, and the everyday moments that made this journey both lighter and more enjoyable.

Finally, I would like to express my deepest gratitude to my family for their unconditional support throughout this journey. To my mom, dad, and my sister "*Momo*"—thank you for your constant encouragement and for always believing in me. Your support has been the foundation that made this journey possible. Your patience, understanding, and the sacrifices you have made along the way have meant more to me than words can express, and even from afar, your presence has always been a source of strength and motivation. I am especially grateful to my wife, Abantika, for her patience, understanding, and unwavering support during my PhD. Your presence has been my greatest strength through both the challenging and rewarding moments. I would also like to thank my in-laws for their continued support and encouragement. A heartfelt thanks to Subha di, Ananda da, and Rishik for making us feel at home here in Helsingborg, Sweden—your warmth and care created a sense of belonging far away from home.

To those who continue reading this thesis —I hope it makes for an enjoyable and insightful read. Thank you.

Popular science summary

Heavy-duty transport plays a crucial role in the modern society by enabling the movement of goods over long distances and supporting global trade and economic activity. Although this sector represents a relatively small share of the total vehicle fleet, it contributes significantly to the global greenhouse gas emissions. At present, a majority of the heavy-duty vehicles operate with diesel-powered engines, which produce not only CO_2 but also other harmful pollutants that negatively affect the environment and public health. Decarbonizing this sector has therefore become an urgent priority to meet climate targets and reduce environmental impact.

Electrification enables zero tailpipe CO_2 emissions and is often considered a promising pathway to rapidly decarbonize freight transport. However, its application in long-haul transport is not straightforward. Driving a heavy-duty vehicle require large amounts of energy, and batteries capable of providing sufficient range for long-haul freight are heavy and bulky, which can reduce the available payload. They also require extensive charging infrastructure along the roads. Hydrogen fuel cell electric powertrains, on the other hand, have recently gained attention as an alternative, as they can offer longer driving ranges and faster refueling while also producing zero tailpipe emissions. But fuel cell systems are still relatively expensive and technologically complex. While ongoing research focuses on improving both battery-electric and fuel cell solutions, internal combustion engines (ICEs) are expected to continue playing an important role in the transition towards sustainable heavy-duty transportation. Their main environmental challenge lies in the fossil-derived fuels rather than the engine itself. Replacing these fuels with low- or zero-carbon renewable alternatives can enable combustion engines to operate with significantly lower climate impact while maintaining the robustness and high-power output required for heavy-duty applications.

Among the renewable fuels explored for heavy-duty engines, biogas and hydrogen are particularly interesting. Biogas, which mainly consists of methane, can be produced from organic waste and therefore contribute to a more circular use of resources. Hydrogen has also attracted growing interest in recent years because it can be produced using renewable electricity and can offer low greenhouse gas emissions over its life cycle. Both biogas and hydrogen are well suited for use in spark ignition engines, where the fuel-air mixture is ignited by a spark. The spark is a very small and short-lived electrical discharge (similar to lightning) that ignites the mixture and initiates combustion. In spark ignition engines, the spark is provided by a spark plug in the combustion chamber.

Although the spark ignition engine is a well-established technology, it has mainly been developed for passenger cars. In heavy-duty engines, the ignition is more challenging. The spark must be strong enough to ignite the mixture robustly, especially when the engine is operated with a large surplus of air to improve

efficiency and reduce emissions. At the same time, the spark energy must be carefully controlled, as excessive energy can accelerate spark plug wear, increase maintenance frequency and overall operating costs of a vehicle.

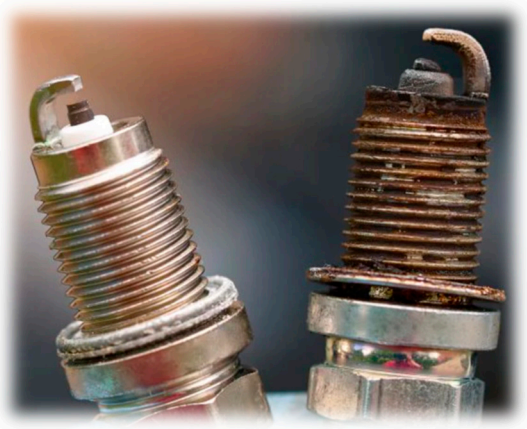

New versus worn-out spark plug. [108]

Ignition becomes even more crucial for hydrogen combustion since it requires an extremely low energy to ignite (one-tenth compared to biogas). Adding higher than necessary electrical energy to the spark plug can overheat the electrodes which become hot surfaces in the combustion chamber. As hydrogen ignites easily on hot surfaces, the hot electrodes can ignite the charge before the spark is fired. This is called pre-ignition and can lead to severe engine damage. For this reason, it is important to optimally control the spark so that it provides the right amount of spark energy to achieve a robust ignition, while avoiding unnecessary energy losses to the spark plug electrodes. Addressing this balance between robust ignition, spark plug wear, and safe engine operation for both hydrogen and biogas heavy-duty engines is the focus of this thesis work. It involves two main stages of research:-

Fundamental insights on spark ignition:

The fundamental aspects of the spark ignition process are studied to understand how electrical energy from the spark is transferred to the surrounding gas to initiate combustion. These investigations are performed under controlled conditions in a specially designed chamber "*calorimeter*" to provide a clearer understanding of the ignition process. The study also examines how the electrical spark interacts with the spark plug electrodes, gaining insights into how spark ignition requirements may change as the spark plug wears over time.

Optimizing spark ignition for biogas and hydrogen engines:

The knowledge gained from the fundamental studies is applied to real engines to develop optimized spark ignition control strategies for heavy duty engines operating on biogas and hydrogen. The investigations explore different engine operating conditions and spark plug geometries to develop knowledge on the ignition requirements over spark plug lifespan. Additionally, this research project also explores different types of spark discharges (AC versus DC) affecting ignitability and spark plug wear.

This thesis work advances the understanding and control of spark ignition in heavy duty engines operating on renewable gaseous fuels such as biogas and hydrogen. By combining fundamental studies with engine-based investigations, this research establishes a foundation that can support the development of more efficient and optimized ignition control strategies for such engines. The findings are relevant for reducing operational challenges such as abnormal combustion and spark plug wear, while maintaining a robust engine performance. At a system level, this work demonstrates how conventional engine technologies can be adapted to operate with cleaner gaseous fuels, supporting a practical and scalable pathway toward sustainable heavy duty transport.

Populärvetenskaplig sammanfattning

Tunga transporter spelar en avgörande roll i det moderna samhället genom att möjliggöra transport av varor över långa avstånd samt stödja global handel och ekonomisk aktivitet. Trots att denna sektor utgör en relativt liten andel av den totala fordonsflottan bidrar den i betydande grad till de globala utsläppen av växthusgaser. I dagsläget drivs en majoritet av de tunga fordonen av dieselmotorer, vilka inte bara genererar koldioxid (CO_2) utan även andra skadliga föroreningar som påverkar miljön och människors hälsa negativt. Att minska koldioxidutsläppen från denna sektor har därför blivit en prioriterad och brådskande åtgärd för att uppnå klimatmål och begränsa miljöpåverkan.

Elektrifiering möjliggör drift utan direkta CO_2-utsläpp och betraktas ofta som en lovande väg för att snabbt minska koldioxidutsläppen från godstransporter. Samtidigt är tillämpningen inom långväga transporter inte okomplicerad. Drift av tunga fordon kräver stora mängder energi, och batterier som kan ge tillräcklig räckvidd för långväga transporter är både tunga och skrymmande, vilket kan minska den tillgängliga lastkapaciteten. De kräver dessutom en omfattande laddinfrastruktur längs vägnätet. Vätgasbaserade bränslecellsdrivlinor har å andra sidan fått ökad uppmärksamhet som ett alternativ, eftersom de kan erbjuda längre räckvidd och snabbare tankning utan direkta utsläpp. Bränslecellsystem är dock fortfarande relativt kostsamma och tekniskt komplexa. Samtidigt som pågående forskning fokuserar på att förbättra både batterielektriska och bränslecellsbaserade lösningar, förväntas förbränningsmotorer fortsatt spela en viktig roll i omställningen mot hållbara tunga transporter. Den huvudsakliga miljöutmaningen är kopplad till de fossila bränslena snarare än till själva motorn. Genom att ersätta dessa bränslen med förnybara alternativ med låga eller inga koldioxidutsläpp kan förbränningsmotorer drivas med avsevärt lägre klimatpåverkan, samtidigt som den robusthet och höga effekt som krävs för tunga tillämpningar bibehålls.

Bland de förnybara bränslen som studeras för tunga motorer är biogas och vätgas särskilt intressanta. Biogas, som huvudsakligen består av metan, kan produceras från organiskt avfall och därmed bidra till en mer cirkulär resursanvändning. Vätgas har också fått ett ökat intresse under de senaste åren, eftersom den kan produceras med hjälp av förnybar el och kan ge låga utsläpp av växthusgaser över hela sin livscykel. Både biogas och vätgas är väl lämpade för användning i gnisttända motorer, där bränsle–luftblandningen antänds med hjälp av en gnista. Gnistan är en mycket liten och kortvarig elektrisk urladdning (liknande blixtar) som initierar förbränningen. I gnisttända motorer genereras gnistan av ett tändstift i förbränningskammaren.

Även om gnisttända motorer är en väl etablerad teknik, har de huvudsakligen utvecklats för personbilar. I tunga motorer är tändningen mer utmanande. Gnistan måste vara tillräckligt stark för att på ett robust sätt antända bränsle–luftblandningen, särskilt när motorn drivs med ett stort luftöverskott för att förbättra

verkningsgraden och minska utsläppen. Samtidigt måste gnistenergin kontrolleras noggrant, eftersom alltför hög energi kan påskynda slitaget på tändstiftet, öka underhållsbehovet och därmed de totala driftkostnaderna för fordonet.

Tändningen blir ännu mer kritisk vid vätgasförbränning, eftersom vätgas kräver en mycket låg energi för antändning (cirka en tiondel jämfört med biogas). Detta gör vätgas mycket känslig för förbränningsrelaterade avvikelser, såsom förtändning och knackning. Om mer elektrisk energi än nödvändigt tillförs tändstiftet kan elektroderna överhettas och fungera som heta ytor i förbränningskammaren. Dessa heta ytor kan i sin tur leda till okontrollerad förbränning och allvarliga motorskador. Av denna anledning är det viktigt att optimera tändningen så att rätt mängd gnistenergi tillförs för att säkerställa en robust antändning, samtidigt som onödiga energiförluster till tändstiftets elektroder undviks. Att hantera denna avvägning mellan robust antändning, slitage på tändstiftet och säker motordrift för både vätgas- och biogasdrivna tunga motorer utgör fokus för detta avhandlingsarbete. Arbetet omfattar två huvudsakliga forskningssteg:-

Grundläggande insikter om gnisttändning:

De grundläggande aspekterna av gnisttändningsprocessen studeras för att förstå hur elektrisk energi från gnistan överförs till den omgivande gasen och initierar förbränning. Dessa undersökningar genomförs under kontrollerade förhållanden i en specialutformad kammare, en så kallad kalorimeter, för att ge en tydligare förståelse av tändningsprocessen. Studien analyserar även hur den elektriska gnistan samverkar med tändstiftets elektroder, vilket ger insikter i hur kraven på tändning kan förändras i takt med att tändstiftet slits över tid.

Optimering av gnisttändning för biogas- och vätgasmotorer:

Den kunskap som erhålls från de grundläggande studierna tillämpas på verkliga motorer för att utveckla optimerade styrstrategier för gnisttändning i tunga motorer som drivs med biogas och vätgas. Undersökningarna omfattar olika driftförhållanden och tändstiftsgeometrier för att skapa förståelse för tändningskrav över tändstiftets livslängd. Vidare studeras även olika typer av gnisturladdningar (AC respektive DC) och deras inverkan på antändbarhet och slitage på tändstiftet.

Detta avhandlingsarbete bidrar till en fördjupad förståelse och förbättrad styrning av gnisttändning i tunga motorer som drivs med förnybara gasformiga bränslen såsom biogas och vätgas. Genom att kombinera grundläggande studier med motorbaserade undersökningar etablerar denna forskning en grund som kan stödja utvecklingen av mer effektiva och optimerade tändstrategier för sådana motorer. Resultaten är relevanta för att minska driftrelaterade utmaningar, såsom okontrollerad förbränning och slitage på tändstift, samtidigt som en robust motorprestanda upprätthålls. På systemnivå visar detta arbete hur konventionella motorteknologier kan anpassas för att drivas med renare gasformiga bränslen, vilket möjliggör en praktiskt genomförbar och skalbar väg mot hållbara tunga transporter.

Abbreviations

GHG	Greenhouse gas emissions
SI	Spark ignition
ICE	Internal combustion engine
HDV	Heavy-duty vehicle
BET	Battery-electric truck
FCET	Fuel cell electric truck
TCO	Total cost of ownership
CAD	Crank angle degree
ICM	Ignition control module
BMS	Battery management system
DC	Direct current
AC	Alternating current
TDC	Top dead center
BDC	Bottom dead center
MBT	Maximum brake torque
IMEP	Indicated mean effective pressure
$IMEP_g$	Gross indicated mean effective pressure
COV	Coefficient of variation
IJT	Injection timing
NO_x	Nitrogen oxides
CA10	Crank angle at 10% mass fraction burnt
CA50	Crank angle at 50% mass fraction burnt
CA90	Crank angle at 90% mass fraction burnt

Chapter 1
Introduction

1.1 Background

Global transportation is one of the major sources of greenhouse gas (GHG) emissions [1]. Although several gases contribute to the greenhouse effect, such as methane (CH_4), nitrous oxide (N_2O), and fluorinated gases, carbon dioxide (CO_2) is the most dominant and is therefore often used as the main indicator when assessing climate impact [2]. Transport sector accounts for about 14% of total CO_2 emissions worldwide as shown in Figure 1a, making it as the fourth largest emitting sectors after electricity generation, agriculture and industry. Within transportation, the heavy duty vehicle (HDV) segment plays a significant role. They are responsible for more than 30% of all transport-related CO_2 emissions, even though they represent a smaller share of the total vehicle fleet (see Figure 1b) [3, 4]. It reflects the high energy demand and long-distance operating patterns of freight trucks, buses, and other commercial vehicles. Therefore, decarbonizing the heavy duty transport sector has become an urgent global priority [5].

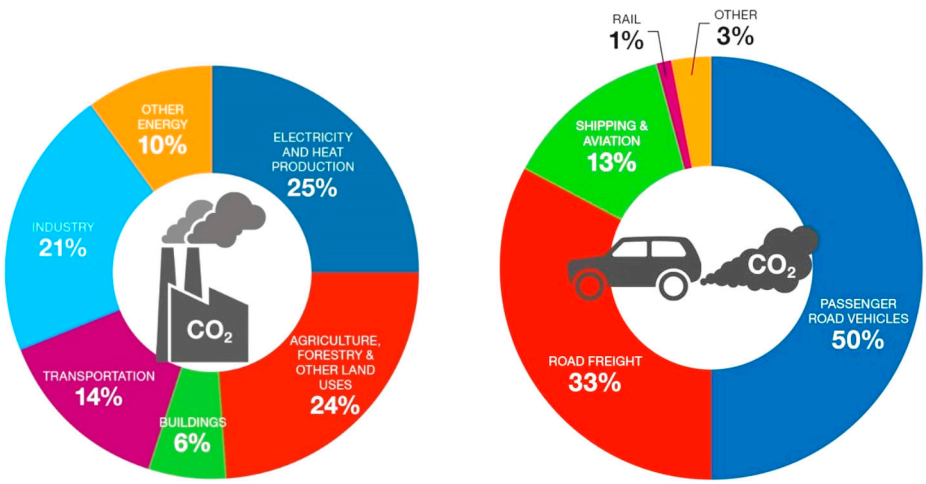

Figure 1a: Global CO2 emissions by sectors. [4]
Figure 1b: Global CO2 emissions from different transport modes. [4]

In Europe, transport sector accounts for about a quarter of total CO_2 emissions, and more than 70% of these emissions come from road transport [6]. Heavy-duty vehicles make up a significant share of this, as shown in Figure 2 [7]. Projections indicate that in the absence of strong policy interventions or technological transitions, CO_2 emissions from heavy duty transport are expected to increase significantly between 2010 and 2030, driven by economic growth, rising freight demand, and expanding logistics networks. This reinforces the critical need for scalable, carbon-neutral propulsion solutions tailored specifically to heavy duty applications [8].

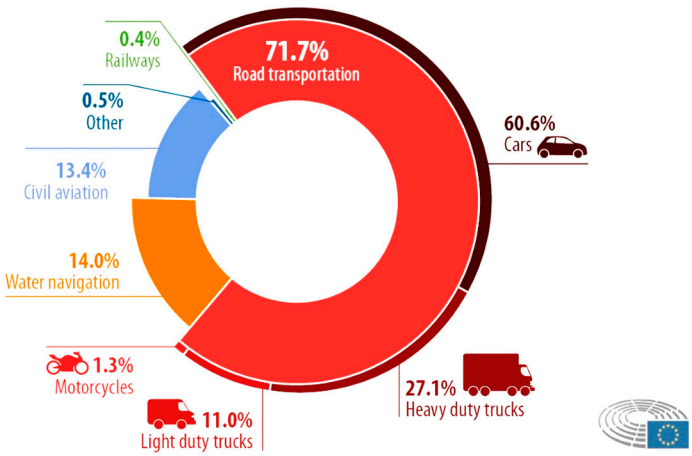

Figure 2: Share of GHG emissions in EU for different transport modes in 2019. [7]

To address this, the European Commission introduced strict policies to reduce GHG emissions from the transport sector as part of the European Green Deal. The commission adopted its first CO_2 regulation for new HDVs in 2019. The regulation requires manufacturers to reduce the average fleet CO_2 emissions by 15% from 2025 and 30% from 2030, compared to 2019 levels [8, 9]. In 2023, the European Commission has proposed a revision of the regulations, aiming for even faster emission reductions. As shown in Figure 3, the new proposal sets much stricter targets: 45% CO_2 reduction by 2030, 65% by 2035, and 90% by 2040. These revised targets showcase the EU's clear intention to accelerate the decarbonisation of heavy duty transport and strengthen the development and adoption of zero-emission mobility in Europe [10].

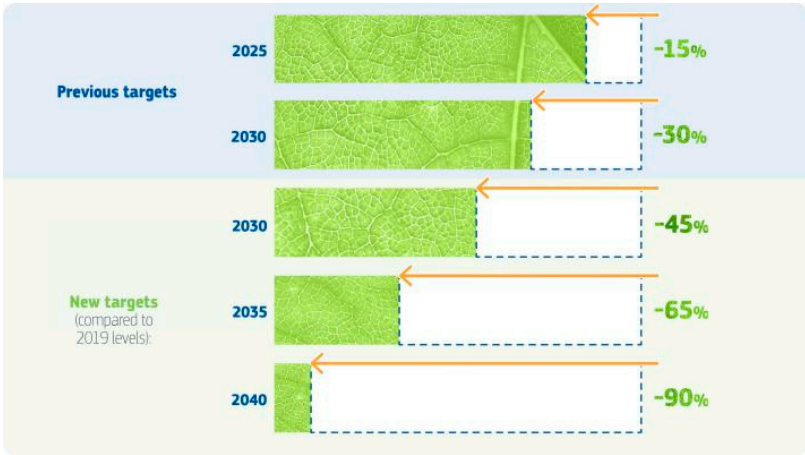

Figure 3: Proposed CO2 emissions standards for HDVs by European Commission in 2023. [10]

Electrification is widely regarded as a key pathway toward achieving climate-neutral transport, primarily due to its high energy efficiency and the absence of tailpipe emissions [11]. Battery electric trucks (BETs) offer a simple and efficient powertrain solution and are particularly well suited for short- and medium-distance transport. However, their application in long-haul heavy-duty transport still remains challenging due to the high energy demand, which requires large and heavy battery packs, as well as limitations in charging infrastructure and operational downtime due to long charging times [12, 13].

Fuel cell electric trucks (FCETs), on the other hand, are gaining increasing attention as an alternative solution for long-haul applications. In FCETs, hydrogen is converted to electricity through an electrochemical process, with water as the only direct by-product [14]. They offer longer driving range and short refueling times, while maintaining relatively high fuel efficiency at low-to-medium loads. However, FCETs are currently associated with high cost, primarily due to the use of platinum-based catalysts. In addition, they require a steady supply of high-purity hydrogen, as impurities can degrade performance over time [15]. Moreover, thermal management is also challenging due to the relatively low operating temperature of fuel cells, which necessitates large radiators for cooling. These factors increase system complexity, cost, and overall vehicle weight [16–18].

Internal combustion engine (ICE) powertrains remain a practical and widely used solution for heavy-duty transport, particularly in long-haul applications. They offer high power density, robust operation, and fast refueling, making them well suited for high-load and long-distance operations. In addition, ICE technology benefits from a mature technology base, and a well-established global fuel supply and refueling infrastructure. However, ICEs rely primarily on fossil fuels, resulting in significant emissions of CO_2 and air pollutants such as nitrogen oxides (NOx) and

particulate matter. These emissions represent a major limitation of ICE technology under increasingly stringent environmental regulations [19, 20].

In short, no single technology can meet all the needs of today's heavy-duty transport while complying with strict emissions legislation. BETs work well for short and regional routes, while FCETs offer longer range but still face challenges with upfront cost, and system complexity [21]. While conventional ICEs are associated with significant emissions, it is important to note that a substantial share of these emissions originates from the use of fossil-derived fuels rather than the engine technology itself. Because of this, the author believes that ICEs using alternative gaseous fuels, particularly both hydrogen and biogas will play an important role for long-hauled transportation for the foreseeable future, particularly where full electrification is impractical.

One of the main advantages of biogas and hydrogen is that they can greatly reduce, or even remove, CO_2 emissions during engine operation [22, 23]. This is primarily because both fuels can be produced from renewable energy sources. Biogas can be made by anaerobic digestion of organic waste or by methanation using captured CO_2 while hydrogen can be produced through water electrolysis powered by renewable electricity [24–26].

An interesting property of both biogas and hydrogen is their high octane rating, making them suitable as fuels for spark ignition (SI) engines. [27–29]. In SI engines, the air–fuel mixture is ignited by a spark plug. The spark creates a small flame kernel, which then propagates through the unburned mixture until it reaches the chamber walls and extinguishes [30, 31]. One of the challenges in improving the thermal efficiency of an SI engine is to keep combustion stable, especially when the mixture is too lean or diluted. Combustion stability is important for engine performance and is often measured using the coefficient of variation of IMEP (COV_{IMEP}). A robust ignition process is therefore essential, since higher COV_{IMEP} decreases efficiency and increases noise, vibrations, and harshness (NVH) [32, 33].

1.2 Motivation

Achieving a robust ignition is challenging for both biogas and hydrogen SI engines. These engine often operate at very lean or diluted conditions to improve efficiency and reduce emissions, which makes flame kernel formation more sensitive to the spark characteristics. Ignitability becomes even more difficult to achieve in hydrogen engines. This is primarily due to the higher breakdown voltage required for spark initiation, which results from the elevated gas pressure and density at the time of ignition. These conditions arise from several factors, including the high boost levels needed to achieve the desired load under lean operation, the use of higher compression ratios compared to biogas engines, and the faster flame speed

of hydrogen, which brings the maximum brake torque (MBT) timing closer to top dead center (TDC) [28, 34].

There is a widespread assumption that ignitability is directly related to the spark energy. However, when a stable flame kernel has already formed, adding more energy to the spark may not improve ignitability. Recent studies show that a very short spark delivering approximately 6 mJ of spark energy, is enough to ensure stable combustion in biogas engines under many operating conditions [32, 35]. While the minimum energy threshold has not been determined, studies indicate that using more-than-necessary spark energies lead to increased spark plug wear [36]. High spark energies raise the temperature of the electrodes and accelerate erosion, which shortens the service life of the spark plug. Apart from a short service lifetime, contemporary high-endurance spark plugs are often expensive due to the use of precious metals like platinum and iridium on their electrodes [36–38].

Spark energy becomes even more critical in hydrogen engine operation [39]. Hydrogen has a very low minimum ignition energy but a high auto-ignition temperature. Its minimum ignition energy is roughly ten times lower than that of methane [40]. This makes hydrogen more sensitive to pre-ignition–unintended ignition that could catastrophically damage the engine. Pre-ignition can be triggered by hot spark plug electrodes or even by residual spark energy released from the ignition system [41, 42].

Therefore, we need a better understanding of the spark ignition process for both biogas and hydrogen fueled ICEVs. This knowledge is essential for designing optimal spark ignition strategies that improve ignitability across different operating conditions. At the same time, these strategies must avoid excessive heating of the spark plug electrodes. By doing so, we can suppress abnormal combustion events, limit spark plug wear while ensuring robustness in future gaseous-fueled ICEs.

1.3 Scope and approach

This thesis focuses on improving the understanding of spark ignition process in heavy-duty SI engines operating on hydrogen and biogas. In particular, the work addresses key challenges related to ignitability, combustion stability, and spark plug wear for a wide range of operating conditions, with particular emphasis on lean and high-load operation, as well as suppression of combustion anomalies in hydrogen engines.

To achieve this, multiple experimental platforms are used. Fundamental investigations of the spark ignition process are carried out using a spark calorimeter, while a dedicated constant-volume chamber is used to study spark plug wear. Ignitability studies of hydrogen and biogas are utilized in two different single-

cylinder engine test benches at different operating conditions. In addition, an optical engine is employed to investigate misfire mechanisms and the role of spark ignition parameters in premixed hydrogen combustion at ultra-lean operations.

The research is presented through a number of scientific publications, which form the core of this thesis. Each paper contributes a specific perspective to the overall goal of understanding the spark ignition process with an aim towards designing optimized spark ignition control strategies for hydrogen and biogas heavy-duty engines.

Chapter 2
Heavy-duty vehicles (HDVs)

The HDVs market encompasses large vehicles primarily designed for transporting goods and passengers over long distances. These vehicles include trucks, buses, and trailers used in logistics, construction, and public transportation sectors. The market's significance lies in its crucial role in global trade and infrastructure development, enabling efficient movement of raw materials, finished products, and people. Its share is increasing throughout the world because of globalization, rising incomes, and shifting patterns of production and consumption [43].

There is growing interest in shifting to zero tailpipe CO_2 emissions HDVs in response to the expected growth of freight demand and the contribution of trucks to air pollution and GHG emissions [43]. However, their powertrain must satisfy several demanding requirements due to the operating conditions of these vehicles.

2.1 Powertrain requirements of HDVs

The requirements for HDVs' powertrains depend strongly on the operating conditions and duty cycles of the vehicles. Long-haul trucks typically operate over long distances under relatively steady and high load conditions, which requires powertrains capable of delivering high torque, high efficiency, and long service life. In contrast, urban and regional freight vehicles operate under more transient conditions with frequent stop–start operation and lower average loads. In such applications, fast dynamic response, and low noise become more important. In addition, short refueling or recharging times are essential to maintain high vehicle utilization in urban freight transport. Table 1 summarizes the key powertrain requirements for both long-haul and urban heavy-duty vehicle applications [44, 45].

Table 1: Powertrain requirements for long-haul and urban HDVs. [44, 45]

Requirement	Long-haul hdvs	Urban / regional hdvs
Driving distance	Very long range	Short to medium range
Engine load	High and steady	Highly transient
Tank-to-wheel efficiency	Very critical	Important but less dominant
Refueling / charging time	Very low	Short–moderate
Powertrain durability	Very high	High
Emission constraints	Very strict	Very strict (zero emissions)
Noise	Moderate-to-low	Very low (urban driving)

2.2 Battery electric powertrains

Battery electric HDVs are considered as one of the main technological pathways for decarbonizing the freight transport sector [11]. In battery electric HDVs, propulsion is provided by one or more electric motors powered by the energy stored onboard battery packs.

Lithium-ion batteries are commonly used due to their relatively high energy density compared to other battery types (as shown in Figure 1), high energy efficiency, and long lifespan. A typical battery electric powertrain consists of a battery pack, a power electronics unit such as a DC/AC inverter, and one or more electric motors [45, 46]. Compared with IC engines, battery electric powertrain configuration is mechanically simpler because it contains fewer moving components and hence, they operate noise-free. In addition, this simplicity can reduce maintenance requirements and improve overall system efficiency [47]. Furthermore, many battery electric vehicles employ regenerative braking systems that recover part of the vehicle's kinetic energy during deceleration and store it back in the battery, which can improve the overall energy efficiency [48].

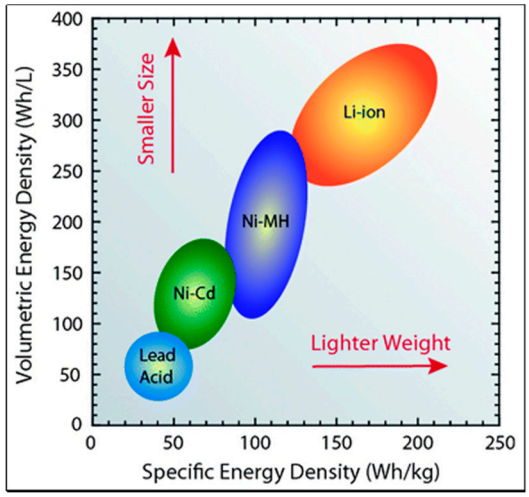

Figure 4: Energy densities of different battery technologies. Adapted from [49].

Battery-electric HDVs offer several advantages for freight transport. They produce zero tailpipe CO_2 emissions during operation and generally exhibit tank-to-wheel energy efficiency close to 70%, which is substantially higher than that of IC engines [50]. Additionally, battery electric HDVs benefit from the operating characteristics of electric motors. Electric motors can deliver instantaneous torque at vehicle start. This characteristic improves drivability, particularly when transporting heavy loads or operating on steep gradients. As a result, electric powertrains can provide smooth and responsive acceleration without the need for complex multi-gear transmissions [51].

Despite these advantages, several challenges remain for the widespread adoption of battery electric powertrains in heavy-duty vehicles. One major limitation is the relatively low specific energy of current battery technologies in comparison to different fuels (see Figure 2), which often requires large and heavy battery packs to achieve long driving ranges. For long-haul freight applications, the battery capacity required to achieve ranges of several hundred kilometers can result in significant additional vehicle weight, which may reduce the available payload capacity [52].

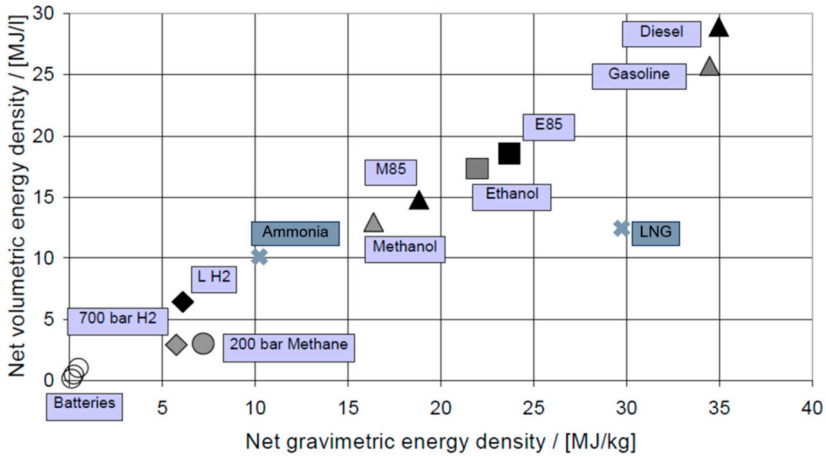

Figure 5: Net volumetric energy density versus gravimetric energy density of different fuels. [53]

In addition, charging times for large battery systems can be long, particularly when high-capacity batteries are used in HDVs. Although high-power charging systems with power levels approaching 1 MW have been proposed to significantly reduce charging time, rapid charging may accelerate battery degradation, hence, shortening overall battery life [54]. This is particularly critical for HDVs as they are expected to operate over long service lifetimes under demanding duty cycles. Accelerated degradation may therefore necessitate battery replacement during the vehicle lifetime, which can significantly increase the total cost of ownership (TCO).

Operating under high charging powers also requires advanced battery management systems (BMS) to ensure safe and reliable operation. The BMS must continuously monitor and regulate cell voltage, temperature, state of charge and state of health during high-power charging and discharging conditions to prevent conditions that may lead to thermal runaway and accelerated battery degradation [55]. This task becomes increasingly challenging as battery capacity and system complexity increase for HDVs.

Furthermore, the large-scale deployment of charging infrastructure for electric HDVs can introduce challenges for existing power grid infrastructure. Studies have shown that simultaneous charging of a relatively small fraction of electric HDVs can lead to voltage violations and reliability issues in transmission and distribution networks, highlighting the need for significant grid upgrades to support widespread electrification [56]. In addition, the selection of battery chemistry introduces further trade-offs between energy density, cost, lifetime, and safety. For example, lithium iron phosphate (LFP) batteries can offer improved durability and safety but lower energy density, whereas nickel manganese cobalt (NMC) batteries can provide

higher energy density at the expense of higher cost and potentially reduced lifetime [107].

Because of these limitations, battery electric HDVs are currently considered more suitable for short-distance or urban freight transport where driving distances are relatively limited and charging opportunities are more accessible. In such applications, the required driving range is typically lower than in long-haul transport, allowing the use of smaller battery capacities. This can reduce the additional vehicle weight associated with large battery packs and may improve the overall feasibility of battery electric powertrains for urban and regional freight operations [44]. However, ongoing researches are focused on improving battery energy density, developing fast-charging technologies, and optimizing BMS to expand the applicability of battery electric powertrains in the long-hauled freight transport sector.

2.3 Hydrogen fuel cell electric powertrains

Fuel cell electric powertrains operate similarly to battery-electric powertrains as both systems use electric motors for vehicle propulsion. Unlike BETs which store electrical energy in batteries, FCETs generate electricity onboard using a hydrogen fuel cell system. In FCETs, hydrogen stored in high-pressure tanks is supplied to a fuel cell stack, where it reacts electrochemically with oxygen from the air to produce electricity, heat, and water. The generated electricity is then used to power the electric motor that drives the vehicle, while water is released as the only by-product at the tailpipe. Proton exchange membrane fuel cells (PEMFCs) are the commonly used fuel cell technology in automotive applications due to their relatively low operating temperature and high power density [57].

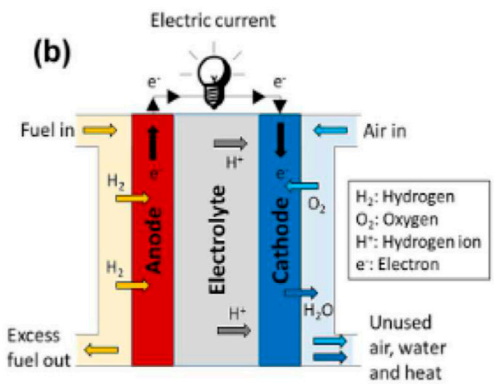

Figure 6: Schematic of a Proton Exchange Membrane Fuel Cell. [58]

FCETs offer several key advantages over battery-electric powertrains, which makes them suitable for long-haul freight transportation. In the first place, hydrogen offers high gravimetric energy density compared to batteries (see Figure 1), which allows fuel cell trucks to achieve long driving ranges comparable to H_2-ICE trucks. In addition, hydrogen vehicles can be refueled within a few minutes, like conventional ICE trucks, which helps maintain high vehicle utilization in freight transport. Furthermore, electricity is generated electrochemically in the fuel cell without a combustion process, and hence, FCETs produce zero tailpipe emissions during operation [58].

Fuel cell systems typically provide relatively high energy conversion efficiency compared to ICEs, particularly at part- to medium-load operations. The electrochemical conversion of hydrogen to electricity in a fuel cell stack typically achieves efficiencies of around 50–60% at such operating conditions. However, at higher loads, the efficiency of the fuel cell stack may decrease due to increased voltage losses at higher current densities and may approach the efficiency levels of conventional ICEs. Nevertheless, when combined with the high efficiency of electric motors, fuel cell powertrains can still achieve higher overall efficiencies than ICE powertrains [59].

While fuel cell electric powertrains offer several advantages, their widespread application in long-hauled transportation is still associated with important challenges. One of the main limitations is the relatively high cost of fuel cell systems, which is largely attributed to the use of precious metal catalysts such as platinum for PEMFC due to its good catalytic activity, stability to withstand the operating environment and resistance to corrosion. This results in a significant increase in the cost of ownership of the FCETs compared to ICE trucks [58]. In addition, PEMFCs require hydrogen of very high purity of greater than 99.9% to ensure reliable operation, since impurities such as carbon monoxide or sulphur compounds in the gas can poison the catalyst and significantly reduce fuel cell performance and lifespan [60].

Furthermore, FCETs typically requires an effective thermal management. Because PEMFCs operate at relatively low temperatures, the generated heat is low-grade (usually 60–100^{o}C), which makes heat rejection more difficult and requires relatively large cooling systems to dissipate the waste heat. Such cooling systems can increase vehicle weight, require additional packaging space, and add complexity to the overall powertrain system [61]. Finally, fuel cell systems have a limited capability to respond to rapid load transients. Sudden changes in power demand may lead to voltage fluctuations and can accelerate degradation of the fuel cell stack. Therefore, modern FCETs typically incorporate auxiliary energy storage systems, such as batteries, that handle transient power demands while allowing the fuel cell to operate in a more stable and efficient load range [62].

Above all, the large-scale adoption of FCETs is limited by the availability of hydrogen refueling infrastructure. At present, hydrogen infrastructure is still in an early stage of development and remains a potential barrier for hydrogen-powered transportation. Studies indicate that by the end of 2018 there were only about 370 hydrogen refueling stations in operation worldwide, with most of them located in Europe, Japan, and North America. Half of the refueling stations are currently accessible while the others are used mainly for research or demonstration purposes. Therefore, the expansion of hydrogen mobility requires the development of a much larger network of refueling stations. A typical hydrogen refueling station is a complex system consisting of several components, including hydrogen production units, purification systems, compressors, storage tanks, hydrogen gas boosters, cooling units, and dispensing equipment. The installation of such infrastructure requires substantial investments and coordinated development of hydrogen production, distribution, and refueling systems, which continues to represent a major challenge for the widespread deployment of all hydrogen-powered HDVs [63].

2.4 Internal combustion engines

Heavy-duty long-haul transportation is often considered one of the most difficult segments of the road transport sector to fully electrify due to the high energy demand associated with long driving distances and high payload requirements. Consequently, ICE powertrains are expected to remain an important solution for long-haul freight transport despite the rapid development of electrified powertrains. Compared with battery-electric and fuel cell powertrains, ICEs benefit from a mature and well-established technology base, together with a highly developed global fuel supply and refueling infrastructure.

In addition, ICE powertrains provide high power density and robust operation, allowing them to deliver the large power outputs required for heavy-duty applications while remaining relatively insensitive to variations in fuel quality. ICEs can also operate reliably under a wide range of ambient conditions, including both very low and very high temperatures, and are generally less sensitive to environmental conditions compared to battery-electric and fuel cell powertrain technologies.

Furthermore, ICEs are manufactured using widely available and recyclable materials, and their production, maintenance, and service infrastructure is already well established worldwide. This contributes to a significant reduction in the TCO of the vehicle – an important requirement for HDVs. Another important advantage is the fuel flexibility of ICEs, as they can operate on a wide range of fuels including conventional fuels, biofuels, synthetic fuels, and hydrogen, enabling their potential role in decarbonization of heavy-duty transportation systems [64, 65].

ICEs also play a dominant role in other sectors that are hard-to-electrify, for instance, maritime transportation and large-scale power generation [66]. Marine transport relies almost entirely on IC engines for propulsion due to their ability to deliver high power output, long operational range, and reliable performance required for long-distance shipping. Although several alternative propulsion technologies are currently being investigated, ICEs are expected to remain widely used in marine applications for the foreseeable future, potentially operating with low-to-zero carbon fuels such as biogas, ammonia, or hydrogen. In addition to transportation, ICEs are commonly used as power gensets for electricity generation. These gensets can respond rapidly to fluctuations in electricity demand and variations in renewable energy production, thereby supporting grid stability and reliability. These operational requirements make ICEs particularly irreplaceable in such applications, highlighting their continued importance in several critical sectors.

However, ICEs face an important challenge – tailpipe emissions of greenhouse gases and air pollutants from the combustion process. Conventional ICE powertrains predominantly operate on fossil-derived fuels such as diesel and gasoline, which leads to significant carbon dioxide (CO_2) emissions during operation. In addition to CO_2, combustion engines also produce nitrogen oxides (NO_X), particulate matter, and unburned hydrocarbons that negatively affect air quality. These emissions represent a major drawback of ICE technology and have led to increasingly strict emission regulations in the transportation and power generation sector [19, 20].

However, it is important to note that a major portion of the carbon emissions associated with ICEs originates from the fossil nature of the fuels rather than from the engine technology itself. By replacing conventional fossil fuels with renewable alternatives such as biogas or hydrogen, the overall greenhouse gas emissions from ICE-based powertrains can be significantly reduced.

2.5 Renewable fuels

Renewable fuels are increasingly considered as an important pathway to reduce greenhouse gas emissions from ICEs. In general, renewable fuels are produced from sustainable resources such as biomass, renewable electricity, or other non-fossil energy sources, and therefore offer the potential to significantly lower lifecycle carbon emissions compared with conventional fossil fuels. In recent years, renewable gaseous fuels, particularly biogas and hydrogen, have gained significant interests as potential alternatives to conventional fossil fuels in ICEs [67]. The following subsections therefore focus on these two fuels and their key properties relevant to ICE operation.

2.5.1 Biogas

Biogas has gained increasing attention as a renewable gaseous fuel for ICEs in recent years, primarily due to the wide availability of organic feedstocks and its potential to reduce greenhouse gas emissions. Biogas can be produced from organic waste streams such as agricultural residues, manure, sewage sludge, and food waste through anaerobic digestion processes [68]. Biogas is primarily composed of methane along with some ethane, propane, nitrogen, and CO_2. Since, it has a chemical composition like natural gas, biogas allows its use in existing natural gas engine technologies with minor modifications [69].

However, biogas exists in gaseous form under normal conditions and therefore has relatively low energy density in its non-compressed state. To improve its energy storage characteristics, biogas can be either compressed to high pressures (typically around 200 bar) as compressed biogas or liquefied at approximately −162 °C to produce liquefied biogas, which significantly increases its volumetric energy density [70]. Biogas also present environmental challenges when used in ICEs – unburned methane emissions, commonly referred to as methane slip. Methane is a 25 times more potent GHG than CO_2 and hence, it is of serious concern [71, 72].

In this thesis, pure methane was used to represent upgraded biogas. While methane captures the main combustion characteristics of upgraded biogas, it does not account for the effects of CO_2 dilution and other impurities present in raw biogas. Consequently, the results should be interpreted with this limitation in mind.

2.5.2 Hydrogen

In recent years, hydrogen has gained significant attention as a potential fuel for internal combustion engines due to its potential for low lifecycle greenhouse gas emissions, particularly when produced from renewable electricity through water electrolysis. In this context, hydrogen is often referred to as “green hydrogen” [73]. Hydrogen also serves as a fundamental building block for many synthetic fuels, commonly referred to as e-fuels. Compared with other synthetic fuels, hydrogen production involves fewer processing steps, which can result in more efficient power-to-fuel conversion pathways.

Hydrogen contains no carbon atoms, and therefore its combustion theoretically eliminates carbon-based emissions such as CO, CO_2, and soot. In practice, experimental studies have reported trace amounts of these emissions, which are typically attributed to the presence of lubricating oil entering the combustion chamber. However, the primary emission concern during hydrogen combustion is NOx, which can be mitigated through appropriate combustion strategies and exhaust after-treatment technologies [74, 75].

Despite these advantages, hydrogen also presents important challenges related to storage and distribution. Under ambient conditions hydrogen has a very low volumetric energy density. To increase its storage density, hydrogen is typically compressed to high pressures ranging from 200 to 700 bar or liquefied at cryogenic temperatures around −253 °C [76]. These storage and transportation requirements introduce additional technical complexity and cost, which currently remain important challenges for the large-scale deployment of hydrogen as a fuel.

2.5.3 Properties of biogas and hydrogen

Both biogas and hydrogen are particularly suitable for spark ignition (SI) engines due to their high octane rating and high autoignition temperature, which provide excellent resistance to engine knock. Table 1 summarizes a comparison of important fuel properties of methane (the main constituent of biogas) and hydrogen. Hydrogen exhibits a wide flammability range and high laminar burning velocity, as shown in Table 2, which enables hydrogen engines to operate under significantly leaner conditions compared to methane.

Table 2: Net volumetric and gravimetric density of different fuels [75, 77, 78]

Property	Hydrogen	Methane
Research Octane Number (RON)	> 130	120
Lower heating value (MJ/kg)	120	50
Minimum ignition energy at λ = 1 (mJ)	0.02	0.28
Self-ignition temperature at λ = 1 (K)	858	873
Flammability limits in air (vol%)	4 – 75	5 – 15
Flammability limits (λ)	10 – 0.14	2 – 0.6
Laminar burning velocity at λ = 1 (cm/s)	290	48

To summarize, HDVs require powertrains that can deliver high efficiency, durability, long driving range, and rapid refueling or recharging. Both battery-electric and fuel cell electric powertrains offer important pathways toward zero tailpipe emissions, but they still face limitations in long-haul applications related to energy storage, infrastructure, cost, and system complexity. Internal combustion engines therefore remain a practical and competitive solution, particularly when operated with renewable gaseous fuels such as biogas and hydrogen. These fuels can significantly reduce lifecycle greenhouse gas emissions while retaining the robustness, high power output, and operational flexibility required for heavy-duty transport. Since both hydrogen and biogas are well suited for spark ignition operation, the following chapter focuses on the fundamentals of spark ignition for such applications.

Chapter 3
Spark ignition

Ignition plays a very important role in all SI-ICE applications. It is an energy-exchange phenomenon where electrical energy, in the form of a spark plasma, is converted to thermal energy that is transmitted to the fuel-air mixture present in the spark plug electrode gap to ensure a successful initiation of the combustion process [79, 35]. The energy discharged at the gap provides a local rise in temperature of the fuel-air mixture to several thousand Kelvin, hence exceeding auto-ignition temperature of the fuel. The auto-ignition temperature triggers breakdown of hydrocarbon chains (by reaching the activation energy of the fuel) and the charge possesses sufficient internal energy to oxidize carbon and hydrogen into CO_2 and water in the vapour state [80].

3.1 Phases of spark

Every spark discharge event undergoes three distinctive phases:

- Breakdown
- Arc
- Glow

Initially, the gas volume within the electrode gap represents a perfect insulator. Once the circuit is triggered to stop charging the ignition coil, the voltage across the spark plug electrode gap rises rapidly but no spark is present yet. This is the pre-breakdown stage where random electrons gain energy in the rising electric field and therefore are accelerated towards the anode. As soon as the applied electric field reaches sufficiently high values (5-10 kV/mm in air and ambient conditions), the field-accelerated electrons ionize the fuel-air molecules by collisions and generates additional electrons and ions like an avalanche, also known as the impact ionization effect [81, 82]. Once this avalanche becomes self-sustained, the spark discharge enters the breakdown phase, as shown in Figure 7.

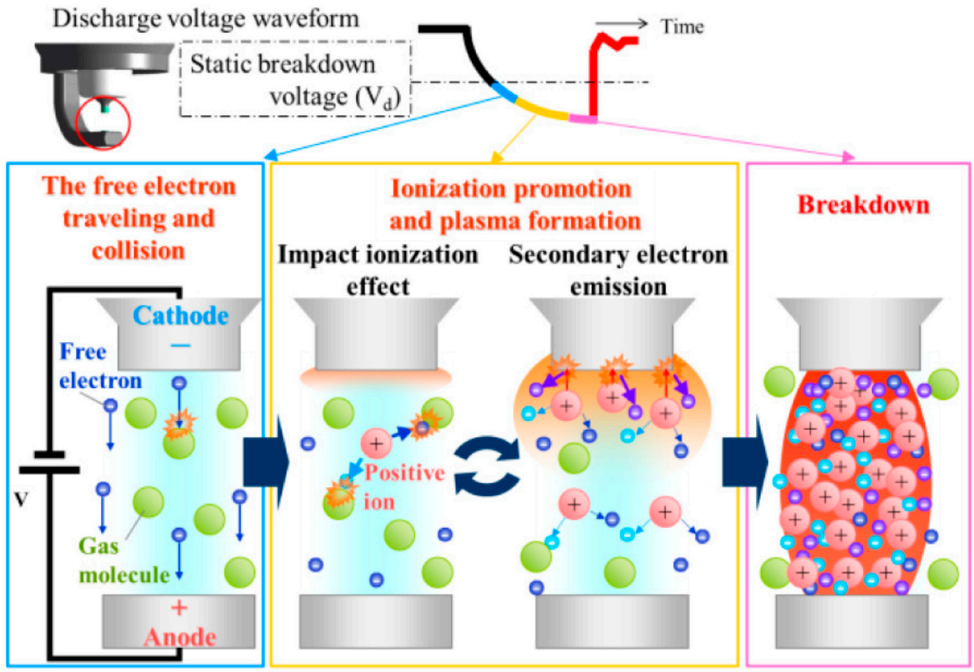

Figure 7: Schematic of spark discharge formation mechanism during pre-breakdown stage. [82]

Breakdown

Breakdown is the abrupt formation of a highly conductive plasma channel across the spark plug electrodes' gap. This is the phase where plasma starts to become visible between the gap. This phase has a duration on the order of tens of nanoseconds and requires a voltage of 10 kV or higher. Figure 8 shows the distribution of spark voltage over time at different phases during a spark event. The breakdown voltage is linearly dependent on the in-cylinder gas pressure and the electrode gap, according to Paschen's law. During the breakdown phase, the plasma temperature can rise to 60,000 kelvin, while the current can rise to several hundred amperes. The end of breakdown is marked by the formation of a conductive plasma channel, and the electrodes are heated up due to the intense energy flux, which leads to the next phase, the arc phase [28].

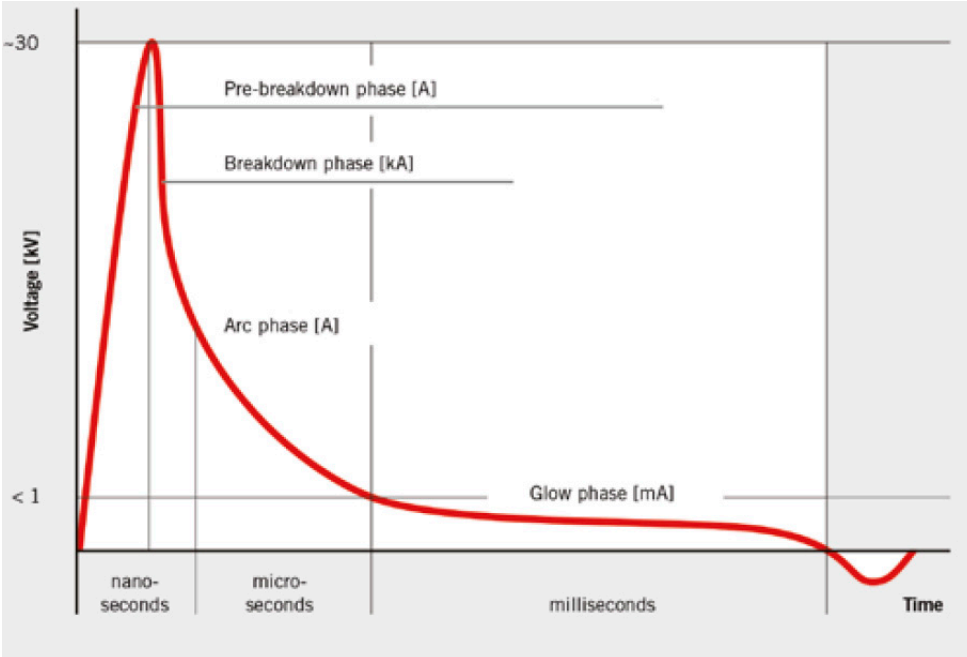

Figure 8: Distribution of spark voltage over time at different phases during a spark event.

Arc

The arc phase is characterized by a highly conductive thin plasma where the heated cathode during the breakdown phase emits thermionic electrons and supply a large electron current. Here, the current typically ranges from 10 to 20 A, primarily supplied by the parasitic capacitances in the spark plug and ignition coil extension. As a result, the voltage needed to sustain the discharge is low (see Figure 8) and the temperature of the plasma falls to below 10,000 K. The arc phase typically lasts for a few microseconds after the breakdown [28, 83].

Glow

As the energy stored in the parasitic capacitances is depleted, the spark discharge finally transitions into the glow phase. The primary mechanism of sustaining the plasma during this phase becomes secondary electron emission from the cathode by photons or ions, rather than thermionic emission [**83**]. The current typically decreases from 10 to 200 mA and hence, the voltage drop near the cathode increases and becomes much higher to sustain the current. During the glow phase, the current is supplied by the ignition system through the primary and secondary coil windings. A strong enough glow current is required to sustain the plasma channel. In the presence of turbulence, the plasma channel is stretched by the surrounding flow field, forming a bow-shaped trajectory. A higher glow current

can sustain a longer plasma than a lower current, increasing the flame kernel area, which in turn is expected to increase the capability to trigger a self-sustained combustion [84 – 88].

The ability to ignite a fuel–air mixture depends on the characteristics of the spark discharge, which in turn depends on the ignition system that generates and controls the spark. An overview of the ignition systems relevant to this thesis work is presented in the following section.

3.2 DC inductive spark

Conventional ignition systems typically produce a unidirectional spark discharge, commonly referred to as a DC spark. In this type of discharge, the current flows in a single direction across the electrode gap. As a result, one electrode remains the cathode while the other acts as the anode throughout the spark duration [84]. One of the most widely used ignition systems in SI-ICE applications is the DC inductive discharge ignition (IDI) system. A schematic representation of this system is shown in Figure 9.

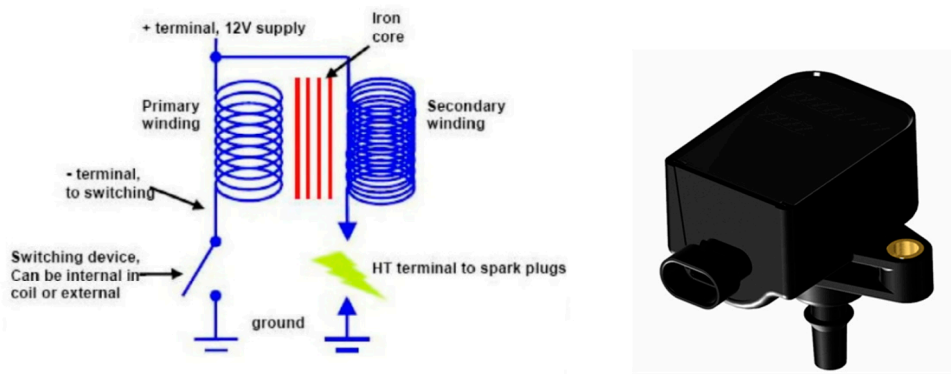

Figure 9: DC inductive system. Left: Schematic diagram. Right: Typical DC inductive coil. [89]

In this type of ignition system, electrical energy is stored in the magnetic field of an ignition coil consisting of a primary and a secondary winding. The energy stored in the coil is controlled by the dwell time, which is the duration during which current flows through the primary winding from the battery or power supply. During this period, the magnetic field in the coil gradually increases. When the current is suddenly interrupted by triggering the ignition pulse, the magnetic field collapses rapidly and induces a high voltage in the secondary winding. This high voltage initiates the spark discharge across the spark plug gap [90].

The dwell time is the only control parameter in an IDI system. In practice, the maximum available voltage required to initiate a spark increases with longer dwell time. However, a longer dwell time also increases the energy stored in the ignition coil. This results in higher spark current and longer spark duration during the discharge. Consequently, a very high spark energy is discharged across the electrode gap, which can often exceed the energy required to achieve a robust combustion [90]. Figure 10 shows typical spark voltage and current waveforms of a DC inductive spark at different dwell times.

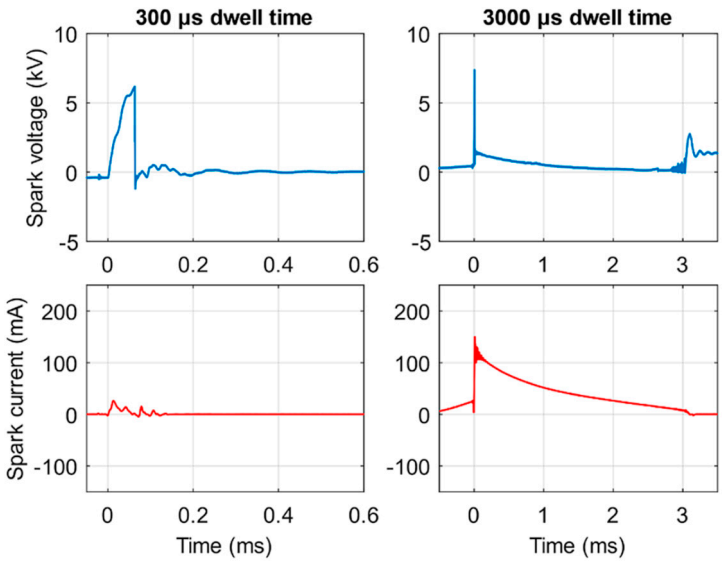

Figure 10: Examples of spark voltage and current waveforms of a DC inductive ignition system at 300 µs and 3000 µs dwell times.[Paper III].

3.3 AC capacitive spark

Unlike conventional DC sparks, an alternating-current (AC) spark periodically changes the polarity of the electrodes. As a result, the current flows in both directions across the spark gap, resulting in a bidirectional discharge. Figure 11 shows typical spark voltage and current waveforms produced by an AC capacitive ignition for spark durations of 70 µs and 500 µs. In both cases, the spark current was maintained at 100 mA.

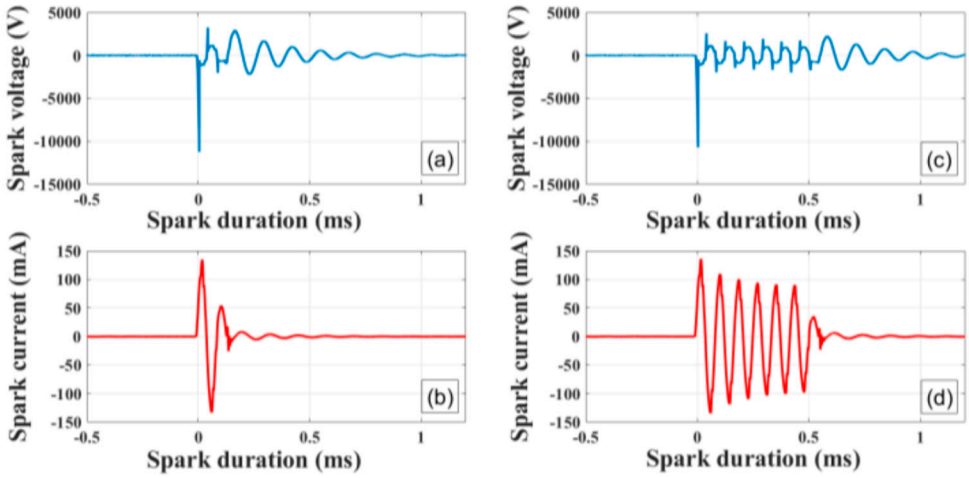

Figure 11: Examples of spark voltage and current waveforms of an AC capacitive ignition system at 70 µs and 500 µs spark durations.[Paper I].

At the beginning of the discharge, electrical breakdown occurs when the voltage across the spark gap exceeds the breakdown threshold. This initiates the spark and forms the initial plasma channel. During the first half-cycle, the discharge behaves similarly to a DC spark. The current flows in one direction until it naturally decreases to zero at the end of the half-cycle. At this point the plasma channel can no longer be sustained, and the spark temporarily extinguishes.

In the following half-cycle, the voltage builds up again with opposite polarity and the spark re-ignites. The voltage required for this re-ignition is typically lower than the initial breakdown voltage. This occurs because residual ionized gas remains in the spark gap after the previous discharge. The remaining charged particles facilitate the re-ignition process and enable the next half-cycle discharge. From the voltage and current behavior, each half-cycle of an AC spark can therefore be considered as a short DC-like spark discharge [84].

In this thesis work, the AC spark is generated using a newly developed capacitive ignition system by Phinia (formerly Swedish Electromagnets – SEM AB). Unlike inductive ignition systems, capacitive ignition systems store electrical energy in one or more capacitors before the spark is released. The stored energy is then discharged through the ignition coil to generate the spark [91]. A schematic representation of this system is shown in Figure 12.

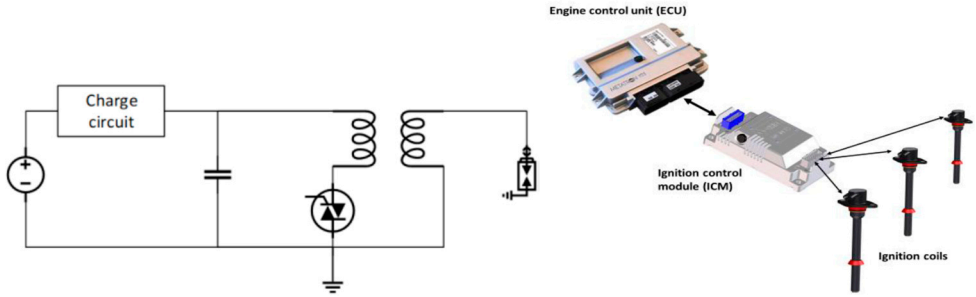

Figure 12: AC capacitive system. Left: Schematic diagram. Right: Typical AC capacitive ICM communicating with ECU and ignition coils. [91]

The AC capacitive ignition system provides a higher degree of freedom in controlling the spark characteristics. The available spark voltage (ASV), spark current and spark duration can be adjusted independently on a cycle-by-cycle basis using a patented microprocessor, controlled embedded power-electronic system, and CAN communication. By controlling the switching of capacitors and power electronics from the ignition control module (ICM), the system can generate sparks with durations ranging from a single half AC wavelength to significantly longer discharges [91]. This capability allows the spark energy to be adjusted according to the ignition requirement and helps avoid unnecessary spark energy being delivered to the electrode gap.

3.4 Ignitability versus spark plug wear – an inherent trade-off

Achieving robust ignition is essential for SI engines because it directly influences combustion stability. A stable combustion is important for maintaining consistent engine performance and efficient operation. It is commonly evaluated using the coefficient of variation of the indicated mean effective pressure (COV_{IMEP}) [33]. Higher values of COV_{IMEP} indicate increased cycle-to-cycle variability, which can reduce thermal efficiency and lead to increased noise, vibration, and harshness (NVH).

Ignitability is commonly associated with the characteristics of the spark discharge, particularly the spark energy [92]. Several studies have investigated the influence of ignition energy on combustion performance in SI engines. Chen et al. [93] studied the effect of spark energy on natural gas combustion in a high-compression-ratio optical engine operating under lean conditions and reported that higher ignition energy improved combustion stability by accelerating early flame kernel growth. Similar observations have been reported in [94], which showed that increasing

ignition energy improves combustion stability, especially for lean mixtures, although the beneficial effect becomes marginal beyond a certain energy level.

In recent years, advanced ignition concepts, capable of delivering higher spark energies, have gained significant interest to further improve combustion performance, particularly for engines operating with gaseous fuels. Cruccolini et al. [95] demonstrated that a corona discharge igniter can extend the lean operating limit and reduce cycle-to-cycle variability compared with a conventional spark igniter in an optical engine fuelled with methane and hydrogen–methane blends. Similar improvements in early flame development and combustion stability have also been reported using non-equilibrium low-temperature plasma ignition systems in hydrogen engines [96]. However, increasing spark energy is not without limitations, as it may accelerate spark plug wear. The repeated high-energy spark discharges lead to gradual erosion of the spark plug electrodes caused by thermal loading, electrical erosion, and material oxidation. As the electrodes wear, the spark gap increases, which may affect ignition robustness and engine performance over time [**18**]. Spark plug durability is a critical aspect for heavy-duty SI engines. Frequent spark plug replacement increases TCO through costs for labour, material and vehicle downtime.

To address this issue, significant research efforts have focused on the development of high-endurance spark plugs. However, these spark plugs are often expensive since they employ precious metals such as platinum or iridium on the electrode surfaces to improve resistance to erosion, as illustrated in Figure 13 [97–98, 38]. Alternatively, optimizing the spark ignition process may provide a viable solution as it can help reducing electrode wear by maximizing the energy transfer from the spark plasma to the gas while minimizing thermal losses to the electrodes during flame kernel formation and early flame development.

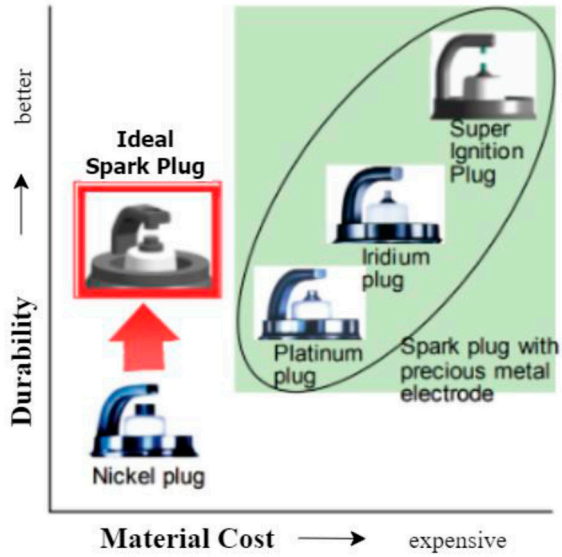

Figure 13: Durability versus material cost of different spark plugs.[Paper I]

3.5 Special considerations for hydrogen in SI-ICE

Ignition energy becomes even more important in hydrogen engine operation. Hydrogen has a very low minimum ignition energy, which makes the fuel relatively easy to ignite. At the same time, hydrogen exhibits a high autoignition temperature. This combination creates unique challenges for the spark ignition control design and increases the susceptibility of hydrogen engines to pre-ignition – an unintended ignition before the scheduled spark timing during the compression stroke. Pre-ignition may be triggered by hot surfaces, such as overheated spark plug electrodes, or by residual electrical energy released from the ignition system [40–42, 99] and can lead to catastrophic engine damage.

On the other hand, the high autoignition temperature of hydrogen enables the use of higher compression ratios to improve engine efficiency. Higher compression ratios increase the in-cylinder pressure at the time of ignition, which requires elevated secondary voltage to achieve electrical breakdown across the spark gap. At the same time, it is necessary to limit the spark energy deposited at the electrode gap by actively controlling the spark current and discharge duration, particularly during the glow phase. In addition, minimizing stray/parasitic capacitances in the ignition coil design can help reduce unnecessary energy release from the ignition system [99,41–42]. The combination of elevated secondary voltage and higher compression ratios can increase the temperature of the spark plug electrodes. This may further increase

the risk of pre-ignition in hydrogen engines. As a result, spark ignition design for H_2-ICEs involves a challenging balance between achieving a robust ignition and avoiding conditions that promote pre-ignition.

These considerations highlight the importance of improved control over the ignition process in spark-ignition engines operating with gaseous fuels. A smart ignition system capable of delivering only the required energy at the spark gap—without excessive energy discharge—could provide a potential solution to achieve a robust ignition while limiting spark plug wear and reducing the risk of abnormal combustion events, particularly in hydrogen operation.

Conventional DC inductive ignition system offers limited flexibility in controlling the characteristics of the spark discharge. In such systems, the available spark voltage is closely linked to the dwell time, which determines the amount of energy stored in the ignition coil prior to the spark discharge. As a result, achieving the required breakdown voltage under demanding operating conditions often increases the total energy released during the spark event. In contrast, the newly developed AC capacitive ignition system used in this thesis work provides greater flexibility in controlling individual spark parameters. It allows independent control of available spark voltage, spark current, and duration, thereby offering additional degrees of freedom to tailor the spark characteristics. This improved controllability may enable the development of optimized ignition strategies for gaseous-fuelled SI engines, including those operating with biogas and hydrogen.

However, to optimally design ignition control strategies requires a better understanding of the spark ignition process. Several knowledge gaps remain regarding how electrical energy from the spark is transferred to the gas and how this process influences ignitability and combustion performance in both hydrogen and biogas-fueled ICEs. This thesis aims to address these knowledge gaps by investigating the following research questions:

- How efficiently is electrical energy transferred from the spark to the gas during the different phases (breakdown, arc, and glow)?
- How do spark control parameters, spark plug geometries, and gas pressure interact, and how can this be used to maximize the energy transfer from the spark to the gas?
- What is the minimum effective spark energy required to achieve a robust ignition in both hydrogen and biogas-fueled engines at different operating conditions?
- Can optimized spark ignition parameters improve combustion performance and avoid abnormal combustion events in hydrogen engines, particularly at high-load operations?

Chapter 4
Platforms for spark ignition and engine research

The research presented in this thesis is based on experiments performed on multiple platforms designed to investigate the spark ignition processes at different levels of complexity. These platforms include both constant-volume chambers and single-cylinder research engines. Each platform serves a specific purpose, ranging from fundamental studies of spark discharge to the evaluation of ignitability and combustion performance of hydrogen and biogas at engine-relevant conditions. The use of multiple experimental platforms enables a systematic investigation of spark ignition, where fundamentals can first be studied under well-controlled conditions and then evaluated in practical engine operation.

The experiments were conducted in test facilities located at Lund University, Chalmers University of Technology, and the Wärtsilä Sustainable Technology Hub (STH).

4.1 Constant-volume chambers

Constant-volume chambers were used in this work to study spark ignition under well-controlled conditions. These chambers allow independent control of key parameters such as gas pressure and temperature, making it possible to investigate the influence of individual spark parameters without the complexity introduced by engine operation.

In this thesis, two types of constant-volume chambers were used. A spark calorimeter was employed to quantify the transfer of electrical energy from the spark to the gas, while a dedicated chamber is was used to study spark plug wear under controlled thermodynamic conditions. Together, these setups provide fundamental insight into the efficiency of spark energy utilization and the mechanisms governing electrode erosion.

4.1.1 Spark calorimeter

A constant-volume spark calorimeter, shown in Figure 14, was developed by the author at Lund University to study the spark ignition process and quantify energy transfer from the spark to the gas. The design of the calorimeter was based on previous studies on pressure-based energy deposition measurements and was further refined through several design iterations to reduce thermal losses and improve measurement [100, 101].

To minimize heat losses, the calorimeter body was constructed from plexiglass, which has a significantly lower thermal conductivity than metals such as stainless steel. It ensures that a larger fraction of the deposited spark energy remains within the gas, thereby improving the accuracy of the energy transfer measurements. The chamber has a cylindrical volume of 7.5 cm^3, selected to provide a measurable pressure response to the spark energy input. A small gas volume enhances the temperature and pressure rise for a given energy input, which improves the signal-to-noise ratio. In addition, the small volume limits heat losses, enabling a more accurate estimation of the energy transferred from the spark to the gas. The chamber is equipped with inlet and outlet ports for gas filling and purging respectively, and an additional volume of 3.4 cm^3 is associated with the intake and purge lines connected to the chamber. Experiments were conducted using nitrogen supplied from a high-pressure gas bottle with regulated pressure control. Nitrogen was chosen as the working gas instead of air to avoid ozone build-up in the chamber during repeated spark discharges, which may influence the spark behavior and introduce uncertainty in the measurements.

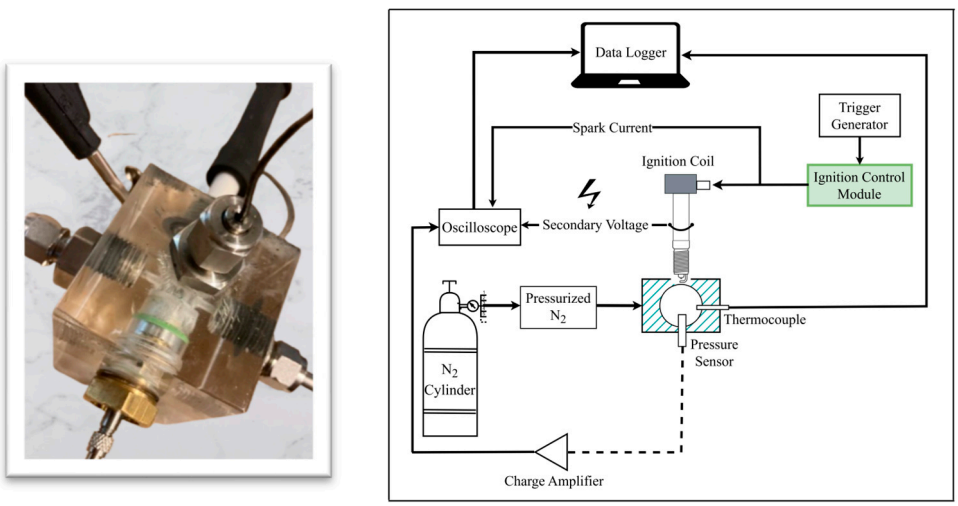

Figure 14: Left: Spark calorimeter at Lund University. **Right:** Schematic diagram of the test-rig.
Source: Paper II

The pressure rise inside the chamber was measured using a high-sensitivity differential pressure transducer (PCB 106B51), shown in Figure 15. The transducer has a sensitivity of 131 μV/Pa, a measurement range of 35 kPa, and a resolution of 0.00034 kPa. Its fast dynamic response (rise time of 12 μs and resonant frequency above 40 kHz) enables accurate capture of the rapid pressure increase generated by the spark discharge. The transducer was mounted on the calorimeter using an acetal adapter to provide electrical isolation, and the signal was amplified using a Kistler 5134B coupler.

Figure 15: The PCB 106B51 pressure transducer.

The spatial arrangement of the spark plug and pressure transducer is an important design consideration. The two components were positioned opposite each other at a distance of 12.5 mm. This results in a delay of approximately 37 μs between the spark onset and the arrival of the pressure wave at the transducer, as shown in Figure 16. This delay is compatible with the travelling time of the pressure wave across the calorimeter at the speed of sound, from the electrode tip to the sensor. The selected distance represents a compromise between measurement accuracy and sensor protection. Positioning the transducer closer to the spark plug would enhance the measurement accuracy, but would also increase the risk of exposure of the transducer to the spark plasma, leading to measurement errors or potential damage.

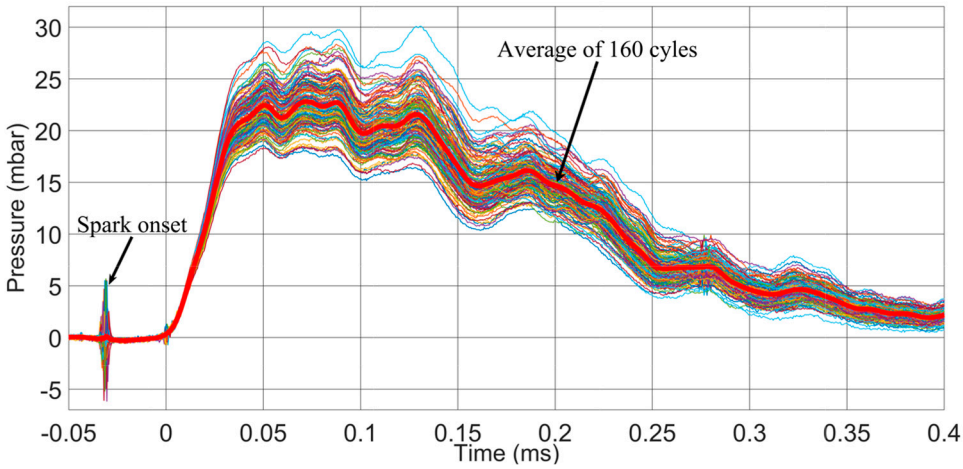

Figure 16: Pressure data from the spark calorimeter at 150 mA–40 µs spark. *Source: Paper II*

In addition to pressure measurements, the electrical characteristics of the spark discharge were recorded. The spark voltage was measured using a capacitive high-voltage probe (MI074), while the spark current was determined from the voltage drop across a 10 Ω resistor placed in the return path of the ignition circuit. The gas temperature inside the chamber was monitored using a K-type thermocouple. A signal generator was used to trigger the ignition system at frequencies corresponding to different engine speeds. All signals were recorded using a PC-based 80 MHz PicoScope 6000 automotive oscilloscope. The setup thus enables accurate quantification of the energy transferred from the spark to the gas and forms the basis for the analysis presented in chapter 6.2.

4.1.2 Spark-plug wear chamber

A dedicated constant-volume chamber was developed at the test facility of Wärtsilä STH to study spark plug wear, as discussed in chapter 6.1. While the chamber is similar in concept to the spark calorimeter, its primary purpose is to investigate electrode erosion over extended operating periods. The setup is designed for long-duration operation, allowing continuous test runs of up to 24 hours. The chamber has a significantly larger volume of 400 ml compared to the spark calorimeter, which helps maintain stable thermodynamic conditions during repeated spark discharges by reducing the influence of pressure rise and heat accumulation. The experiments were conducted using pressurized air, with the chamber pressure regulated through a pneumatic control system. In addition, the chamber was continuously purged with air at a flow rate of approximately 5 liters/min to prevent the accumulation of ozone, which could otherwise affect electrode erosion rates. To

better represent engine-relevant conditions, spark plugs were externally heated. The ground electrode was continuously heated using a laser to 750 °C, and its temperature is measured using an optical pyrometer. In addition, the spark plug head is maintained at 120 °C using an external heater.

Spark plug wear is quantified by monitoring the breakdown voltage over time, which serves as an indirect measure of electrode gap growth. As the electrodes erode, the gap increases, leading to a corresponding rise in breakdown voltage. The breakdown voltage was continuously measured during the test using a Tektronix P6015 high-voltage probe, allowing electrode wear to be monitored over time.

4.2 Single-cylinder research engines

In addition to the fundamental studies conducted in constant-volume chambers, engine experiments were performed to investigate ignitability of hydrogen and biogas combustion at different operating conditions. Single-cylinder research engines are particularly suitable for this purpose, as they provide a high level of control over operating parameters while retaining the key characteristics of practical engine operation. The experimental work in this thesis was carried out using three different single-cylinder engine platforms.

4.2.1 Wärtsilä W31SCE

The Wärtsilä W31SCE single-cylinder engine was used to investigate ignitability in large-bore marine biogas engines operating under lean-burn conditions, as discussed in chapter 6.1. The engine is based on the Wärtsilä W31 platform (see Figure 17), which is currently in commercial production. The designation “W31” refers to its bore diameter of 31 cm. It has a displacement of 32.4 L and is equipped with an active pre-chamber system. It delivers a nominal power output of approximately 600 kW at 750 rpm. The engine is located at the test facility of Wärtsilä STH in Vaasa, Finland. The specifications are summarized in Table 3.

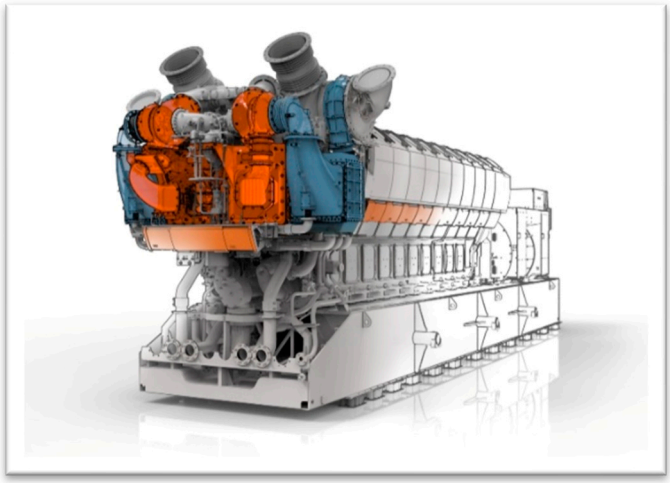

Figure 17: Wärtsilä W31 full-scale gas engine used as reference for the W31SCE engine platform. [102]

Table 3: Specifications of the Wärtsilä W31SCE single cylinder engine. *Source: Paper I*

Engine type	**W31SCE**
Swept volume	32.4 L
Main injection type	Port-injected
Bore	310 mm
Stroke	430 mm
Length of con rod	1095.2 mm
λ (main chamber)	2.0
λ (pre-chamber)	1.4

The overall engine control system is managed by Wärtsilä, and detailed control strategies were not accessible due to proprietary restrictions. In addition, detailed information regarding the pre-chamber design—such as geometry, orifice configuration, and internal flow characteristics—was not provided by Wärtsilä. However, the spark-trigger signal from the engine control unit was made available, enabling external control of spark ignition parameters through an ignition control module (ICM). Communication with the ICM was established via CAN using Vehicle Spy 3 software.

For the ignitability study, in-cylinder pressure traces were recorded using a piezo-electric pressure transducer with 0.1 CAD resolution. In addition, the electrical characteristics of the spark discharge were measured. The spark voltage was measured using a Tektronix P6015 high-voltage probe, while the spark current was determined from the voltage drop across a 10 Ω resistor placed in the return path of

the ignition circuit. Both signals were recorded using a PC-based 80 MHz PicoScope 6000 automotive oscilloscope.

4.2.2 Scania D13 optical engine

The Scania D13 optical research engine, shown in Figure 18, was used in this work to investigate ignitability and flame kernel development in hydrogen combustion under premixed conditions. The platform enables direct visualization of flame kernel formation, growth, and extinction, which are not accessible through pressure-based measurements alone. This is essential for understanding the mechanisms governing misfire under highly diluted conditions, as discussed in chapter 6.4.

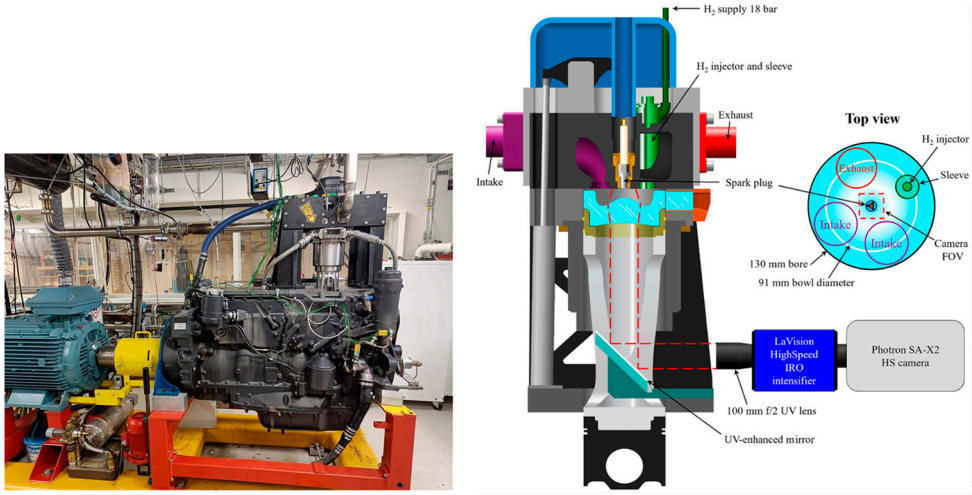

Figure 18: The Scania D13 optical engine at Lund University. **Left:** Engine test cell. **Right:** Cross-sectional schematic of the optical engine and camera setup. The top view shows the spark plug and injector placement as well as the camera field of view. **Source: Paper III**

The engine is modified based on the Bowditch design. The modified cylinder is equipped with a gas-engine-type cylinder head featuring a centrally located spark plug. One of the exhaust valves has been removed to accommodate a low-pressure hydrogen injector of the outward-opening hollow-cone type. Table 4 summarizes the specifications of the engine. Hydrogen is supplied at 18 bar absolute pressure through a buffer tank of 0.5 L, which stabilizes pressure fluctuations during injection. The hydrogen flow rate is measured using a Bronkhorst F-112AC mass flow meter. Air is supplied by compressors and cooled using heat exchangers, with the airflow measured upstream using a Bronkhorst F-106BI flow meter.

Table 4: Specifications of the Scania D13 optical single cylinder engine. *Source: Paper III*

Engine type	Scania D13
Swept Volume	2.1 L
Bore	310 mm
Stroke	430 mm
Length of con rod	255 mm
Compression ratio	11.5:1
Swirl ratio	2.2
No. of intake valves	2
No. of exhaust valves	1

In contrast to the production ECU that operates based on pre-defined control strategies, this engine is equipped with a flexible in-house control and data acquisition system. The control system is implemented in a LabVIEW-based environment, allowing independent control of key parameters such as injection timing, ignition timing, and other operating conditions. It enables synchronized acquisition of both crank-angle-resolved and time-based signals. High-frequency signals (up to 30 kHz), such as in-cylinder pressure and ignition characteristics, were recorded on a crank angle basis, while low-frequency signals (up to 50 Hz), including temperatures, pressures, and flow rates, were recorded on a time basis. In addition, both spark voltage and current were measured using the same approach described in chapter 4.1.1.

Optical access to the combustion chamber was achieved from below through a fused-silica piston and an UV-enhanced aluminium mirror. The piston features a "Mexican hat" geometry, which magnifies the central region of the combustion chamber around spark timing, improving the visualization of the flame kernel development. A high-speed camera was used to capture the evolution of the early flame kernel.

4.2.3 Volvo D13 engine

A Volvo D13 single-cylinder engine was used to investigate ignitability and cycle-to-cycle variability in DI hydrogen combustion at high load operation. This platform complements the optical engine studies by enabling evaluation of spark ignition where both mixture dilution and injection timing influence the combustion performance, as discussed in chapter 6.5.

The cylinder head of the engine is modified to accommodate a centrally mounted hydrogen injector while the spark plug is mounted off-center between the intake and exhaust valves. The injector operated at injection pressures up to 40 bar and was equipped with a single-hole flow-guiding cap. The injection strategy is designed to utilize jet momentum to generate a strong in-cylinder flow structure, promoting

mixture formation while maintaining turbulent kinetic energy near TDC. Since the base engine was originally designed for compression ignition operation, the compression ratio was reduced from 18:1 to 10:1 by introducing a concave piston geometry. This modification enables stable hydrogen combustion while avoiding severe combustion anomalies such as knock. Due to design constraints, several features of the original cylinder head are retained, resulting in a weak swirl motion generated by the intake system. Engine specifications are summarized in Table 5.

Table 5: Specifications of the Volvo D13 single cylinder engine. Source: Paper V

Engine base type	Volvo D13
Displaced volume (cm^3)	2116
Bore (mm)	131
Stroke (mm)	158
Con rod length (mm)	254
Compression ratio	10:1
No. of intake valves	2
No. of exhaust valves	2

Hydrogen is supplied from external high-pressure storage and regulated prior to injection. A small buffer volume was installed upstream of the injector to reduce pressure fluctuations during operation. The hydrogen flow rate was measured using a Coriolis mass flow meter. A throttle valve was installed in the intake line but it remained fully open during the experiments. Engine load was controlled by adjusting the intake pressure and the hydrogen fuel flow rate. The intake air flow rate was measured using a hot-wire anemometer. A schematic diagram of the test bed is shown in Figure 19.

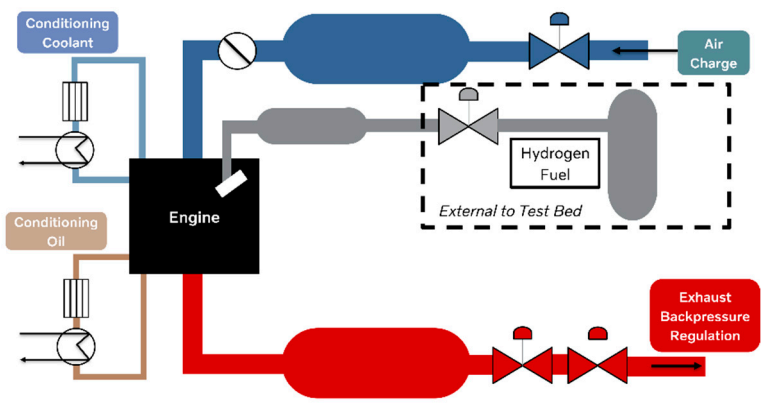

Figure 19: Schematic diagram of Volvo D13 engine test bench at Chalmers University of Technology. *Source: Paper V*

The engine test bench is controlled using an AVL PUMA system, which enabled automated operation and integration of data acquisition from both high and low frequency measurement systems connected to the engine. In-cylinder pressure was measured using a piezoelectric pressure transducer with a resolution of 0.1 CAD. In addition, both spark voltage and current were measured and recorded using the similar approach explained in chapter 4.1.1.

Chapter 5
Research methods

This chapter presents the research methods employed in this thesis. The experimental platforms described in the previous chapter were used to generate data over a wide range of operating conditions. These data require systematic methods to analyze the spark ignition process and combustion performance in hydrogen and biogas engines. The methods include both experimental design approaches and combustion analysis techniques. Together, they provide a structured framework for analyzing the experimental data and gaining deeper insight into the factors governing robust spark ignition at different operating conditions.

5.1 One factor at a time (OFAT)

The OFAT approach is a widely used experimental method in which one parameter is varied at a time to establish its primary effects on the system while keeping all other parameters constant [103]. This approach is particularly useful in combustion engine studies for identifying trends and thresholds, such as the onset of unstable combustion or misfire.

In this thesis, OFAT is employed in the initial stages of the experimental investigations. For example, in the ignitability analysis of the biogas engine (chapter 6.1), spark energy was varied while maintaining constant engine operating conditions to identify the combustion instability. Similarly, in the electrical-to-thermal energy transfer analysis (chapter 6.2), both spark current and duration were varied one at a time to evaluate their influence on the net energy deposited to the gas and to estimate energy transfer efficiencies at different phases of a spark.

A key limitation of the OFAT approach is that it does not capture interactions between parameters [104]. As illustrated in Figure 20, the experimental points obtained using OFAT lie along one-dimensional paths in a multi-parameter space. In practical engine operation, multiple parameters vary simultaneously, and their combined effects may differ from the sum of their individual influences. As a result, OFAT cannot fully describe the complex relationships governing combustion performance. This limitation motivates the use of design of experiments (DoE)

methods, which allow systematic investigation of both individual effects and interactions between parameters.

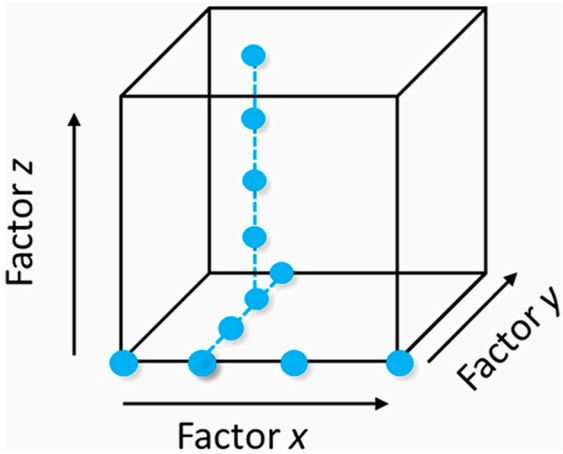

Figure 20: Example of an OFAT approach with three factors. [103]

5.2 Design of experiments (DoE)

DoE provides a systematic framework to investigate both the individual and combined effects of multiple parameters. By varying several parameters simultaneously according to a designed experimental plan, DoE enables efficient exploration of the parameter space and identification of interactions with other variables. In particular, the use of orthogonal designs allows the effects of individual factors to be separated, even though all are varied at the same time. With less structured or non-orthogonal test matrices, the effects become confounded with each other.

In this thesis, a central composite design (CCD) was used. It is a commonly used response surface methodology (RSM) technique, typically built on a two-level factorial design, with superimposed axial points (face-centered) and center points. Factorial points represent combinations of high and low levels of each parameter, axial points extend the design space to capture curvature, and center points are used to estimate experimental variability and improve the robustness of the model. Thus, the design structure enables estimation of both main and interaction effects, as well as curvature through quadratic terms, by fitting a second-order regression model. A schematic illustration of the CCD structure is shown in Figure 21, using a three-factor experiment. For a more detailed explanation of the CCD method and its statistical properties, refer to [105, 106].

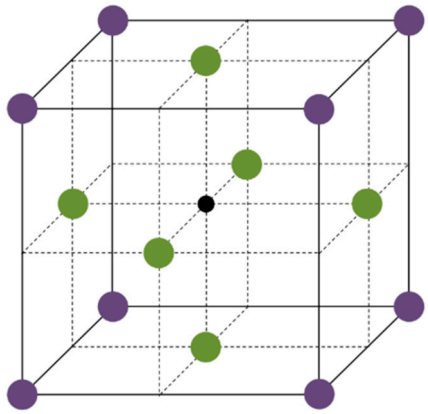

Figure 21: Schematic of a central composite design with three factors.

The use of CCD forms the basis for the analyses presented in chapters 6.3 and 6.5. In chapter 6.3, CCD was used to study the influence of multiple physical and electrical spark parameters on the energy deposition to the gas. In chapter 6.5, CCD was utilized to closely evaluate the combined effects of mixture dilution, injection timing, and spark parameters on engine stability and combustion performance in DI hydrogen engine. By using this DoE method, it becomes possible to identify optimal spark parameter combinations for achieving a robust ignition while minimizing excess spark energy discharge.

5.3 Heat release analysis

Heat release analysis is a fundamental tool to evaluate the combustion performance and efficiency in ICEs [30]. In this thesis, heat release analysis is used to evaluate both the combustion process in engines and the net electrical-to-thermal energy deposition to the gas in the spark calorimeter.

The analysis is based on the first law of thermodynamics, which relates to heat addition to the working fluid to changes in internal energy and the work done by the gas during combustion. The general form for a closed system is:

$$dQ = dU + pdV \quad (1)$$

where dQ is the heat added to the system, dU is the change in internal energy, p is the cylinder pressure, and dV is the change in cylinder volume.

Using the ideal gas law and assuming a constant ratio of specific heats, the rate of heat release with respect to crank angle can be expressed as:

$$\frac{dQ}{d\theta} = \frac{\gamma}{\gamma-1} p \frac{dV}{d\theta} + \frac{1}{\gamma-1} V \frac{dp}{d\theta} \quad (2)$$

where Q is the heat released, θ is the crank angle, γ is the ratio of specific heats, and V is the cylinder volume.

In engine applications, heat release analysis is performed based on in-cylinder pressure measurements. The heat release rate is integrated to obtain cumulative heat release, which allows the determination of key combustion parameters such as ignition delay, combustion phasing, and burn duration.

In the spark calorimeter, the same thermodynamic principle is applied in a simplified form to estimate the net energy deposited from the spark to the gas. Since the chamber volume is constant, the analysis is based only on the measured pressure rise (see equation 3), which is directly related to the thermal energy added to the gas. In this case, the heat release rate is expressed as a function of time rather than crank angle:

$$\frac{dQ}{dt} = \frac{1}{\gamma-1} V \frac{dp}{dt} \quad (3)$$

5.4 Engine performance analysis

In this thesis, combustion performance is evaluated using a set of metrics derived from in-cylinder sampling and heat release analysis. These metrics are used to quantify ignitability, combustion phasing, and cycle-to-cycle variability at different operating conditions.

MFB: Mass fraction burned (MFB) represents the fraction of the total fuel energy released during combustion. It is obtained from the cumulative heat release and describes the progression of the combustion process.

CA_X: It is defined as the crank angle degree at which x% of the total heat release has occurred during the combustion process. The crank angle corresponding to 5% MFB (CA05) and 10% MFB (CA10) are used to describe early flame development. The crank angle at 50% MFB (CA50) represents the combustion phasing while the crank angle at 90% MFB (CA90) is used to indicate burn duration.

IMEP: In addition to heat-release-based metrics, the indicated mean effective pressure (IMEP) is used to quantify the work output associated with the combustion process. IMEP is calculated from the pressure–volume diagram as:

$$\text{IMEP} = \frac{1}{Vd} \int p \, dV \quad (4)$$

where p is the in-cylinder pressure, V is the cylinder volume, and V_d is the displacement volume, defined as the volume swept by the piston between TDC and BDC. The integral $\int p\, dV$ represents the net indicated work produced over one engine cycle. By normalizing the work with the V_d, IMEP can be interpreted as an equivalent constant pressure that would produce the same amount of work when acting over the displaced volume. It therefore provides a convenient and size-independent measure of the effectiveness of combustion in converting released energy into useful work. In this thesis, the gross IMEP ($IMEP_g$) is considered, which represents the work produced during the compression and expansion strokes and does not include the pumping work.

COV_{IMEP}: The coefficient of variation of indicated mean effective pressure (COV_{IMEP}) is a commonly used metric for quantifying combustion stability of an engine. It is defined as:

$$COV_{IMEP} = \frac{\sigma_{IMEP}}{IMEP_{mean}} \quad (5)$$

where σ_{IMEP} is the standard deviation of IMEP and $IMEP_{mean}$ is the average IMEP of a number of combustion cycles considered. The parameter hence describes the variation of IMEP in relation to its mean value.

5.5 Spark energy analysis

Spark energy is defined as the electrical energy delivered to the spark plug gap. In this thesis, spark energy is an important parameter for studying its relationship with ignitability and spark plug wear in hydrogen and biogas engines. It is calculated from the measured voltage (U) and current (I) at the electrode gap by integrating the instantaneous electrical power (U*I) over the spark duration (t_s).

During the experiments, both secondary voltage and current were measured from the ignition coil. However, these measurements include resistive losses in the ignition cable and the spark plug. Therefore, to estimate the spark energy at the gap, the resistance in the spark plug and the ignition cable were measured and then the resistive losses (R) were finally subtracted.

$$E = \int_0^{ts} (UI) - (I^2R)\, dt \quad (6)$$

Chapter 6
Results

6.1 Ignitability versus spark plug wear in biogas engine

This section examines the relationship between spark ignition characteristics, combustion stability, and spark plug durability in a Wärtsilä W31SCE large-bore biogas engine. A central question is whether increasing spark energy beyond the point of successful flame kernel formation improves ignitability or instead leads to unnecessary thermal loading and accelerated electrode wear. To address this, two fundamentally different ignition concepts are evaluated: a conventional DC inductive system, and an AC capacitive system, which allows independent control of spark voltage, current, and duration. In addition, standard J-gap spark plugs with electrode gaps ranging from 0.22 mm to 0.51 mm was used, representing both new and worn conditions. This is particularly relevant, as electrode gap increases over time due to wear and directly influences ignition requirements.

The analysis is based on two complementary experimental approaches. Engine-based measurements are used to assess ignitability and combustion stability under high-load conditions, while a dedicated test rig is employed to quantify spark plug wear under controlled conditions representative of engine operation.

6.1.1 Ignitability analysis

Ignitability in the engine is assessed indirectly through combustion stability, as a stable combustion process indicates reliable flame kernel formation following spark discharge. In this work, combustion stability is quantified using COV_{IMEP}, with a threshold of 2% used to define stable operation. Additional metrics, including the coefficient of variation of peak pressure COV_{PP} and early flame development angles (CA05 and CA10), are analyzed to provide further insight into the sensitivity of ignition behavior to variations in spark energy. Table 6 summarizes the engine operating points considered in this work.

Table 6: Engine Operating Points. *Source: Paper I*

Operating point	Engine speed (rpm)	Imep (bar)	Engine load (%)
1	750	30	90
2	750	33	100

Figure 22 shows COV_{IMEP} and COV_{PP} as a function of dwell time for different electrode gaps at 90% engine load. In a DC inductive ignition system, dwell time is the primary control parameter and simultaneously influences spark voltage, current, and duration. Consequently, increasing dwell time leads to a monotonic increase in total spark energy. A complete description of a DC inductive ignition system is provided in the Chapter 3. It is seen from the figure that increasing dwell time initially improves combustion stability, as reflected by a reduction in both COV_{IMEP} and COV_{PP}. However, beyond a certain threshold, further increases in dwell time do not yield additional improvements. This behavior is consistent across all investigated operating conditions, including full load, and is further supported by the early flame development analysis shown in Figure 23. These observations indicate that once the flame kernel becomes self-sustained and starts to propagate, there is nothing more to gain by adding more energy to the spark.

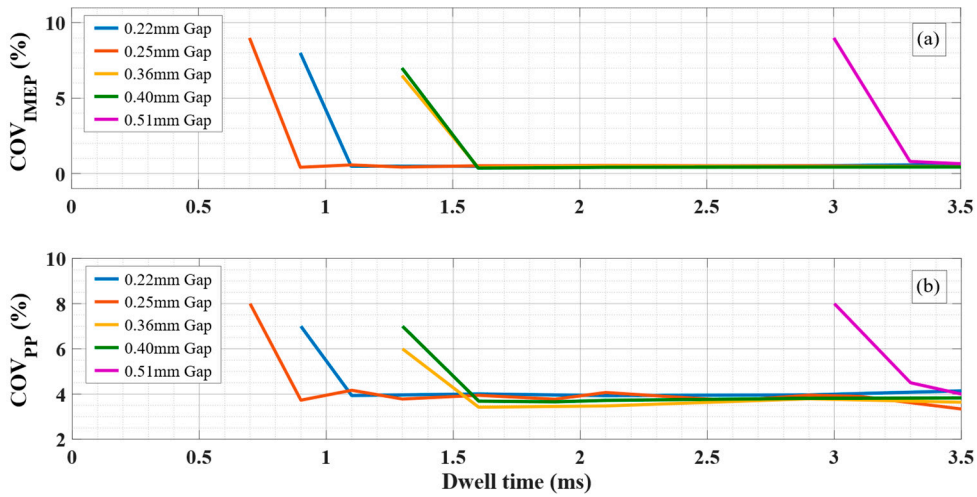

Figure 22: DC Inductive – COVIMEP and COVPP versus dwell time, engine operated at 90% engine load. *Source: Paper I*

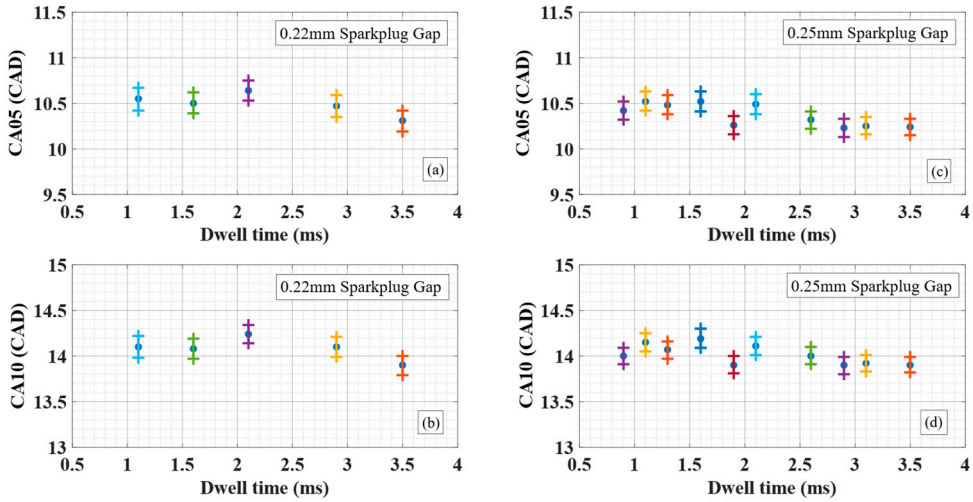

Figure 23: DC Inductive – CA05 & CA10 versus dwell time at 0.22 mm and 0.25 mm electrode gaps, engine operated at 90% engine load. *Source: Paper I*

A notable deviation is observed for the narrowest electrode gap (0.22 mm), which requires slightly higher dwell time compared to the 0.25 mm gap to achieve stable combustion. This is likely due to enhanced quenching effects during the early stages of flame kernel development, as the narrower gap increases heat losses to the electrode surfaces, effectively cooling the flame kernel. As a result, a relatively higher spark energy input was required to ensure a robust combustion.

Similar trends are observed with the AC capacitive ignition system, despite its ability to independently control spark parameters. Once stable combustion is achieved, increasing spark voltage, current, or duration does not result in further improvements in combustion stability. This indicates that the limitation is not related to the flexibility of the ignition system, but rather to the fundamental physics of flame kernel formation.

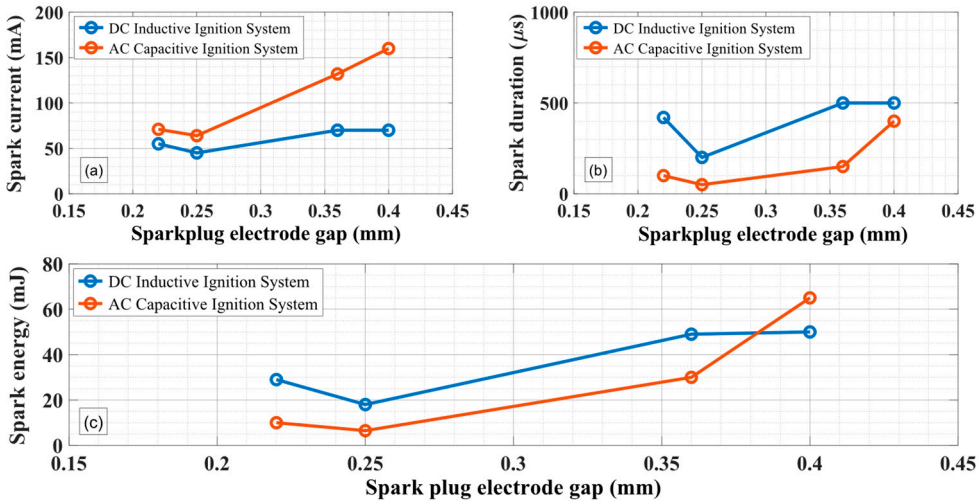

Figure 24: (a): Spark Current vs Spark plug electrode gap at 90% engine load. (b): Spark Duration vs Spark plug electrode gap at 90% engine load. (c): Spark Energy vs Spark plug electrode gap at 90% engine load. *Source: Paper I*

Figure 24 compares the spark characteristics of the DC inductive and AC capacitive systems across different electrode gaps. While both systems achieve stable combustion, the AC capacitive system does so with significantly lower total spark energy. This is enabled by its ability to tailor spark parameters independently, allowing very short spark durations (~50 μs) while maintaining sufficient ignition capability. In contrast, the DC inductive system exhibits limited flexibility. Increased breakdown voltage demand at larger electrode gaps results in longer spark durations and consequently higher total energy discharge. This excess energy does not contribute to improved ignitability, suggesting that a substantial portion of the energy is not effectively utilized in the ignition process.

6.1.2 Spark plug wear analysis

To assess the implications of excess spark energy on component durability, spark plug wear was evaluated using a dedicated test rig under controlled conditions representative of engine operation. The minimum spark energy profiles required to achieve stable combustion at 90% engine load were selected for electrode gaps of 0.25 mm, 0.36 mm, and 0.40 mm. Each test was conducted over 200 hours, corresponding to approximately 4.5 million spark events. Spark plug wear is quantified through continuous measurement of breakdown voltage, which serves as an indirect measure of changes in electrode gap. The rate of increase in breakdown voltage is used to estimate the electrode erosion rate.

Figure 25 shows the breakdown voltage and its rate of increase over time for both DC inductive and AC capacitive ignition systems at a 0.25 mm electrode gap. It is observed that the breakdown voltage increases significantly faster for the DC inductive system compared to the AC capacitive system. In addition, the DC inductive system fails to sustain operation for the full test duration under the same spark energy profile, whereas the AC capacitive system maintains stable operation throughout. This behaviour can be attributed to differences in both the magnitude and nature of the spark discharge. The DC inductive system operates with higher total spark energy, leading to increased thermal loading of the electrode surfaces and accelerated material erosion. As the electrode gap increases, the required breakdown voltage rises accordingly, eventually exceeding the capability of the ignition system. In contrast, the AC capacitive system operates at significantly lower energy levels, limiting thermal loading and reducing electrode wear. Moreover, the alternating nature of the current promotes a more uniform distribution of thermal stresses across the electrode surfaces, further mitigating localized erosion.

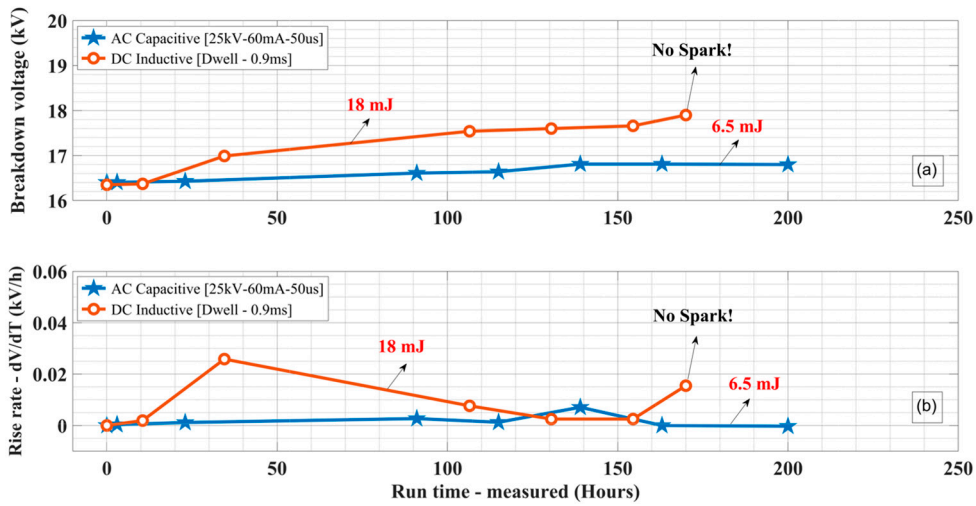

Figure 25: (a): Breakthrough voltage vs Run time at 0.25 mm gap. (b): Rise-rate of Breakthrough voltage vs Run time at 0.25mm gap. *Source: Paper I*

This effect is further confirmed in Figure 26, where a high-energy AC capacitive profile (~1.5 times the energy of the DC system) is tested. Despite the higher energy input, the AC system exhibits a slower increase in breakdown voltage and maintains stable operation throughout the test. This demonstrates that spark energy alone does not govern electrode wear; the characteristics of the spark discharge, particularly current directionality and temporal distribution, play a critical role.

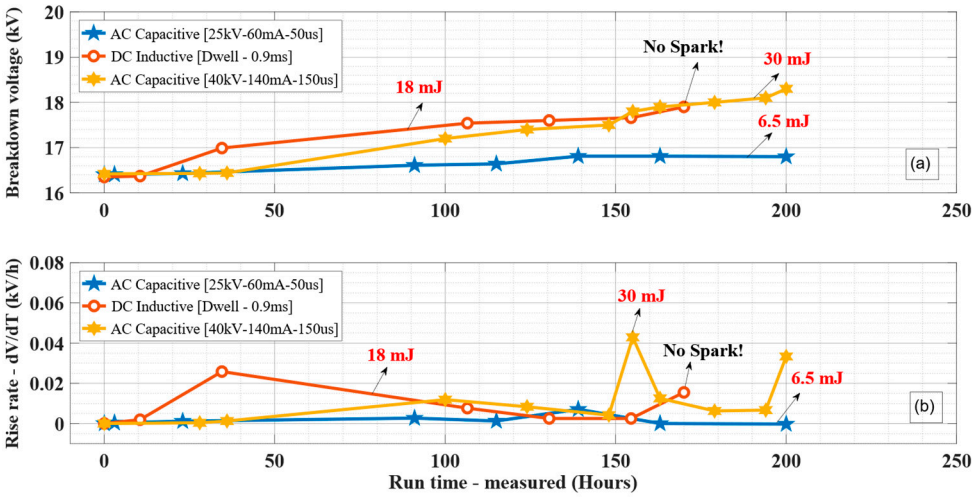

Figure 26: (a): Additional Findings - Breakthrough voltage at 0.25 mm gap. (b): Additional Findings - Rise-rate of Breakthrough voltage at 0.25 mm gap. *Source: Paper I*

To summarize, the results from this work clearly demonstrate that ignitability is not governed by total spark energy, but seems to be related to how effectively this energy contributes to flame kernel formation. Once a self-sustained flame kernel is established, additional energy does not improve combustion stability and instead leads to increased thermal loading of the spark plug electrodes. Furthermore, spark plug wear is influenced not only by the magnitude of the energy discharge but also by the nature of the spark. The AC capacitive system, through its ability to control spark parameters and distribute heat losses more uniformly across the spark-plug electrodes, achieves comparable ignition performance with significantly reduced electrode erosion.

These findings highlight a fundamental trade-off between ignition robustness and spark plug durability and emphasize the importance of controlled energy delivery rather than increased spark energy. This insight forms the basis for further investigation into energy transfer mechanisms from the spark to the gas and ignition optimization strategies presented in the following sections.

6.2 Energy transfer characteristics from spark to gas

This section examines how efficiently the electrical energy delivered by the spark is transferred to the gas at different phases during a spark event. The electrical energy supplied by the ignition system is not entirely transferred to the gas. While a portion of it is dissipated as heat in the spark plug electrodes, additional losses

occur in the ignition system components such as cables and internal resistances. Only the fraction of the total electrical energy is transferred to the gas which contributes to ionization and leads to spark formation, while the remaining energy can be considered as waste.

A spark discharge consists of three distinct phases—namely breakdown, arc, and glow—each characterized by different plasma properties and energy transfer mechanisms (discussed in Chapter 3). Understanding the relative contribution of these phases to the total energy deposited in the gas is essential, as robust ignition is governed not only by the total spark energy, but by how efficiently that energy is deposited into the combustible mixture at different phases.

To fulfil this research objective, experiments were conducted in a custom-built spark calorimeter (see Chapter 4 for detailed specifications) where nitrogen (N_2) gas was used under pressurized conditions. The chamber pressure was varied up to 5 bar at a constant temperature of 25 ± 1°C to enable controlled variation of gas density which corresponds to the in-cylinder gas density around TDC. The energy deposited to the gas was determined from the measured pressure rise using a high-sensitivity pressure transducer. An AC capacitive ignition system was employed to enable independent control of spark current and duration, allowing systematic investigation of discharge characteristics. Standard J-gap spark plugs of nickel on both electrodes were used in this study.

6.2.1 Breakdown and arc phase efficiency

The breakdown and arc phases represent the initial stage of the spark discharge, typically lasting a few microseconds. To evaluate the energy transfer during these early phases, experiments were performed by varying the total spark duration between 40 µs and 1000 µs at different current amplitudes. The corresponding thermal energy deposited in the gas was calculated using the heat release equation (see chapter 5) from the measured pressure rise in the chamber.

Figure 27 shows the net energy transferred to the gas as a function of spark duration at a gas pressure of 4 bar, for current amplitudes ranging from 60 mA to 300 mA. It is seen that the deposited energy increases with spark duration up to approximately 150 µs for all current levels, except at the lowest current (60 mA), where the increase in energy deposition saturated earlier at around 80 µs. Furthermore, increasing the current amplitude by a factor of five resulted in only a modest increase in deposited energy (approximately 30% at 150 µs), indicating a diminishing return of higher current levels in terms of effective energy transfer. Beyond the spark duration of 150 µs, the net energy transferred to the gas decreased despite continued energy input to the spark. This behavior indicates that prolonged discharge leads to increased thermal losses, primarily due to heat transfer from the plasma channel to

the electrodes and surrounding surfaces. Finally, the net energy transfer to the gas levelled off after 500 µs for all the glow current levels.

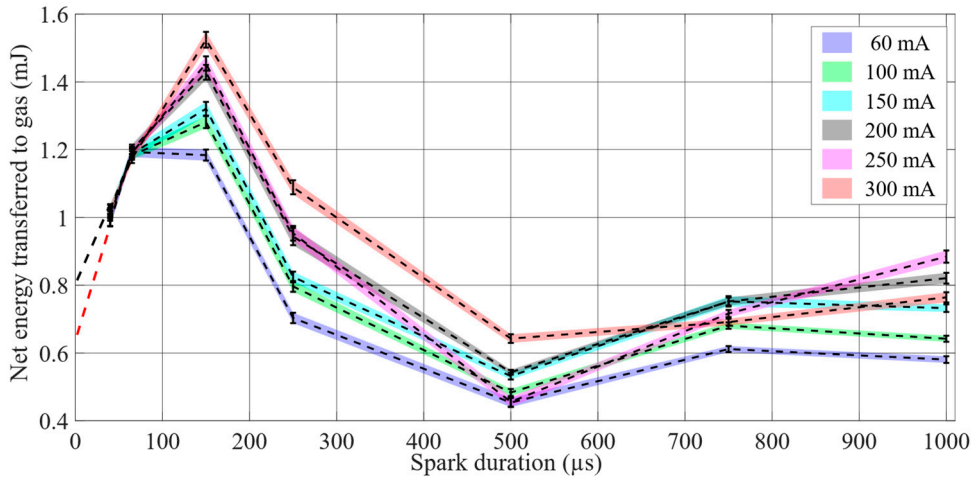

Figure 27: Net energy transferred to the gas with extrapolation vs spark duration at various current amplitudes. **Source: Paper II**

To assess the contribution of the breakdown and arc phases, the measured energy deposition was extrapolated from 40 µs to 2 µs (corresponding to the end of these phases) using the two shortest spark durations (40 µs and 80 µs), assuming a linear trend in this region. While this approach introduces some uncertainty, it can be considered reasonable over the short interval of spark duration where the initial increase in energy deposition exhibits an approximately linear trend. The extrapolated values were further supported by the results from the analysis of glow phase efficiency (for details, see Paper II).

Finally, an envelope of net energy transfer to the gas during the breakdown and arc phases was established, as shown at the far left in Figure 27. Comparing this envelope with the electrical energy delivered to the spark gap yields an estimated electrical-to-thermal energy conversion efficiency in the range of 45–64%.

6.2.2 Glow phase efficiency

After the breakdown and arc phases, the spark transitions into the glow phase where it persists for the rest of the spark duration and can be actively controlled from an ignition system. To evaluate the energy transfer efficiency during this phase, experiments were conducted at a fixed spark duration of 40 µs while varying the glow current at three levels. The influence of gas density on the glow phase efficiency was also assessed by repeating the experiments at different chamber pressures.

Figure 28 shows the electrical-to-thermal energy conversion efficiency during the glow phase as a function of glow current at different gas densities. The efficiency ranges between approximately 6% and 15%, which is significantly lower than that observed during the breakdown and arc phases. In addition, a clear dependence on the gas density is observed, with glow phase efficiency increasing at higher densities. This is likely due to the increased number of gas molecules in the vicinity of the plasma channel, which enhances collisional heat transfer from the plasma to the gas. Consequently, higher gas densities improve the coupling between the spark discharge and the surrounding gas. Another important trend is observed with the glow current, which exhibits a non-monotonic behavior. The glow phase efficiency increases with current up to approximately 85 mA, beyond which it decreases for all investigated density levels. This reduction in efficiency can be attributed to increased heat losses to the electrodes at higher current levels. As the electrode temperature rises, a larger fraction of the electrical energy is conducted into the solid material rather than transferred to the gas. This effect is particularly pronounced at lower gas densities, where the reduced number of gas molecules limits the ability of the spark plasma to transfer energy to its surrounding gas.

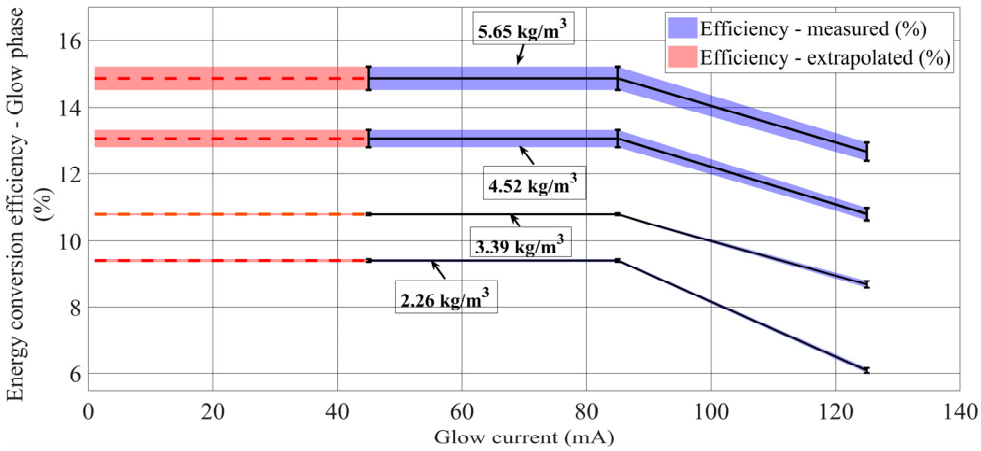

Figure 28. Glow phase efficiencies at different gas densities versus glow current amplitudes. *Adapted from Paper II*

To summarize, the results demonstrate a fundamental distinction between the different phases of the spark discharge. The breakdown and arc phases are highly efficient in transferring energy to the gas. However, they are mainly governed by system properties such as gas density, electrode gap, and parasitic or stray capacitances present within the ignition system and therefore cannot be directly controlled. In contrast, the glow phase is less efficient but provides a degree of controllability through adjustment of current and duration from an ignition system. Importantly, the results identify a threshold behavior in both spark duration and

current. Beyond this threshold, additional electrical energy does not lead to increased energy deposition in the gas, but instead results in increased thermal losses, primarily to the spark plug electrodes. This finding provides a fundamental explanation for the observations in Section 6.1, where increasing spark energy beyond a certain level did not improve combustion stability but led to accelerated electrode wear. Furthermore, the strong dependence of glow phase efficiency on gas density suggests that ignition strategies must be adapted to engine operating conditions. At higher loads, where gas density is elevated, the efficiency of energy transfer improves, whereas at low loads or highly diluted conditions, longer discharges may be required to achieve a robust ignition.

Note that this work was conducted using spark plugs with fixed geometry. In practice, spark plug geometry–particularly center electrode diameter and electrode gap–affect the size of the plasma channel and thereby the energy transfer to the gas. Furthermore, electrode wear during engine operation influences these parameters over time by increasing the gap and reducing the effective center electrode diameter. This highlights the need to explore the combined effects of spark discharge parameters, gas density, and spark plug geometries on the energy transfer to the gas, which is addressed in the following section.

6.3 Multi-parameter investigation of energy transfer to the gas

Building on the phase-resolved energy transfer analysis presented in Section 6.2, this section evaluates how spark plug geometry, ignition control parameters, and gas density jointly influence the net energy transferred from the spark to the gas. While the previous section characterized the energy transfer to the gas during different discharge phases, a key challenge remains: in practical engine operation, these parameters can vary simultaneously and interact in a non-linear manner. Therefore, a systematic multi-parameter analysis is required to identify the dominant factors and their interactions. The experiments were conducted in the same spark calorimeter described in Section 4, using nitrogen under pressurized conditions. The AC capacitive ignition system was used to enable independent control of spark current and duration.

Five input parameters were considered in this work: center electrode diameter, electrode gap, gas density, glow current, and glow duration. Each parameter is varied over three levels, as summarized in Table 7, allowing both individual and combined effects to be evaluated systematically.

Table 7: Physical values of the input factors at three coded levels. *Source: Paper IV*

Coded units	Physical units				
	Center Electrode Diameter (mm)	Electrode Gap (mm)	Gas density (kg/m^3)	Glow current (mA)	Glow duration (µs)
-1	0.70	0.30	2.2	100	250
0	1.70	0.80	4.5	200	750
1	2.70	1.30	6.8	300	1250

6.3.1 Parameters affecting spark energy deposition

The statistically significant effects of the parameters on the energy deposition to the gas (E_{gas}) are shown in the Pareto plot in Figure 29. The results clearly indicate that electrode gap is the dominant parameter governing energy transfer to the gas, followed by gas density and the interaction between these two factors. In comparison, glow current exhibits a smaller but still noticeable influence, particularly through its interaction with electrode gap. This highlights that the energy transfer is primarily governed by electrode gap and gas density, which define the size of the plasma channel and its interaction with the surrounding gas, rather than by the controllable spark parameters alone.

Interestingly, both glow duration and electrode diameter are found to be statistically insignificant within the investigated range. This suggests that extending the glow duration does not necessarily increase the effective energy transferred to the gas, but rather prolongs the presence of the plasma channel. This may be beneficial for flame kernel stabilization under less optimal fuel-air mixture conditions. Similarly, variations in electrode diameter have limited influence on the net energy transfer, despite their potential impact on heat losses to the electrode material.

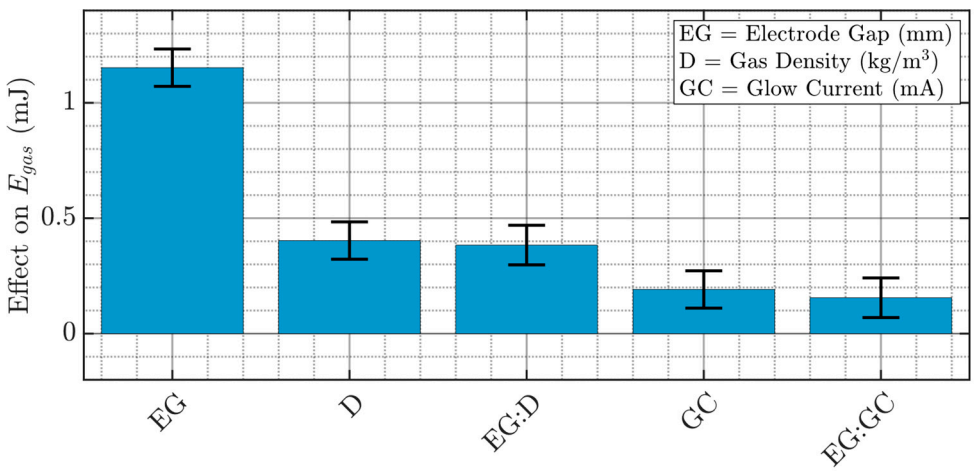

Figure 29. Pareto plot of statistically significant factors. *Source: Paper IV*

To further comprehend the combined influence of the statistically significant parameters on the response, interaction plots are studied. This is important because, in real engines, multiple variables often change simultaneously. Studying these interactions therefore provides deeper insight into the spark ignition process and helps identify conditions that maximize energy transfer to the gas.

Figure 30 shows the interaction between electrode gap and gas density on the energy deposition to the gas, E_{gas}. It is observed that at narrow electrode gaps (0.3–0.5 mm), the energy transfer to the gas remained low even at higher gas densities. Once the electrode gap widened to approximately 0.7 mm, energy deposition increased significantly and this effect became steeper as the gas density increased. This behavior is likely due to the size of the plasma channel. At narrow electrode gaps, the plasma channel is short, limiting the volume of gas that can be ionized and heated. As a result, a larger fraction of the spark energy is lost to the electrodes. As the electrode gap increases, the plasma channel becomes elongated and interacts with a larger volume of gas, improving the coupling between the electrical discharge and the surrounding gas. Higher gas density further enhances this coupling by increasing the number of gas molecules available to absorb energy from the spark plasma.

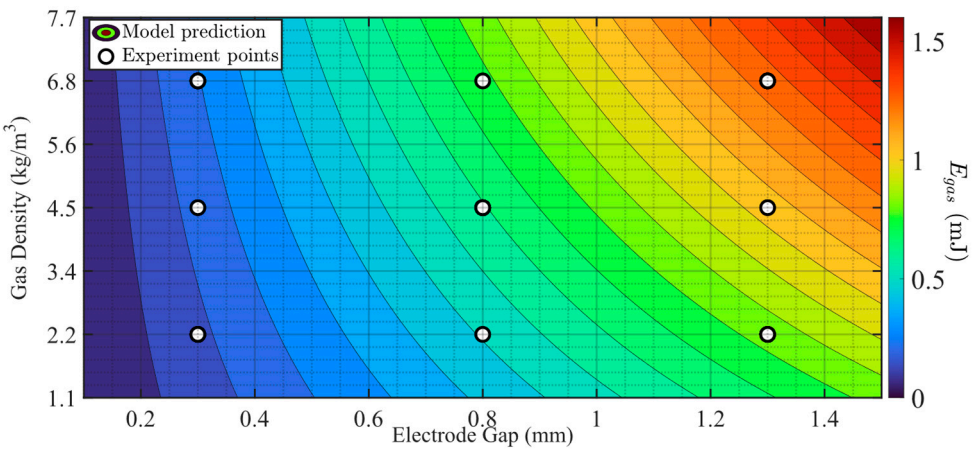

Figure 30. Interaction between the spark plug electrode gap and the gas density. *Source: Paper IV*

A similar interaction is observed between electrode gap and glow current. At narrow gaps, increasing the glow current has little effect on energy deposition to the gas, indicating that the limited plasma volume constrains energy transfer. At larger gaps, however, increasing glow current leads to higher energy deposition, although the relative gain is smaller compared to the effect of electrode gap. This is consistent with the reduced efficiency of the glow phase at higher current levels, as discussed in Section 6.2, where increased thermal losses to the electrodes limit the effectiveness of

adding spark energy. Nevertheless, their combined influence still leads to increased energy transfer to the gas when both parameters are set to high levels.

6.3.2 Optimal spark ignition control maps

Based on the combined insights from sections 6.2 and 6.3, conceptual ignition control strategies are developed for both biogas- and hydrogen-fueled SI-ICEs. The aim is to maximize effective energy transfer to the gas while minimizing thermal energy losses, particularly to the spark plug electrodes.

Figure 31 illustrates the proposed control strategy for biogas-fueled SI-ICEs as a function of engine load and electrode gap. At medium-to-high loads and narrow electrode gaps, increasing glow duration is beneficial, as it provides sufficient time for the plasma to interact with the mixture while compensating for heat losses. This trend is reflected in the right-hand plot, where long spark durations are shown as red-to-green field (corresponding to high-to-intermediate glow duration). Under these conditions, increasing glow current is less effective, as indicated by the blue region in the left-hand plot. As the electrode gap increases over time, the plasma channel becomes elongated, providing efficient energy coupling. At such conditions, increasing glow current becomes more effective, while glow duration can be substantially reduced. However, the current should not be too high to prevent excess heat losses.

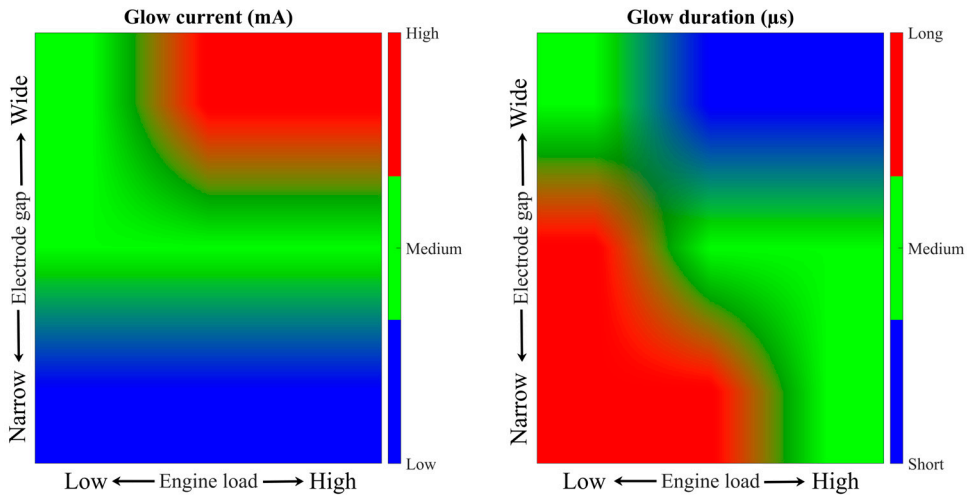

Figure 31: Spark ignition control map for biogas fueled SI-ICEs. *Source: Paper IV*

At idling or low loads, where gas density is low, ignition becomes challenging, particularly at narrow electrode gaps. In such conditions, longer spark durations

(shown in red in right-hand plot) are recommended to ensure sufficient interaction between the plasma and the fuel-air mixture. As the electrode gap increases, the role of glow current becomes prominent, although sufficient duration must still be maintained to ensure a robust ignition.

Figure 32 outlines the corresponding strategy for hydrogen-fueled SI-ICEs. Due to the inherently low ignition energy requirement of hydrogen, both glow current and duration are recommended to keep to their minimum to avoid excessive electrode heating and the associated risk of pre-ignition from the hot surface of the electrodes. However, at narrow electrode gaps, the limited plasma-arc length necessitates an increase in spark duration to ensure a stable flame kernel formation. This is especially relevant for hydrogen ICEs since they tend to operate at extremely lean fuel-air mixtures. As the gap increases, glow current becomes more effective and thus, recommended to slightly increase, while keeping the duration to its minimum.

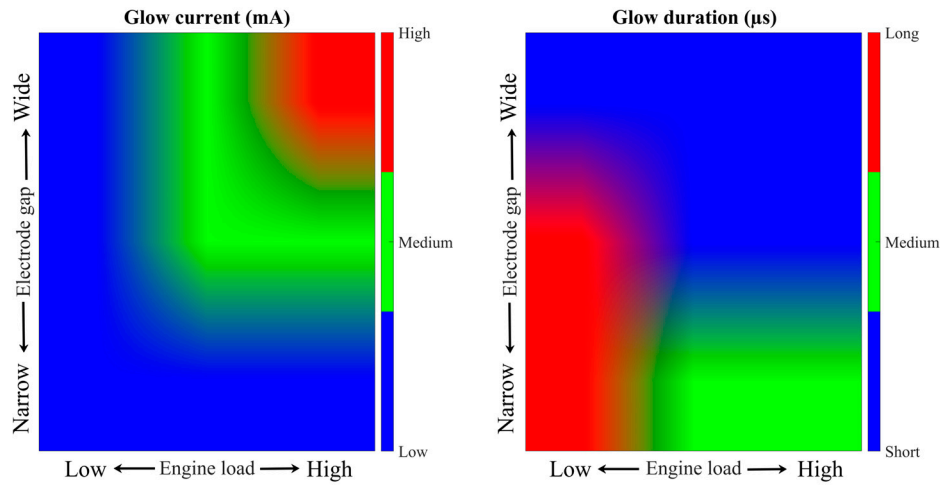

Figure 32: Spark ignition control map for H2 – fueled SI-ICEs. **Source: Paper IV**

In summary, the results from this work demonstrate that electrode gap plays a central role in governing energy transfer from the spark to the gas. Although it cannot be actively controlled during engine operation, it increases over time due to electrode wear and can therefore serve as an important input for adaptive ignition control strategies. Gas density and glow current also influence energy transfer, but their effects are strongly coupled to electrode gap. At narrow gaps, their impact is limited due to restricted plasma development, whereas at larger gaps their influence becomes more pronounced. This highlights the need to adjust ignition parameters dynamically based on both operating conditions and spark plug condition over time. Interestingly, neither center electrode diameter nor glow duration show a statistically significant effect on energy transfer to the gas within the tested range.

However, these parameters may still influence spark plug wear and should not be neglected.

While this analysis establishes how spark plug geometry, gas density, and ignition control parameters influence energy transfer, ignitability cannot be fully described by electrical-to-thermal energy-based considerations alone. In ultra-lean hydrogen-air mixtures, combustion stability remains strongly dependent on the subsequent development of the flame kernel, even when sufficient energy is delivered to the mixture. The following section therefore investigates ignitability limits and misfire behavior using optical diagnostics, providing direct insight into flame kernel formation and quenching mechanisms at different engine operating conditions.

6.4 Ignitability and misfire limits of hydrogen combustion

This section examines the mechanisms governing ignitability and misfire behavior in hydrogen-fueled combustion under ultra-lean conditions. The study is based on a two-stage experimental approach conducted in an optical single-cylinder Scania D13 (more details can be found in Chapter 4) heavy-duty engine. In the first stage, ignitability limits are mapped over a wide range of equivalence ratios and spark discharge parameters using both DC inductive and AC capacitive ignition systems. In the second stage, selected operating conditions are investigated using an intensified high-speed camera to directly observe early flame kernel development and identify the mechanisms responsible for misfires and combustion instability. The key operating conditions considered in this study are summarized in Table 8.

Table 8: Engine operating conditions. *Source: Paper III*

Engine speed	1200 rpm
Engine load – $IMEP_g$	4 bar & 7 bar
Skip-fire mode	1 fired cycle, 4 motored cycles
Injection pressure	18 bar (absolute)
Start of injection	- 340 CAD aTDC

6.4.1 Ignitability analysis

Ignitability was assessed through combustion stability, quantified using COV_{IMEP}. Increasing COV_{IMEP} was found to be strongly correlated with a higher frequency of misfires, indicating that combustion instability is primarily linked to unsuccessful or inconsistent flame kernel development. From the results, equivalence ratios are found to have the strongest influence on ignitability. As the mixture becomes increasingly lean, combustion stability deteriorates rapidly, with COV_{IMEP}

increasing exponentially. This behavior was independent of ignition system type and load when sufficiently high spark energy was supplied, indicating that fuel-air mixture conditions fundamentally limit ignitability.

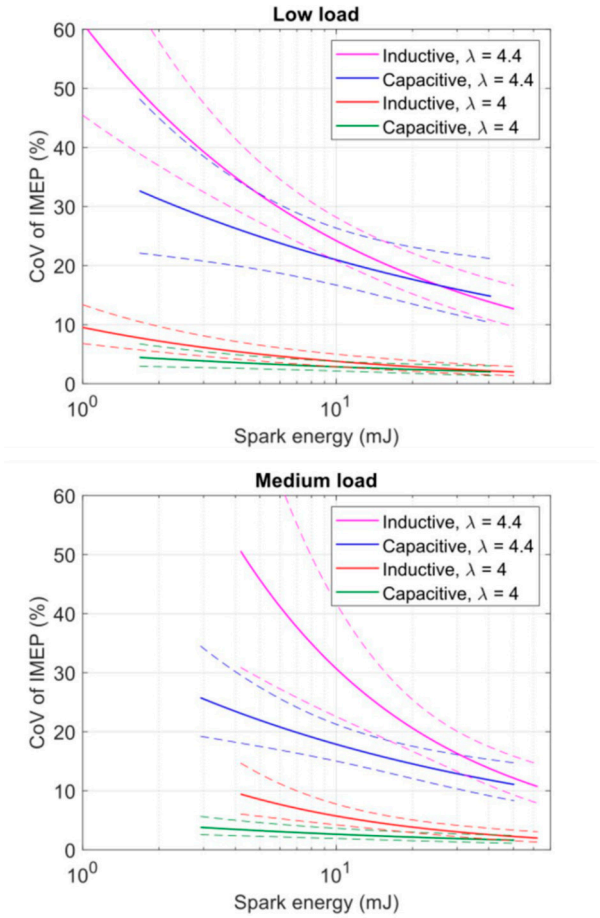

Figure 33: COV_{IMEP} as function of spark energy, for both ignition systems and two equivalence ratios and engine loads. *Source: Paper III*

Figure 33 shows the variation of COV_{IMEP} as a function of spark energy for both DC inductive and AC capacitive ignition systems at two equivalence ratios and engine loads. It is observed that both ignition systems provided similar performance at high spark energies. Once the spark energy was reduced, significant differences in ignitability emerged. The inductive system exhibited a more rapid increase in COV_{IMEP} compared to the capacitive system. This behavior indicates that spark energy alone cannot reliably predict ignitability. One contributing factor is the increased cycle-to-cycle variability in spark formation as the delivered voltage

approaches the breakdown threshold. This was detected from the spark voltage traces measured during the experiments. At low spark energies—approximately 3–4 mJ for medium load and around 1 mJ for low load—the spark initiation became increasingly unstable using the inductive system. This led to increased COV_{IMEP} even before complete spark failure occurred. In contrast, the capacitive system maintained a stable spark discharge, resulting in a slower increase in COV_{IMEP} and more consistent combustion stability across both load conditions.

A further distinction between the ignition systems is observed at intermediate spark energies, at medium load and $\lambda \approx 4.4$, where the spark discharge is relatively stable for both systems. Despite operating at similar energy levels (approximately 20 mJ), the capacitive system demonstrated improved ignitability compared to the inductive system. This difference can be attributed to the significantly lower current of the inductive system. The inductive discharge delivered a spark current of 30 mA, whereas the capacitive system delivered 2–6 times higher current at comparable energy levels due to its ability to independently control the spark parameters. The higher spark current enhances plasma channel stability, making it less susceptible to turbulence and allowing it to stretch further [], leading to improved ignitability [88].

6.4.2 Optical investigation into misfire mechanisms

To further investigate the physical mechanisms underlying misfires, an intensified high-speed camera was used to visualize early flame kernel development. This enabled direct observation of the processes that govern successful and failed ignition events. The experiments were carried out at both low and medium loads for $\lambda = 4.0$, 4.5, and 4.8 using the AC capacitive ignition system. It was found that the formation of a flame kernel did not always lead to successful ignition. In many cases, a flame kernel was formed but extinguished shortly afterwards. Two main mechanisms responsible for such misfires were identified during the investigations.

The first mechanism involves the formation of a flame kernel that is subsequently convected away from the spark plug and extinguished within a few crank angle degrees. These flame kernels were observed to move with the in-cylinder flow at relatively high velocities, indicating that convection and turbulence play a dominant role in their extinction. Under ultra-lean conditions, the flame kernel was weak and unable to sustain itself against these flow-induced losses.

The second mechanism is associated with quenching of the flame kernel within the spark plug region. In this case, the flame kernel remained in close proximity to the electrodes and was extinguished due to heat losses to the surrounding metal surfaces. The geometry of the spark plug, particularly the confined region between the central and ground electrodes, promoted such quenching, especially for weak flame kernels.

In addition to these two mechanisms, a number of misfiring cycles showed no clearly visible flame kernel. This suggests that ignition either fails at a very early stage or that the flame kernel is too weak to be detected with the optical setup used in this study. This highlights the inherent difficulty of achieving robust ignition under ultra-lean conditions.

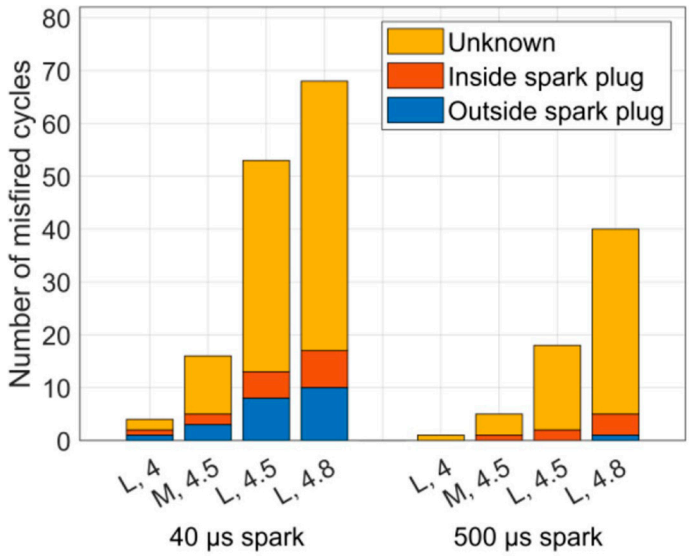

Figure 34: The number of misfired cycles identified by heat release, out of 200 cycles per run. The labels are shown as (load, lambda), where L represents low load and M represents medium load. The bars are divided into the different types of misfires: flame kernels that were extinguished in the open, flame kernels that were quenched in the spark plug, and cycles where the cause could not be determined. *Source: Paper III*

Figure 34 shows the number of misfired cycles and their classification based on the observed flame kernel behavior for two different spark durations. Notably, increasing the spark duration from 40 µs to 500 µs significantly reduced the total number of misfires, indicating that longer spark duration improves ignitability. A closer examination of the results shows that this improvement is mainly due to a reduction in misfires where the flame kernel is extinguished in the bulk flow. In other words, longer spark duration helps the flame kernel survive the effects of convection and turbulence. By providing energy over a longer time, the spark increases the chance that the flame kernel can grow into a stable flame. On the contrary, misfires caused by quenching near the electrodes are only slightly reduced when the spark duration is increased. This indicates that these ignition failures are primarily governed by the excessive heat losses to the spark plug electrodes, which are difficult to affect by longer spark duration.

Further analysis of flame kernel lifetime shows that most kernels in misfiring cycles are extinguished within 300 μs after the spark event. This suggests the flame kernels are formed during the early part of the spark and may extinguish even before the spark has ended. Therefore, the initial phase of spark discharge is critical for achieving a robust ignition, probably due to high breakdown and arc phase energy transfer efficiency.

To summarize, the results demonstrate that ignitability in hydrogen engines is governed by a complex interaction between spark characteristics, mixture conditions, and in-cylinder flow. While spark energy provides a useful first-order measure of ignitability, it does not fully capture the underlying mechanisms. Instead, successful ignition depends on the formation of a sufficiently robust flame kernel during the early stages of the spark discharge, as well as its ability to survive bulk flow/turbulence and heat losses. The findings also reveal different misfire mechanisms dominate under different conditions. At ultra-lean conditions, flame kernel extinction due to convection and turbulence becomes critical, whereas quenching effects near the spark plug are strongly influenced by electrode geometry and heat losses to the electrodes.

These insights provide an explanation for the observations in the previous sections of this chapter. In particular, they explain why increasing spark energy beyond a certain threshold does not necessarily improve combustion stability, and why independent control over spark parameters—such as spark current and duration—is essential for achieving a robust ignition while minimizing spark plug wear.

6.5 Ignitability and cycle-to-cycle variations in DI hydrogen combustion

This section extends the analysis of ignitability to a direct injection (DI) hydrogen engine operating at high load conditions. While section 6.4 focuses on flame kernel development and misfire mechanisms at low-to-medium loads, ignition behavior at high load introduces additional challenges related to mixture formation and abnormal combustion.

In hydrogen engines, port fuel injection is often limited by backfire, i.e. unintentional ignition during while the intake valve is open, leading to a flame travelling into the intake system. This restricts engine power density—a key requirement for heavy-duty applications. Direct injection after intake valve closing (IVC), or so-called early direct injection, eliminates this limitation, thereby enabling hydrogen engines to operate at higher loads. However, the risk of pre-ignition remains a concern. Due to the high reactivity of hydrogen and its strong sensitivity

to temperature, prolonged residence time of the fuel in the cylinder can increase the likelihood of unintended ignition at hot surfaces during the compression stroke.

Direct injection after the compression stroke, or so-called late direct injection, can reduce this risk by limiting the residence time of hydrogen under high-temperature conditions. At the same time, however, it reduces the available mixing time, which can lead to locally lean regions near the spark plug at ignition timing. Under such conditions, flame kernel formation becomes more sensitive to spark characteristics and in-cylinder flow, increasing the risk of combustion instability and cycle-to-cycle variations. To address these challenges, this work investigates the combined influence of λ, injection timing (IJT), and spark parameters on combustion stability and cyclic variability in a heavy-duty hydrogen DI engine at high load operation.

The study is based on an experimental investigation conducted in a single-cylinder Volvo D13 heavy-duty engine (further details are provided in Chapter 4). The key operating conditions are summarized in Table 9. An AC capacitive ignition system was used in this study, enabling independent control of spark parameters such as spark current and duration.

Table 9: Engine operating conditions. *Source: Paper V*

Engine speed (rpm)	**1400**
IMEP (bar)	12
Injection pressure (bar)	35
Intake temperature (ºC)	40 ± 2
Ignition timing	At constant CA_{50} MFB to 8ºCA aTDC

6.5.1 Combustion stability analysis

In this work, combustion stability is quantified using COV_{IMEP}, with a threshold of 2% used to define stable operation. Figure 35 shows the interaction between λ and IJT and their combined effect on combustion stability. It is observed that at moderately lean conditions ($\lambda \approx 2.0$), combustion remained stable across the investigated range of injection timings (between 180ºCA and 110ºCA bTDC). However, as the mixture became increasingly diluted, combustion stability became more sensitive to IJT. Delaying the injection led to a clear increase in COV_{IMEP}. Finally, at $\lambda \approx 2.6$, combustion was no longer within the stability threshold, even with IJT at 180ºCA bTDC. Further delaying the injection resulted in a rapid increase in COV_{IMEP} to values exceeding 5%, indicating risks of partial combustion or misfires. This behavior can be attributed to the reduced mixing time associated with late injection. When the injection is retarded, the fuel has less time to mix with air before ignition, increasing the likelihood of locally lean regions near the spark plug. These locally lean conditions make flame kernel formation increasingly difficult, leading to high combustion instability and reduced ignitability.

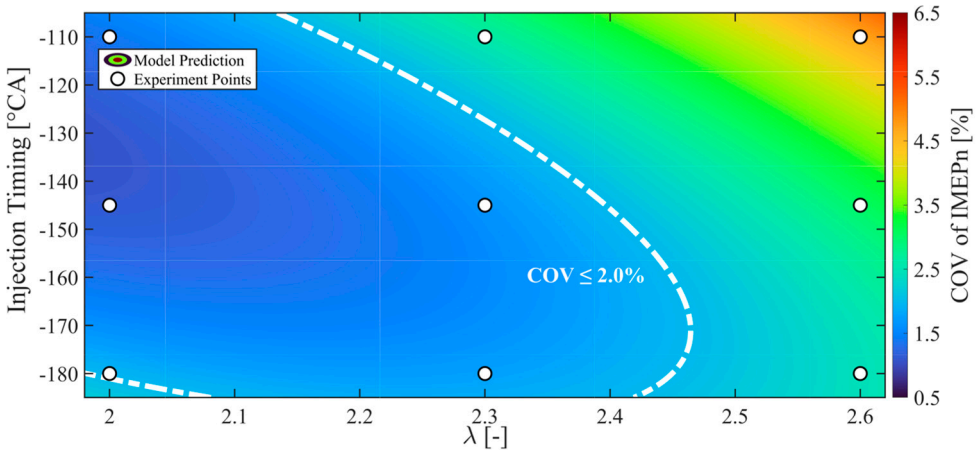

Figure 35: Interaction between λ and IJT on COV_{IMEP}, at spark current = 200mA and spark duration = 270 µs. *Source: Paper V*

In hydrogen engines, operating at lean fuel-air mixtures is desirable to increase thermal efficiency, while late injection is preferred to reduce the risk of pre-ignition. However, the combination of high dilution and late injection leads to critical conditions for achieving robust ignition. It is therefore important to assess whether spark ignition parameters can improve combustion stability at these conditions.

Figure 36 shows the interaction between λ and spark duration and their combined influence on COV_{IMEP}. At $\lambda \approx 2.0$, combustion remained stable even at the shortest spark duration (~40 µs), and increasing the spark duration had little influence on COV_{IMEP}. However, as the mixture became more diluted, combustion stability became increasingly sensitive to spark duration. As the spark duration increased, COV_{IMEP} improved significantly. At $\lambda \approx 2.6$, increasing the spark duration from 40 µs to 500 µs restores stable engine operation, bringing COV_{IMEP} below 2%. This can be explained by the longer spark duration, which provides more time for the plasma to interact with the fuel–air mixture and increases the likelihood of forming a stable flame kernel.

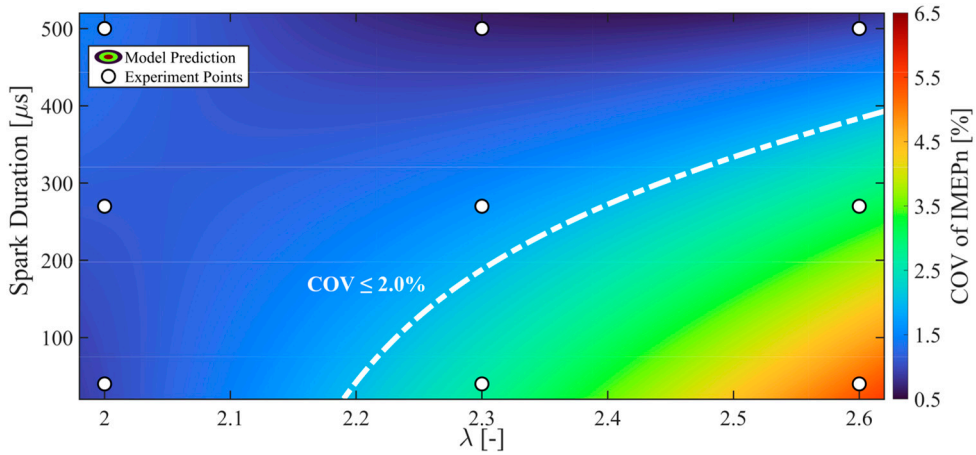

Figure 36: Interaction between λ and spark duration on COV_{IMEP}, at spark current = 200mA and IJT = 145 °CA bTDC. *Source: Paper V*

A similar trend is observed under late injection conditions, where combustion stability is further challenged by reduced mixing time. In such cases, short spark durations (~40 µs) resulted in highly unstable combustion, with COV_{IMEP} exceeding 10%. Increasing the spark duration to 500 µs significantly reduced COV_{IMEP} to below 2% and restoring stable engine operation.

6.5.2 Combustion cycle-to-cycle variations

While COV_{IMEP} is a widely used metric to quantify combustion stability, it represents only the variation in total work output and does not fully capture how combustion develops within each cycle. Figure 37 illustrates this limitation, where two operating conditions (a) and (b) with similar COV_{IMEP} exhibit noticeably different combustion behavior. Cycles with similar COV_{IMEP} can still follow different combustion paths, as variations in combustion duration may not strongly affect the total work output of an engine.

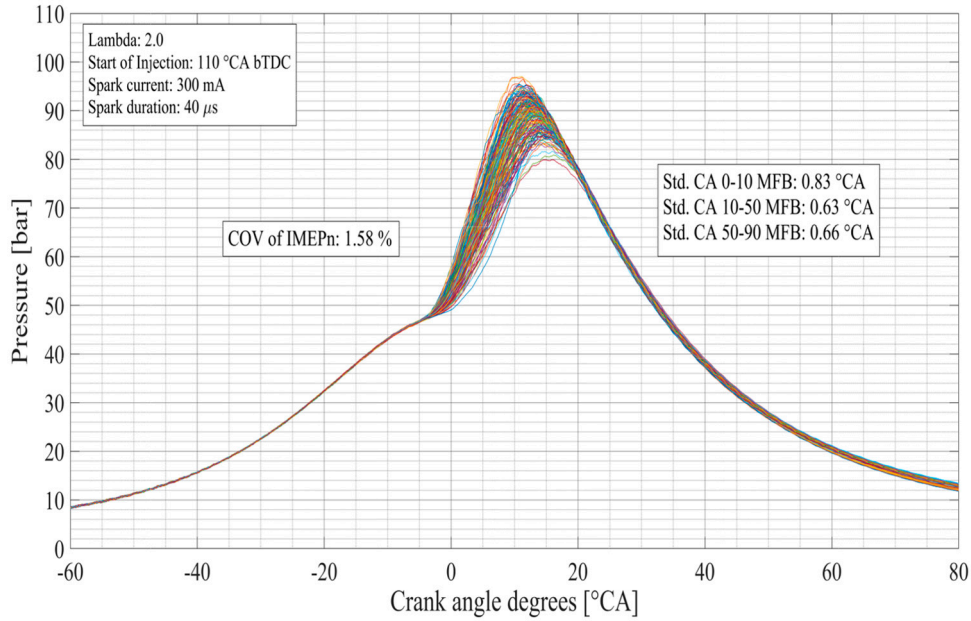

(a)

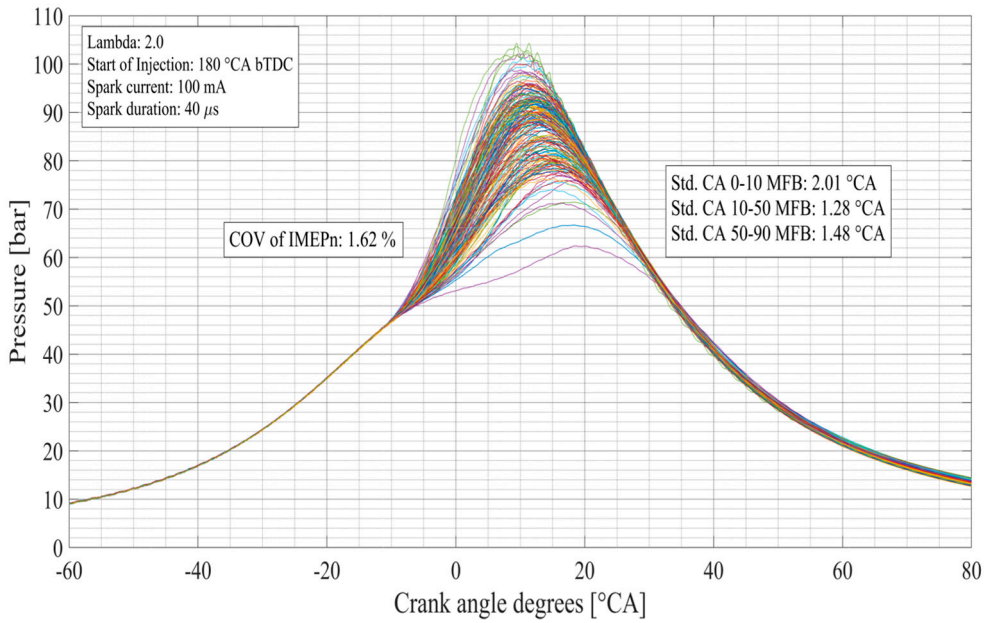

(b)

Figure 37: Pressure traces of 200 combustion cycles at: (a) λ = 2.0 and IJT = 110oCA bTDC, and (b) λ = 2.0 and IJT = 180oCA bTDC. *Source: Paper V*

Although cycle-to-cycle variations can affect the engine's thermal efficiency, they are particularly critical for hydrogen premixed combustion engines. High cyclic variability can influence the end-of-expansion temperature and can increase both residual gas and exhaust valve temperatures. Due to the strong temperature sensitivity of hydrogen ignition, high cyclic variability can increase the risk of pre-ignition and knock in subsequent cycles, especially at high-load operation.

In this study, the overall combustion duration from spark timing (ST) to 90% mass fraction burned (MFB) was divided into three sub-intervals: ST–10% MFB, 10–50% MFB, and 50–90% MFB. The standard deviation of each interval was then computed to quantify the cycle-to-cycle variability associated with each stage of the combustion process. The analysis reveal that both λ and IJT have a significant influence on cyclic variability. λ has the strongest effect, indicating that global mixture dilution primarily governs the combustion variability. IJT also affects combustion repeatability by influencing local charge conditions near the spark plug. While spark ignition parameters have limited influence under moderately lean conditions, their importance increases as the mixture becomes more diluted and less homogeneous.

Figure 38 shows the interaction between spark current and spark duration on the standard deviation of $CA_{50\text{-}90}$ MFB. Although the spark discharge has occurred during the initial stages of the combustion interval, it influences the flame kernel development, and its effect propagates into the subsequent flame propagation and late burn phases.

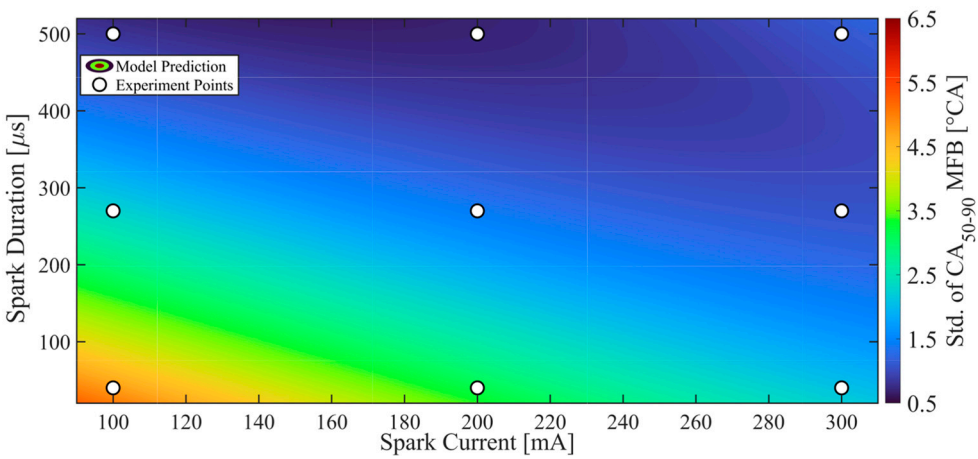

Figure 38: Interaction between spark current and spark duration on Std. of $CA_{50\text{-}90}$ MFB, at λ = 2.3 and IJT = 145 °CA bTDC. *Source: Paper V*

Interestingly, the figure shows that achieving a comparable reduction in the standard deviation requires different levels of adjustment for the two spark parameters. To

maintain std. of $CA_{50\text{-}90}$ MFB below 1°CA, the spark current needs to be increased by roughly a factor of 2.5 from its minimum settings (100 mA) while keeping the spark duration to its minimum (40 µs) possible. On the other hand, if the spark current is kept to its minimum, the spark duration must be increased by roughly a factor of eight from 40 µs to achieve similar level of combustion repeatability. The relative adjustment of spark current and duration required to reduce the cyclic variability, as shown in Figure 38, applies to the specific condition of $\lambda = 2.3$ and IJT at 145 °CA bTDC. At higher levels of dilution and delayed injection, the required adjustment for both spark parameters will tend to increase substantially, where fuel-air mixture conditions become less optimal for stable combustion.

To summarize, the results show that combustion stability in a hydrogen DI engine is primarily governed by the interaction between λ and IJT. Late injection combined with highly diluted mixtures significantly deteriorates stability by reducing mixing time and increasing the likelihood of locally lean regions near the spark plug. Under such conditions, spark parameters play an important role, with spark duration emerging as the dominant control parameter. Increasing the spark duration can significantly restore stable engine operation.

The analysis from combustion cycle-to-cycle variability identifies that COV_{IMEP} alone is not sufficient to describe combustion performance. Similar COV_{IMEP} values can still correspond to different combustion characteristics, as variations in burn durations may not strongly affect the total work output. However, such variations can be critical in hydrogen engines, since they influence temperature levels of residual gas and exhaust valves and therefore increase the risk of pre-ignition and knock in subsequent cycles. Among the investigated parameters, λ has the strongest influence on cyclic variability, indicating that global mixture dilution primarily governs combustion repeatability. IJT further affects the variability by influencing the local charge conditions near the spark plug. Spark current and duration can both be used to reduce cyclic variability under such critical conditions, although the relative adjustment required differs and becomes more pronounced as the mixture becomes increasingly diluted and less homogeneous.

A combined adjustment of spark current and duration may provide an effective approach for reducing combustion cycle-to-cycle variations. Increasing the spark current strengthens the plasma channel, while increasing the duration provides more time for the plasma to interact with the fuel–air mixture. In the end, both parameters contribute to a stable and self-sustained flame kernel development and enhance combustion repeatability. At present, their relative influence on electrode temperature and spark plug wear remains unclear. This is particularly important for hydrogen engines, where the fuel-air mixture is highly susceptible to pre-ignition. Since spark plug electrode can act as potential ignition sources, spark parameters must be carefully controlled to limit the electrodes from overheating while ensuring robust ignition.

Chapter 7
Summary

7.1 Discussion

This section discusses the key findings of the thesis by integrating results from the different experimental approaches. By combining insights from constant-volume chamber experiments, optical diagnostics, and engine studies, it provides an coherent understanding of the spark ignition process studied within this thesis across different levels of complexity.

A common understanding in SI engines is that increasing spark energy improves ignitability. This is largely based on conventional inductive ignition systems, where spark voltage, current, and duration are inherently coupled due to limited controllability. As the engine load increases, the in-cylinder gas density at the time of ignition also increases. It eventually leads to an increase in the required breakdown voltage. To meet this requirement, the ignition coil must be charged with significantly higher energy—often 10 times greater than what is needed to achieve a robust ignition, as has been shown in this thesis—which is then delivered to the gap during the spark discharge.

While inductive ignition systems are robust and widely used in light-duty engines, spark plug wear is typically not a major concern there. Passenger cars operate predominantly at low-to-medium loads and have relatively shorter engine lifetimes, typically around 300,000 km. Under these conditions, the excess spark energy does not significantly impact maintenance requirements. However, this situation is fundamentally different for heavy-duty engines. They operate predominantly at high load conditions and have significantly longer lifetimes, typically around 2,000,000 km. Under such conditions, the higher spark energy delivered by the inductive ignition systems leads to increased thermal loading of the spark plug electrode, resulting in accelerated wear. This necessitates more frequent spark plug replacement, increasing maintenance requirements and operational downtime.

At present, there is limited open literature providing quantitative information on spark plug lifetime in heavy-duty engines using inductive ignition systems. However, the spark plug wear investigations presented in this thesis clearly show that electrode erosion increases significantly over time at high-load operation.

Considering that the spark energy delivered to the gap can be an order of magnitude higher than what is required for robust ignition, this excess energy can reasonably be expected accelerate spark plug wear by a factor of five, depending on operating conditions.

In heavy-duty applications, spark plug replacement is ideally synchronized with regular maintenance events, such as oil changes, which typically occur every 80,000 km. Using an inductive ignition system, the effective spark plug lifetime can be expected to be approximately 20,000 km, leading, to additional maintenance events dedicated solely to spark plug replacement. This increases both maintenance costs and operational downtime. For a six-cylinder engine equipped with six spark plugs, each costing €100, the cost of spark plugs per replacement is €600. Including labor and downtime, the total cost per replacement can reach approximately €1400. Over the engine lifetime, these replacements outside scheduled maintenance intervals lead to an additional cost of approximately €100,000.

In addition to direct maintenance costs, spark plug replacement also leads to significant operation downtime. Over the lifetime of the engine, this can correspond to several hundred hours of lost operation, which translates into several weeks of reduced vehicle availability and revenue generation.

The results of this thesis demonstrate a capacitive ignition system with independent control of spark parameters enables a significant reduction in the spark energy delivered to the gap, while achieving robust ignition at different operating conditions. A quantitative comparison highlights the extent of this improvement. In inductive ignition systems, achieving stable ignition under high-load conditions often requires spark energies exceeding 100 mJ. In contrast, the capacitive ignition system used in this work is able to achieve comparable ignition robustness with spark energies in the range of 2–5 mJ. This reduction in excess spark energy has direct implications for spark plug durability. By minimizing unnecessary thermal loading of the electrodes, the rate of electrode erosion can be significantly reduced. As a result, spark plug lifetime can be extended, reducing the need for standalone maintenance events and improving the overall transport efficiency in heavy-duty applications.

However, there is a trade-off between initial investment cost of the ignition systems and operating cost associated with spark plug replacement over the engine lifetime. Inductive ignition systems are relatively simple and cheap. However, as discussed above, they tend to increase operational costs over the engine lifetime. In contrast, capacitive ignition systems with independent control of spark parameters require more complex hardware, including a dedicated ignition control module (ICM), resulting in higher initial system cost. Nevertheless, the ability to precisely control spark parameters enable a significant reduction in electrode wear, extending maintenance intervals and reducing downtime. When evaluated over the full engine lifetime, these benefits offset the higher initial investment.

Besides spark plug wear, hydrogen heavy-duty engines face an additional challenge. This is particularly evident in hydrogen premixed combustion, where the propensity for pre-ignition at high load operation limit hydrogen engines from achieving power density levels comparable to modern diesel engines. Late DI can minimize such risks by shortening the residence time of the fuel-air mixture before ignition. However, it can significantly affect ignitability likely due to poor mixture conditions close to the spark plug. This thesis finds that spark parameters can play a critical role in addressing these limitations. More specifically, appropriate tuning of both spark current and duration can significantly improve ignitability at unfavorable mixture conditions while maintaining low spark energy levels. Therefore, a high degree of control over spark parameters can be beneficial, not only for decelerating spark plug wear, but also for achieving robust DI hydrogen combustion at high-load operation without overheating the spark plugs.

7.2 Limitations and future work

Within the scope of this thesis, the effect of local flow and turbulence on the spark ignition process is not fully captured. The spark calorimeter utilized to study the energy transfer from spark to the gas was based on a quiescent chamber configuration, where no bulk flow was present. This configuration enables accurate and repeatable measurements of spark-induced pressure rise. However, introducing flow into the calorimeter added significant technical challenges. The pressure rise associated with spark energy deposition is relatively small, and the presence of flow introduced additional pressure fluctuations and measurement noise. As a result, it became difficult to distinguish the pressure signal caused by the spark from flow-induced disturbances, complicating the interpretation of the measured spark energy deposition. In addition, both the biogas and hydrogen engines considered were based on heavy-duty diesel platforms, which employed low-swirl cylinder head designs. Increasing swirl or introducing tumble-enhancing cylinder head designs is currently an active area of investigation, as enhanced in-cylinder flow promotes better fuel–air mixing. This can enable greater flexibility in injection timing, including the possibility of much later injection without significantly compromising mixture quality near the spark plug. However, elevated in-cylinder flow in the vicinity of the spark plug can affect energy deposition from the spark to the fuel-air mixture. In particular, strong flow can stretch the plasma channel, increase the likelihood of spark blow-out long before stable flame kernel formation, and thereby increase the risk of misfire.

This thesis evaluates the influence of the electrode gap and center electrode diameter on the spark energy deposition to the gas. However, the broader influence of spark plug electrode geometry on the ignitability of hydrogen and biogas engines is not fully assessed, mainly due to the limited availability of spark plugs with systematically varied designs. This remains an important limitation, since electrode

geometry directly affects the local electric field distribution, breakdown behaviour, and subsequent spark plasma development. These factors strongly influence how effectively electrical energy is coupled to the fuel-air mixture during ignition. As a result, variations in electrode geometry can affect ignition robustness, the required spark energy, and the sensitivity of the ignition process to operating conditions such as gas density and local flow at spark timing.

Therefore, to build on the findings of this work, several promising avenues for future research are identified:

- Further investigation is required to understand the influence of in-cylinder flow and turbulence on spark ignition. Therefore, future work should focus on extending the spark calorimeter measurements to controlled flow conditions or developing alternative diagnostic approaches capable of isolating spark-induced energy deposition in the presence of flow.
- Further work is required to systematically investigate the influence of spark plug electrode designs on ignitability of hydrogen and biogas SI engines. Therefore, a wider range of electrode designs should be considered to better understand their effect on the electric field distribution and spark plasma development at different operating conditions.
- Idling conditions in biogas engines represent an important operating regime for heavy-duty applications and should be investigated. Under such conditions, the low gas density and unfavorable mixture formation make it challenging to achieve stable combustion.
- This thesis has investigated the ignitability of a hydrogen DI engine at a load of 12 bar $IMEP_g$ at 1400 RPM. However, heavy-duty engines operate over a wider range of high-load conditions, where ignition becomes challenging due to increased gas density. Further investigation at higher load levels is therefore recommended to assess the effectiveness of spark parameter control in achieving robust ignition without excessive thermal loading of the spark plug electrode.

7.3 Conclusions

This thesis has investigated the spark ignition process in heavy-duty engines operating on hydrogen and biogas, with a focus on achieving stable combustion while minimizing spark plug overheating and wear. The work combines experimental studies in constant-volume chambers, optical diagnostics, and engine-based investigations to improve understanding of ignitability over a wide range of operating conditions. Based on the results presented in this thesis, the following main conclusions can be drawn:

Role of spark energy in ignition

Robust spark ignition is not governed by the total spark energy delivered to the gap, but by how the energy is delivered during the discharge. Once a stable and self-sustained flame kernel is formed, additional spark energy does not improve combustion stability. Instead, excess energy leads to increased thermal loading of the spark plug electrodes and accelerated wear.

Energy transfer from spark to gas

The efficiency of energy transfer from the spark to the gas depends strongly on how the energy is distributed over the duration of the spark. The initial phases of the spark discharge–breakdown and arc–are highly efficient in transferring energy to the gas but are short-lived and largely governed by system conditions. In contrast, the glow phase provides greater controllability but contributes less efficiently to energy deposition to the gas. Moreover, increasing glow current or duration beyond a certain threshold does not improve energy deposition, but instead increases thermal losses to the electrodes. Moreover, energy transfer from the spark to the gas is governed by the combined effect of multiple parameters rather than individual spark parameters. Both spark plug electrode diameter and gas density at the time of ignition interact with electrical spark parameters to govern the effectiveness of energy deposition to the gas.

Early flame kernel development in hydrogen combustion

Ignitability is primarily governed by the early development of the flame kernel. At ultra-lean conditions, flame kernels are weak and can be extinguished either due to in-cylinder flow at relatively high velocities or due to the heat losses to the surrounding metal surfaces of the spark plug electrode. Moreover, the flame kernel extinction occurs within a very short time after the spark event, often before the spark has fully ended. This indicates that the initial phases of the spark, during which the plasma is most energetic, are critical for achieving a self-sustained flame kernel.

Ignitability of hydrogen DI combustion

Combustion stability in hydrogen DI engine is governed by the interaction between mixture preparation and ignition control. Under non-ideal conditions, such as high dilution and limited mixing due to delayed injection, ignition becomes increasingly sensitive to local conditions near the spark plug. In such conditions, appropriate control of spark parameters is essential to maintain a stable combustion without excessive thermal loading of the electrodes. While COV_{IMEP} is a widely used metric to define combustion stability, it has been found to be not sufficient enough to fully describe the combustion behavior. Similar values of COV_{IMEP} can correspond to different combustion characteristics, as cycle-to-cycle variations in burn duration may not significantly affect the total work output of an engine. However, these variations can strongly affect in-cylinder thermal conditions, thereby increasing the

risk of pre-ignition and knock, particularly in hydrogen engines. Minimizing the cyclic variability requires coordinated adjustment of spark parameters, particularly the current and the duration, with the required level of control becoming more pronounced as the mixture becomes increasingly diluted and less homogeneous.

7.4 Thesis contributions

- This thesis provides a new perspective towards ignitability in hydrogen and biogas SI engines, shifting the focus from increasing spark energy to how the spark is controlled through its parameters.
- It provides experimental quantification of energy transfer from the spark to the gas at different phases of the spark discharge.
- Through systematic experimental design, this thesis establishes closely-coupled interactions between multiple physical and electrical spark parameters in governing energy deposition to the gas.
- Using optical diagnostics, this thesis identifies two dominant mechanisms responsible for misfires in hydrogen premixed combustion at ultra-lean conditions. Additionally, it finds COV_{IMEP} alone is not a sufficient metric to characterize combustion behavior in hydrogen DI engines, and therefore recommends the use cycle-to-cycle variations of burn duration different stages for a more comprehensive analysis. This is particularly important for high-load operations, where such variations can increase the risk of combustion anomalies, including pre-ignition and knock.

References

1. H. Ritchie, M. Roser and P. Rosado, "Emissions by sector: where do greenhouse gases come from?," OurWorldInData.org, 2020. [Online]. Available: https://ourworldindata.org/emissions-by-sector. [Accessed 27th March 2024].
2. United Nations, "Kyoto Protocol to the United Nations Framework Convention on Climate Change," 1998.
3. H. Ritchie, "Cars, planes, trains: where do CO2 emissions from transport come from?," OurWorldInData.org, 2020. [Online]. Available: https://ourworldindata.org/co2-emissions-from-transport. [Accessed 27th March 2024].
4. Wilkinson, M., Darton, R., Pritchard, C., Knowles, E., Montoro, A., & Petit, C. (2021). Decarbonisation of End Uses. TCE: The Chemical Engineer.
5. Steentjes, K., Pidgeon, N. F., Poortinga, W., Corner, A. J., Arnold, A., Böhm, G., ... & Tvinnereim, E. (2017). *European Perceptions of Climate Change (EPCC): Topline findings of a survey conducted in four European countries in 2016.*
6. Elkerbout, M., Egenhofer, C., Rizos, V., & Bryhn, J. (2021). European Green Deal. *Towards a resilient and sustainable post-pandemic recovery, CEPS Task Force Working Group Report*.
7. European Parliament. (2019, March 22). *CO_2 emissions from cars: facts and figures (infographics)*.https://www.europarl.europa.eu/topics/en/article/20190313STO31218/co2-emissions-from-cars-facts-and-figures-infographics.
8. Broekaert, S., & Fontaras, G. (2022). CO2 emissions of the European heavy-duty vehicle fleet.
9. Regulation (EU) 2019/1242 of the European Parliament and of the Council of 20 June 2019 setting CO2 emission performance standards for new heavy-duty vehicles and amending Regulations (EC) No 595/2009 and (EU) 2018/956 of the European Parliament and of the Council and Council Directive 96/53/EC.
10. European Commission. *Reducing CO_2 emissions from heavy-duty vehicles*. Reducing CO_2 emissions from heavy-duty vehicles (europa.eu).
11. Ö. Andersson and P. Börjesson, "*The greenhouse gas emissions of an electrified vehicle combined with renewable fuels: Life cycle assessment and policy implications*" Applied Energy, vol. 289, p. 116621, 2021.
12. Philibert, C. "Direct And Indirect Electrification Of Industry And Beyond". Oxford Review Of Economic Policy, 04 2019, Vol. 35, No. 2, P. 197–217, Issn 0266-903x, Doi:10.1093/Oxrep/Grz006.

13. Al-Hanahi, B., Ahmad, I., Habibi, D., Et Al. ”Charging Infrastructure For Commercial Electric Vehicles: Challenges And Future Works”. Ieee Access, 2021, Vol. 9, P. 121476–121492, Doi:10.1109/Access.2021.3108817.
14. Cullen,D.A., Neyerlin,K.C., Ahluwalia,R.K.,Etal.”Newroads Andchallenges For Fuel Cells In Heavy-Duty Transportation”. Nature Energy, 2021, Vol. 6, No. 5, P. 462–474, Doi:10.1038/S41560-021-00775-Z.
15. Stępień, Z. (2021). *A comprehensive overview of hydrogen-fueled internal combustion engines: achievements and future challenges.* Energies, 14(20), 6504.
16. Lohse-Busch, H., Stutenberg, K., Duoba, M., Liu, X., Elgowainy, A., Wang, M., ... & Christenson, M. (2020). *Automotive fuel cell stack and system efficiency and fuel consumption based on vehicle testing on a chassis dynamometer at minus 18 C to positive 35 C temperatures.* International Journal of Hydrogen Energy, 45(1), 861-872.
17. Sharaf, O. Z. And Orhan, M. F. ”An Overview Of Fuel Cell Technology: Fundamentals And Applications”. Renewable And Sustainable Energy Reviews, 2014, Vol. 32, P. 810–853, Doi:10.1016/J.Rser.2014.01.012.
18. Doppler, C. And Lindner-Rabl, B. ”Fuel Cell Trucks: Thermal Chal Lenges In Heat Exchanger Layout”. Energies, 2023, Vol. 16, No. 10, Issn 1996 1073, Doi:10.3390/En16104024.
19. Agarwal, A. K., Mounaïm-Rousselle, C., Brequigny, P., Dhar, A., Hespel, C., Patel, C., & Valera, H. (2025). Future of internal combustion engines using sustainable, scalable, and storable E-fuels and biofuels for decarbonizing transport and enabling advanced combustion technologies. *Progress in Energy and Combustion Science*, *110*, 101236.
20. Reitz, R. D., Ogawa, H., Payri, R., Fansler, T., Kokjohn, S., Moriyoshi, Y., ... & Zhao, H. (2020). IJER editorial: The future of the internal combustion engine. *International Journal of Engine Research*, *21*(1), 3-10.
21. Gong, M. (2025). *Decarbonizing heavy-duty engines: advanced optical diagnostics for sustainable gaseous fuel combustion*. Lund University.
22. SHARMA, S. and GHOSHAL, S. K. ”Hydrogen the future transportation fuel: From production to applications”. Renewable and Sustainable Energy Re views, 2015, vol. 43, p. 1151–1158, ISSN 1364-0321, doi:10.1016/j.rser.2014.11.093.
23. KALGHATGI, G., AGARWAL, A. K., LEACH, F., et al. Engines and fuels for future transport. Springer Singapore, 2021. doi:10.1007/978-981-16-8717-4, ISBN 978-981-16-8716-7.
24. SANTHOSH, J., SARKAR, O., and MOHAN, S. V. ”Green Hydrogen Compressed natural gas (bio-H-CNG) production from food waste: Organic load influence on hydrogen and methane fusion”. Bioresource Technology, 2021, vol. 340, p. 125643, doi:10.1016/j.biortech.2021.125643.
25. NEMMOUR,A., INAYAT, A., JANAJREH, I., et al. ”Green hydrogen-based E-fuels (E-methane, E-methanol, E-ammonia) to support clean energy tran sition: A literature review”. International Journal of Hydrogen Energy, 2023, vol. 48, no. 75, p. 29011–29033, doi:10.1016/j.ijhydene.2023.03.240.

26. NIKOLAIDIS, P. and POULLIKKAS, A. ”A comparative overview of hydro gen production processes”. Renewable and sustainable energy reviews, 2017, vol. 67, p. 597–611, doi:10.1016/j.rser.2016.09.044.
27. Lou, D., Ren, Y., Zhang, Y., & Sun, X. (2020). Study on the Effects of EGR and Spark Timing on the Combustion, Performance, and Emissions of a Stoichiometric Natural Gas Engine. ACS omega.
28. Ängeby, J., Tidholm, J., Gustafsson, B., and Johnsson, A., “Ignition Systems for SI-ICE Fueled by Alternative and Renewable Fuels,” in:, *Internal Combustion Engine Division Fall Technical Conference*. Vol. 87561, (American Society of Mechanical Engineers, 2023, October), V001T03A005.
29. Mazloomi, K. and Gomes, C., “Hydrogen as an Energy Carrier: Prospects and Challenges,” *Renewable and Sustainable Energy Reviews* 16, no. 5 (2012): 3024-3033.
30. J. B. Heywood, “Internal Combustion Engine Fundamentals” 2018 ISBN 1-260-11610-7.
31. Duong, J. (2013). Combustion visualization in a large bore gas engine. Division of Combustion Engines, Department of Energy Sciences, Faculty of Engineering (LTH), Lund University.
32. Saha, A. (2021). Ignitability Study of a Spark-ignited Heavy-duty Engine, fueled with Natural Gas (CNG).
33. Tatsch, G. A., (Dwell Calibration DTEC (www.dtec.net.au))s, M. E. S., Lanzanova, T., Sari, R. L., Taglieber, V. H., & Görck, C. L. (2014). Cylinder Pressure Based Engine Calibration of a Formula SAE Racing Engine (No. 2014-36-0350). SAE Technical Paper.
34. Verhelst, S. and Turner, J.W.G., “Hydrogen-Fueled Spark Ignition Engines,” in: Tingas, E.A. (Eds), Hydrogen for Future Thermal Engines, (Cham: Green Energy and Technology. Springer, 2023). https://doi.org/10.1007/978- 3-031-28412-0_8.
35. Ängeby, J., Saha, A., Björnsson, O., & Lundgren, M. (2022, April). Spark ignition-searching for the optimal spark profile. In *International ATZ Conference* (pp. 397-414). Wiesbaden: Springer Fachmedien Wiesbaden.
36. Nishioka, S., Hanashi, K., and Okabe, S., “Super Ignition Spark Plug with Wear Resistive Electrode,” SAE Technical Paper 2008-01-0092 (2008, 2008), https://doi.org/10.4271/2008-01-0092.
37. Hori, T., Shibata, M., Okabe, S., & Hashizume, K. (2003). Super ignition spark plug with fine center & ground electrodes (No. 2003-01-0404). SAE Technical Paper.
38. Rager, J., Böhm, J., Kaiser, T., Flaig, A., & Mücklich, F. (2006). Design and Materials for Long-Life Spark Plugs (No. 2006-01-0617). SAE Technical Paper.
39. Ängeby, J., Gustafsson, B., & Johnsson, A. (2023). Ignition Control Module for Hydrogen Combustion Engines. *MTZ worldwide*, *84*(10), 48-53.
40. Machač, J. and Majer, M., “Hydrogen Fuel in Transportation,” *Multidisciplinary Aspects of Production Engineering* 2, no. 1 (2019): 161-171.
41. Verhelst, S. and Wallner, T., “Hydrogen-Fueled Internal Combustion Engines,” *Progress in Energy and Combustion Science* 35, no. 6 (2009): 490-527.

42. Stockhausen, W.F., Natkin, R.J., AND Reams, L., Crankcase ventilation system for a hydrogen fueled engine. US Patent 6,606,982 B1, August 2003.
43. Giuliano, G., Dessouky, M., Dexter, S., Fang, J., Hu, S., & Miller, M. (2021). Heavy-duty trucks: The challenge of getting to zero. *Transportation Research Part D: Transport and Environment*, *93*, 102742.
44. Moultak, M., Lutsey, N., & Hall, D. (2017, September). Transitioning to zero-emission heavy-duty freight vehicles. Washington, DC, USA: ICCT.
45. Cunanan, C., Tran, M. K., Lee, Y., Kwok, S., Leung, V., & Fowler, M. (2021). A review of heavy-duty vehicle powertrain technologies: Diesel engine vehicles, battery electric vehicles, and hydrogen fuel cell electric vehicles. *Clean Technologies*, *3*(2), 474-489.
46. Pelletier, S., Jabali, O., & Laporte, G. (2014). *Battery electric vehicles for goods distribution: a survey of vehicle technology, market penetration, incentives and practices* (Vol. 43). Montreal, Canada: Cirrelt.
47. Ehsani, M., Gao, Y., Longo, S., & Ebrahimi, K. (2018). Modern electric, hybrid electric, and fuel cell vehicles. CRC press.
48. Wen, J. P., & Zhang, C. W. (2015). Research on modeling and control of regenerative braking for brushless DC machines driven electric vehicles. *Mathematical Problems in Engineering*, *2015*(1), 371725.
49. Chan, C. C. (2007). The state of the art of electric, hybrid, and fuel cell vehicles. *Proceedings of the IEEE*, *95*(4), 704-718.
50. Huang, W. D., & Zhang, Y. P. (2011). Energy efficiency analysis: biomass-to-wheel efficiency related with biofuels production, fuel distribution, and powertrain systems. *PLoS One*, *6*(7), e22113.
51. Yang, J. D., Millichamp, J., Suter, T., Shearing, P. R., Brett, D. J., & Robinson, J. B. (2023). A review of drive cycles for electrochemical propulsion. *Energies*, *16*(18), 6552.
52. Kalghatgi, G. (2018). Is it really the end of internal combustion engines and petroleum in transport?. *Applied energy*, *225*, 965-974.
53. Svensson, M. (2024). *Assessing single-fuel solutions enabling compression ignition of renewable methanol*. Lund University.
54. Han, X.; Lu, L.; Zheng, Y.; Feng, X.; Li, Z.; Li, J.; Ouyang, M. A review on the key issues of the lithium ion battery degradation among the whole life cycle. ETransportation 2019, 1, 100005.
55. Tran, M. K., & Fowler, M. (2020). A review of lithium-ion battery fault diagnostic algorithms: Current progress and future challenges. *Algorithms*, *13*(3), 62.
56. El Helou, R., Sivaranjani, S., Kalathil, D., Schaper, A., & Xie, L. (2022). The impact of heavy-duty vehicle electrification on large power grids: A synthetic Texas case study. *Advances in Applied Energy*, *6*, 100093.
57. Lai, J. S., & Ellis, M. W. (2017). Fuel cell power systems and applications. *Proceedings of the IEEE*, *105*(11), 2166-2190.

58. Aminudin, M. A., Kamarudin, S. K., Lim, B. H., Majilan, E. H., Masdar, M. S., & Shaari, N. (2023). An overview: Current progress on hydrogen fuel cell vehicles. *International Journal of Hydrogen Energy*, *48*(11), 4371-4388.
59. Lohse-Busch, H., Stutenberg, K., Duoba, M., Liu, X., Elgowainy, A., Wang, M., ... & Christenson, M. (2020). *Automotive fuel cell stack and system efficiency and fuel consumption based on vehicle testing on a chassis dynamometer at minus 18 C to positive 35 C temperatures.* International Journal of Hydrogen Energy, 45(1), 861-872.
60. Ohi, J. M., Vanderborgh, N., & Voecks, G. (2016). Hydrogen fuel quality specifications for polymer electrolyte fuel cells in road vehicles. *US DOE EERE*.
61. Stępień, Z. (2021). *A comprehensive overview of hydrogen-fueled internal combustion engines: achievements and future challenges.* Energies, 14(20), 6504.
62. Hames, Y., Kaya, K., Baltacioglu, E., & Turksoy, A. (2018). Analysis of the control strategies for fuel saving in the hydrogen fuel cell vehicles. *International Journal of Hydrogen Energy*, *43*(23), 10810-10821.
63. Apostolou, D., & Xydis, G. (2019). A literature review on hydrogen refuelling stations and infrastructure. Current status and future prospects. *Renewable and Sustainable Energy Reviews*, *113*, 109292.
64. Appl-Scorza, S., Lippelt, J., & Littlejohn, C. (2018). Challenges of electrification of heavy and long-haul traffic. In *CESifo Forum* (Vol. 19, No. 4, pp. 46-59). München: ifo Institut–Leibniz-Institut für Wirtschaftsforschung an der Universität München.
65. Verhelst, S. (2014). Future vehicles will be driven by electricity, but not as you think [Point of View]. *Proceedings of the IEEE*, *102*(10), 1399-1403.
66. Mallouppas, G., & Yfantis, E. A. (2021). Decarbonization in shipping industry: A review of research, technology development, and innovation proposals. Journal of marine science and engineering, 9(4), 415.
67. Saha, A., Ojanperä, A. M., Hyvonen, J., Aengeby, J., Tidholm, J., Andersson, O., & Tunestal, P. (2023). *The influence of ignition control parameters on combustion stability and spark plug wear in a large bore gas engine* (No. 2023-01-0257). SAE Technical Paper.
68. Vasan, V., Sridharan, N. V., Feroskhan, M., Vaithiyanathan, S., Subramanian, B., Tsai, P. C., ... & Ponnusamy, V. K. (2024). Biogas production and its utilization in internal combustion engines-a review. *Process Safety and Environmental Protection*, *186*, 518-539.
69. Nemmour, A., Inayat, A., Janajreh, I., & Ghenai, C. (2023). Green hydrogen-based E-fuels (E-methane, E-methanol, E-ammonia) to support clean energy transition: A literature review. *International Journal of Hydrogen Energy* *48*(75), 29011-29033.
70. Gunatilleke, B., Robinson, C., Scott, S., Arambel, A., & Alotaibi, D. (2024). Liquefied Natural Gas (LNG).
71. Khan, M. I., Yasmin, T., & Shakoor, A. (2015). Technical overview of compressed natural gas (CNG) as a transportation fuel. Renewable and Sustainable Energy Reviews, 51, 785-797.

72. Aakko-Saksa, P., Koponen, P., Roslund, P., Laurikko, J., Nylund, N. O., Karjalainen, P., ... & Timonen, H. (2020). Comprehensive emission characterisation of exhaust from alternative fuelled cars. *Atmospheric environment*, *236*, 117643.
73. Kalaskar, V., Conway, G., Handa, G., Joo, S., & Williams, D. (2023). Challenges and Opportunities with Direct-Injection Hydrogen Engines. SAE Technical Paper, (2023-01-0287).
74. Kahraman, E., Ozcanlı, S. C., & Ozerdem, B. (2007). An experimental study on performance and emission characteristics of a hydrogen fuelled spark ignition engine. *International journal of hydrogen energy*, *32*(12), 2066-2072.
75. Verhelst, S., & Wallner, T. (2009). Hydrogen-fueled internal combustion engines. *Progress in energy and combustion science*, *35*(6), 490-527.
76. Hosseini, S. E. (2023). *Fundamentals of hydrogen production and utilization in fuel cell systems*. Elsevier.
77. Machač, J., & Majer, M. (2019). *Hydrogen fuel in transportation.* Multidisciplinary Aspects of Production Engineering, *2*(1), 161-171.
78. Mazloomi, K., & Gomes, C. (2012). Hydrogen as an energy carrier: Prospects and challenges. Renewable and Sustainable Energy Reviews, 16(5), 3024-3033.
79. Reinmann, R. (1998). *Theoretical and experimental studies of the formation of ionized gases in spark ignition engines*. Lund University.
80. Mitianiec, W. (2012). *Factors Determining Ignition and Efficient Combustion in Modern Engines Operating on Gaseous Fuels*. Internal Combustion Engines, *9*(51000), 3-34.
81. Maly, R. (1984). *Spark ignition: its physics and effect on the internal combustion engine. In Fuel economy* (pp. 91-148). Springer, Boston, MA.
82. Abe, Y., Sugiura, A., Doi, K., Shibata, M., Yokoo, N., & Nakata, K. (2015). *Study of ignition system for demand voltage reduction* (No. 2015-01-0777). SAE Technical Paper.
83. A. Anders. Glows, arcs, ohmic discharges: An electrode-centered review on dis charge modes and the transitions between them. Applied Physics Reviews, 11(3):031310, September 2024.
84. Zhang, K. (2025). *Laser-based Optical Diagnostics of Electrode Wear: A Pioneering Work*. Lund University.
85. Soldera, F. A., Mucklich, F. T., Hrastnik, K., Kaiser, T.: Description of the discharge process in spark plugs and its correlation with the electrode erosion patterns. IEEE transactions on vehicular technology, 53(4), pp. 1257-1265. (2004).
86. Schneider, A., Leick, P., Hettinger, A., Rottengruber, H.: Experimental studies on spark stability in an optical combustion vessel under flowing conditions. In: Internationaler Motorenkongress. pp. 327-348. Springer, Wiesbaden (2016).
87. Suzuki, K., Uehara, K., Murase, E., & Nogawa, S.: Study of ignitability in strong flow field. In: International Conference on Ignition Systems for Gasoline Engines, pp. 69-84. Springer, Cham (2016).

88. Zhu, H., Tan, Q., Yu, X., Yang, Z., Liang, L., Zheng, M., Qian, J.: Impact of Spark Plasma Length on Flame Kernel Development under Flow Condition. SAE International Journal of Advances and Current Practices in Mobility, 2(2020-01-1114), 2172-2182. (2020).
89. (Dwell Calibration DTEC (www.dtec.net.au)).
90. Ängeby, J., Johnsson, A., SEM, J. T., Zhang, K., Richter, M., & Ehn, A. (2024, October). Robust ignition and sparkplug wear for H2 SI-ICE. In *6th International Conference on Ignition Systems for SI Engines—7th International Conference on Knocking in SI Engines* (p. 81). Berlin, Germany: Expert Verlag.
91. Ängeby, J. (2021). Spark Ignition System for Alternative Fuels–Robust Ignition, Minimized Spark Plug Wear and Combustion Process Diagnostics. In *Internationaler Motorenkongress 2021* (pp. 345-368). Wiesbaden: Springer Fachmedien Wiesbaden.
92. Franke, A., & Reinmann, R. (2000, March). Calorimetric characterization of commercial ignition systems. In *SAE 2000 World Congress*. SAE Technical Paper.
93. Chen, L., Wei, H., Zhang, R., Pan, J., Zhou, L., & Feng, D. (2019). Effects of spark plug type and ignition energy on combustion performance in an optical SI engine fueled with methane. *Applied Thermal Engineering*, *148*, 188-195.
94. Zhang, X., & Chen, L. (2023). The synergy effect of ignition energy and spark plug gap on methane lean combustion with addressing initial flame formation and cyclic variation. *ACS omega*, *8*(7), 7036-7044.
95. Cruccolini, V., Discepoli, G., Cimarello, A., Battistoni, M., Mariani, F., Grimaldi, C. N., & Dal Re, M. (2020). Lean combustion analysis using a corona discharge igniter in an optical engine fueled with methane and a hydrogen-methane blend. *Fuel*, *259*, 116290.
96. Ricci, F., Zembi, J., Avana, M., Grimaldi, C. N., Battistoni, M., & Papi, S. (2024). Analysis of hydrogen combustion in a spark ignition research engine with a barrier discharge igniter. *Energies*, *17*(7), 1739.
97. Hori, T., Shibata, M., Okabe, S., & Hashizume, K. (2003). Super ignition spark plug with fine center & ground electrodes (No. 2003-01-0404). SAE Technical Paper.
98. Nishioka, S., Hanashi, K., & Okabe, S. (2008). Super ignition spark plug with wear resistive electrode (No. 2008-01-0092). SAE Technical Paper.
99. Alashaab, A., Salem, H., Abo-Serie, E., Rabee, B., & Aal, M. A. (2016). Gaseous fuel for improving cold starting and reducing emissions of gasoline engines. International Journal of Global Warming.
100. Kim, K., Hall, M. J., Wilson, P. S., & Matthews, R. D. (2020). Arc-phase spark plug energy deposition characteristics measured using a spark plug calorimeter based on differential pressure measurement. *Energies*, *13*(14), 3550.
101. Discepoli, G., Cruccolini, V., Dal Re, M., Zembi, J., Battistoni, M., Mariani, F., & Grimaldi, C. N. (2018). Experimental assessment of spark and corona igniters energy release. *Energy Procedia*, *148*, 1262-1269.
102. Wärtsilä Corporation. (2018, March 28). *Orders stream in for Wärtsilä 31*. Wärtsilä Insights. https://www.wartsila.com/insights/article/orders-stream-in-for-wartsila-31

103. Taylor, C. J., Pomberger, A., Felton, K. C., Grainger, R., Barecka, M., Chamberlain, T. W., ... & Lapkin, A. A. (2023). A brief introduction to chemical reaction optimization. *Chemical Reviews*, *123*(6), 3089-3126.

104. Kyprianou, D., Rarata, G., Emma, G., Diaconu, G., Vahcic, M., & Anderson, D. (2022). Flow chemistry and the synthesis of energetic materials. *Publications Office of the European Union: Luxembourg*.

105. Andersson, O. (2012). *Experiment!: planning, implementing and interpreting*. John Wiley & Sons.

106. Box, G. E., Hunter, J. S., & Hunter, W. G. (2005). *Statistics for experimenters: design, innovation, and discovery*. John Wiley & Sons.

107. Evro, S., Ajumobi, A., Mayon, D., & Tomomewo, O. S. (2024). *Navigating battery choices: A comparative study of lithium iron phosphate and nickel manganese cobalt battery technologies*. *Future Batteries*, *4*, 100007.

108. Integrated Engineering. (n.d.). *Advanced spark plug reading*. IE Auto Blog. https://performancebyie.com/blogs/ie-auto-blog/advanced-spark-plug-reading

Scientific publications

Author contributions

Co-authors are abbreviated as follows: Jakob Ängeby (JÄ), Peter Hallstadius (PH), Ari-Matti Ojanperä (AO), Elvin Zanjani (EZ).

Paper I

The Influence of Ignition Control Parameters on Combustion Stability and Spark plug Wear in a Large Bore Gas Engine
A. Saha, A. Ojanperä, J. Hyvonen, J. Ängeby, J. Tidholm, Ö. Andersson, P. Tunestål
SAE Technical Paper 2023-01-0257, 2023, https://doi.org/10.4271/2023-01-0257

I designed and conducted the experiment together with AO. I then performed the data analysis, wrote the manuscript, and revised it following peer review on my own. AO and the other co-authors reviewed the manuscript and provided their feedback.

Paper II

Characterization of Spark Ignition Energy Transfer at Different Phases Using Pressure-Rise Calorimetry
A. Saha, P. Tunestål, J. Ängeby, Ö. Andersson
SAE Technical Paper 2025-01-8402, 2025, https://doi.org/10.4271/2025-01-8402

JÄ and I jointly designed the experiments, with JÄ initiating the design concept. I then conducted the experiment, performed the data analysis, wrote the manuscript, and finally revised it following peer review on my own. JÄ and the other co-authors reviewed the manuscript and provided their feedback.

Paper III

High-Speed Optical Diagnostics of Misfire Limits in a Spark-Ignited Heavy-Duty Hydrogen Engine
P. Hallstadius, **A. Saha**, A. Sridhara, Ö. Andersson
SAE Int. J. Adv. & Curr. Prac. in Mobility 7(5):2383-2397, 2025, https://doi.org/10.4271/2025-01-8401

I participated in planning the experiment with the first author (PH). I then participated in conducting the experiment and data collection. PH performed the engine and optical data analysis, and I performed the spark energy calculations. PH wrote the manuscript. I provided input on the manuscript.

Paper IV

Calorimetric Study of the Influence of Spark Ignition System Parameters on the Energy Transfer to the Gas
A. Saha, P. Tunestål, J. Ängeby, Ö. Andersson
SAE Technical Paper 2025-24-0033, 2025, https://doi.org/10.4271/2025-24-0033

I designed the experiment, conducted the experiment, performed the data analysis, wrote the manuscript and revised it following the peer review. All the co-authors reviewed the manuscript and provided their feedback.

Paper V

Ignitability Study in a Spark-Ignited Hydrogen Direct Injection Heavy-Duty Engine
A. Saha, E. Zanjani, J. Engström, P. Tunestål, Ö. Andersson
Will be submitted to *International Journal of Hydrogen Energy.*

I designed the experiment on my own. I then conducted the experiment together EZ. Then I performed the data analysis on my own. I wrote the manuscript together with EZ. I will finally revise it following the peer review on my own. EZ and the other co-authors will review the manuscript and will provide their feedback.

Printed by Media-Tryck, Lund 2026 NORDIC SWAN ECOLABEL 3041 0903

About the author

ANUPAM SAHA holds a Bachelor's degree in Mechanical Engineering from West Bengal University of Technology and a Master's degree in Automotive Systems Engineering from HAN University of Applied Sciences, with a specialization in combustion engines. His doctoral research at the Department of Energy Sciences, Lund University, is dedicated to advancing spark ignition systems for combustion engines operating on gaseous fuels. This thesis presents his contributions toward optimizing the spark ignition process to enhance ignitability while minimizing spark plug wear and abnormal combustion in heavy-duty engines fueled by biogas and hydrogen.

LUND UNIVERSITY

Faculty of Engineering
Department of Energy Sciences

LUTMDN/TMHP-26/1187-SE
ISBN 978-91-90202-31-9
ISSN 0282-1990